RETINAL GENE TRANSCRIPTIONAL REGULATION AND NEUROPROTECTION OF PHOTORECEPTORS

By

Gillian Curtis Shaw

A dissertation submitted to Johns Hopkins University in conformity with the requirements for the degree of Doctor of Philosophy

Baltimore, Maryland

October, 2014

Abstract

My PhD research included two distinct projects. Project I examined the transcriptional regulation of two genes expressed in the retina, synaptotagmin 11 (*Syt11*, retinal ganglion cell-enriched) and S-antigen (*Sag*, photoreceptor-enriched). For each, a cloned fragment was identified that showed promoter activity in its respective cell population. A deletion analysis and subsequent bioinformatic analysis were used to predict transcription factors (TF) binding within the region of interest, and then binding site mutant promoter-reporter constructs were generated and tested. Finally, siRNA knockdown of TFs of interest was followed by endogenous expression analysis. I identified regions of interest for each gene (*Syt11* -192 to -41 bp and Sag -279 to -182 bp) but knockdown of multiple TFs in each cell population yielded inconclusive results.

In Project II, I evaluated sunitinib, a multiple kinase inhibitor that is neuroprotective for retinal ganglion cells, for its ability to promote photoreceptor (PR) survival in mouse models of PR degeneration. Based on the findings of a collaborator who found that sunitinib promoted the survival of PRs in a rat model of an autosomal dominant retinal degeneration (*Rho S334ter*), I studied the retinal expression of dual leucine kinase (DLK) protein (known to be a target of sunitinib) during retinal degeneration (RD). I observed an increase in DLK abundance in degenerating retinas, which persisted after most PRs had degenerated, suggesting that DLK accumulation occurs, at least in part, in a cell type other than PRs. I tested the effect of sunitinib on photoreceptor survival in the *Rho Q344ter* and the *rd1* (*Pde6b* mutant) mouse RD models, but under the conditions tested did not observe evidence of increased PR survival. Additionally, I tested the ability of genetic deletion of *Parp1* to promote PR survival in the sodium iodate and *rd1* mouse

models of RD. *Parp1* null PRs did not show evidence of increased survival at 36 days post sodium iodate administration. Several litters of *Parp1* KO/*rd1* animals had increased PR survival. Further studies are needed to more fully define the potential role of sunitinib, DLK inhibition, and PARP1 inhibition in photoreceptor neuroprotection.

Thesis Advisor: Donald J. Zack, MD, PhD

Thesis Reader: Joseph Steiner, PhD

Acknowledgements

I would like to thank Don Zack for taking me on as a PhD student in his laboratory. Without his mentorship, patience and advice I would not have been able to attain this goal. I would also like to thank Cindy Berlinicke without whose guidance, advice and caring demeanor I never would have been able to get as far as I did. Don and Cindy both patiently taught me how to design an experiment, choose proper controls and helped me interpret my results time and time again. Additionally, I thank all of the other members of the Zack lab who were always willing to teach me techniques and discuss experiments with me. The helpful and collaborative nature of the other Zack lab members was integral in my success.

My committee members helped guide me as I navigated the past several years and then gave me the stamp of approval, for which I am grateful. They are: Andrew McCallion, Valina Dawson and Joseph Steiner.

I would also like to thank my mom, dad and brother. Without their love and support, I probably never would have made it this far in life.

TABLE OF CONTENTS

LIST OF TABLES

LIST OF FIGURES

Part II Chapter 1.

Part II Chapter 2.

I: Regulation of Retinal Cell Type-Specific Gene Expression

Introduction

The retina is the multilayered neural tissue that lines the back of the eye and is responsible for converting light into a neurochemical signal. The two most medically relevant cell types are photoreceptors and retinal ganglion cells. The photoreceptors (PRs), the rods and cones, are the cells responsible for converting a light signal into a chemical signal that is then passed through the rest of the retinal cells and eventually through the retinal ganglion cells to the brain. Photoreceptors are medically relevant because they are affected by numerous genetic and degenerative diseases such as retinitis pigmentosa and age-related macular degeneration. Retinal ganglion cells are damaged in glaucoma and other forms of optic nerve disease, and it is their loss that leads to vision loss and potentially blindness in these diseases, and thus they are also medically highly relevant.

Rods, which are more sensitive than cones and are responsible for vision in dim light, are the most numerous photoreceptor-type in most mammalian retinas, and they express the rhodopsin visual pigment. Cone photoreceptors are responsible for bright light, high acuity and color vision. There are several different types of cone photoreceptors characterized by which of several different cone opsin visual pigments they express. Individual cones, with a few exceptions, express only one visual pigment, and the opsin they express dictates the wavelengths of light to which they are most sensitive.

Phototransduction is the extensively studied and remarkable process by which light is converted into a chemical signal within photoreceptor cells (reviewed by Sung & Chuang [1]). Mammalian opsin molecules, with a few exceptions, are covalently linked

to the chromophore 11-*cis*-retinal. The phototransduction process begins when light photo-isomerizes 11-*cis*-retinal to all-*trans*-retinal within photoreceptor cell membranes, causing a conformational change in rhodopsin and initiating a G protein coupled signaling pathway. Transducin, a G protein, is activated by rhodopsin that in turn activates phosphodiesterase which hydrolyzes cGMP. The decrease in cGMP closes the cGMP-gated channels and causes the photoreceptor to hyperpolarize, which decreases the amount of glutamate being released at synapses with second order retinal neurons. These signal changes are ultimately conveyed to the brain where visual perception takes place.

Photoreceptors are affected in a large number of degenerative diseases. Age-related macular degeneration, which is the most common cause of irreversible blindness in the elderly in the Western world, is an example of a degenerative disease that affects PRs and their major supporting cells, the retinal pigment epithelial (RPE) cells. Retinitis pigmentosa and Leber congenital amaurosis (LCA) are genetically heterogeneous groups of retinal degenerative diseases caused by a wide spectrum of genetic mutations that affect PR and RPE cells. LCA can be considered a more severe form of RP that affects young children. The degree and rapidity of vision loss in LCA and RP are variable, but many forms of these diseases ultimately result in blindness. Many of the genes, of which there are more than 200, that when mutated cause retinal degenerative disease, encode proteins that are involved in phototransduction, the visual cycle or transcription factors that regulate the expression of phototransduction proteins (RetNet, http://www.sph.uth.tmc.edu/RetNet/).

Retinal ganglion cells (RGCs) receive and integrate visual information from other cells in the retina and transmit this information via the optic nerve to visual centers in the

brain. A variety of diseases cause damage and loss of RGCs, which can result in vision loss and blindness. Among these diseases, the neurodegenerative disease glaucoma is the most common. Approximately 60 million people have glaucoma, and behind cataracts, it is the second leading cause of blindness in the world [2]. Despite the implication of multiple cellular mechanisms and pathways as contributing to glaucoma-associated RGC cell damage and death, including excitotoxicity, ischemia, oxidative stress, neurotrophin deprivation due to impaired retrograde transport, glial cell changes, and altered local immune status [3], the treatment of glaucoma continues to be based almost solely on the reduction of intraocular pressure [4-6]. A potentially more attractive approach would be to target damage-promoting pathways specifically in RGCs.

Developments of cell-type specific therapeutic approaches are greatly facilitated by understanding the gene expression regulatory pathways in the particular cell of interest. The identity and normal functioning of a tissue is dictated by differential gene expression of the cells that make up that tissue. The development of all six of the retinal neurons (RGCs, rods, cones, horizontal cells, bipolar cells and amacrine cells) and retinal glial cells (Müller glial cells) has been studied extensively in a number of species (reviewed by Xiang [7]). A number of transcription factors necessary for retinogenesis have been identified, including PAX6, RX, CHX10 and SIX3 [8]. PAX6, in particular, is required early on in cells of the developing visual field [9, 10], and in fact when it is genetically deleted, only amacrine cells develop [9]. Photoreceptor development, in particular, and its myriad necessary transcriptional regulatory events, has been studied in great detail (recently reviewed by Swaroop [11] and Ranganathan & Zack [12]). In the rat and mouse retina, cone and then rod photoreceptors are born beginning at embryonic

days 11.5 and 12, respectively, and continue to be born and develop until embryonic day 17.5 for cones and post-natal day 10 for rods [13, 14].

The sequential appearance of several transcription factors (RAX then OTX2 then CRX) is necessary for the initial photoreceptor cell fate specification and differentiation [15-17]. The presence of the RORβ transcription factor in photoreceptor precursor cells is necessary for the eventual rod photoreceptor cell fate as it goes on to stimulate the expression of *Nrl*, another necessary transcription factor, which in turn stimulates the expression of *Nr2e3* [18-21]. The combination of NRL and NR2E3 is necessary for rod-specific gene expression and differentiation, and in the absence of NRL, photoreceptor precursor cells differentiate into cone photoreceptors [20]. The combination of CRX and NRL transcription factors is necessary for the expression of many different rod photoreceptor specific genes [22, 23]. Cone photoreceptor development diverges from that of rods through the actions of a number of transcription factors, which not only specify cone fate, but exact type of cone fate through the stimulation of transcription of the various cone opsin genes. In the absence of NRL, CRX and RORβ act together to promote the expression of S-opsin and the development of short wavelength (or blue) cones [24]. However if TRβ2 is present with its ligand, thyroid hormone, then M-opsin is expressed and the precursor cell develops into a medium wavelength (or green) cone [25].

Although not as well studied as PRs at the gene regulation level, in recent years there has been increasing attention to the study of the mechanisms regulating RGC-specific gene expression. Broad regulatory pathways involved in RGC cell fate determination have been defined in the developing murine retina, and a number of the

transcription factors that are important for RGC development have been identified [7]. Transcriptomic studies of RGC changes associated with RGC damage have also been performed in animal models of glaucoma [26, 27].

RGCs are the first cell type to be born during retinogenesis, and many of the necessary transcription factors and their regulatory network have been established. Of note, however, is that there are many different types of RGCs in the developed retina that have followed various gene regulatory pathways to become fully differentiated RGCs, necessitating a complicated gene regulatory network. As mentioned earlier, PAX6 is required not only for retinal progenitor determination, but specifically for RGC determination [9]. It is known that PAX6 and the Notch pathway have opposite effects on RGC development, and NOTCH inhibits Math5 expression, thus inhibiting RGC development [28]. Additionally, when *Neurod1*, which is required for amacrine cell development, is replaced with *Math5*, amacrine cell fate is prevented and RGC cell fate is promoted [29]. It is known that the ATOH7/MATH5 transcription factor, which is in part dependent on *Pax6* expression [8, 9, 30-32], is important for RGC development, however, not all cells that express *Math5* will become RGCs [33, 34]. Additionally, there is a subset of RGCs that never express *Math5* [35], and instead, expressed *Neurod1* [36]. Nonetheless, targeted disruption in mice results in a reduced number of RGCs and the absence of an optic nerve [37, 38].

MATH5 regulates the transcription of several other genes including islet 1 (*Isl1*), *Eya2* and *Pou4f2/Brn3b* that are critical for continued RGC development and maintenance [30, 39, 40]. Retina-specific knockdown of *Isl1* expression in the developing mouse retina did not prevent RGC development, but did result in early RGC apoptosis

[30]. In this *Isl1* knockdown experiment, the expression of *Brn3b* was also decreased, suggesting *Isl1* lies upstream of *Brn3b* [30]. The POU domain transcription factors, POU4F2/BRN3B, POU4F1/BRN3A and POU4F3/BRN3C are necessary for RGC differentiation, maturation and axon growth [41, 42]. BRN3B regulates a number of other genes including transcription factors with known or postulated roles in the retina as well as genes important for neuron function and integrity [31, 43]. And not unexpectedly, additional players in the retinal and RGC gene regulatory network are being discovered constantly. A recently identified pair of redundant factors (ONECUT1 and ONECUT2) are important for early retinal cell differentiation and double knockout of both factors resulted in abnormal horizontal cell, cone cell and RGC development [44].

A number of gene expression studies have examined whole retina gene expression changes in glaucoma [27, 45, 46] and found an up-regulation in inflammatory and glial activation-related genes including *C1q* and *Gfap*. One study that examined laser capture microdissected RGCs after glaucoma induction found an up-regulation of genes in apoptosis-related pathways and markers of inflammation, including complement pathways (e.g. *Gfap, C1qa, C1qb, C3*) and a down-regulation of neuronal pro-survival genes (e.g. *Stmn2, Ywhaz, Vsnl1, Ywhab, Ret*) [26]. Although many RGC transcriptional pathways have been identified, many molecular details are lacking.

Though some of the pathways directing the development of photoreceptors and RGCs have been elucidated, the exact transcription factors necessary to direct expression of the many different photoreceptor- and RGC-specific genes have not been fully determined. This is an important area of research and advances in post-development transcriptional regulation in these cells could support a number of important pursuits

including gene therapy, stem cell therapy, and neuroprotective drug discovery. Knowing what regulatory sequences are required for cell-specific expression would allow cell type-specific gene therapy to be directed to photoreceptors or RGCs within the retina, and would allow regulating the expression of the gene therapy target genes or neuroprotective genes. Additionally if the regulatory sequences of genes known to contribute to either photoreceptor or RGC survival or death were known, then a screen for drugs that modulate the expression of these genes could be used to identify important novel treatment approaches for diseases that affect these cells.

Retinal transcriptional regulation has often been studied using immortalized cell lines. For example HEK293, COS, and Y79 cells have been used to study photoreceptor promoters [47-51] and RGC5 cells have been used to study a number of aspects of RGC biology [52]. However, although such studies have yielded useful information, immortalized cells, even if originally from the cell type of interest, can differ greatly from the actual cell in a living tissue. For example, the network of other transcription factors and modulators as well as the epigenetic status of primary cells compared to immortalized cells can differ significantly [53]. Related to these differences, promoter reporter activity can also differ in primary cells compared to immortalized cell lines, making the discernment of cell-type specific transcriptional regulatory mechanisms difficult [47]. Therefore, although their use is more technically challenging, for the retinal promoter studies described in the next two chapters I chose to use primary retinal cells because they more accurately recapitulate the *in vivo* genetic and cellular milieu of the retina and thus are better suited to study of the mechanisms that determine cell type-specific gene expression in the retina. Chapter 2 describes studies utilizing synaptotagmin

11 (*Syt11*)-reporter constructs in combination with purified murine RGCs as a model to study RGC transcriptional regulation. Chapter 3 describes parallel studies utilizing S-antigen (*Sag*)-reporter constructs in combination with total mouse retinal cultures, which are predominantly made up of rods, as a model to study photoreceptor transcriptional regulation.

References

1. Sung, C.H. and J.Z. Chuang, *The cell biology of vision.* J Cell Biol, 2010. **190**(6): p. 953-63.
2. Quigley, H.A. and A.T. Broman, *The number of people with glaucoma worldwide in 2010 and 2020.* Br J Ophthalmol, 2006. **90**(3): p. 262-7.
3. Rieck, J., *The pathogenesis of glaucoma in the interplay with the immune system.* Invest Ophthalmol Vis Sci, 2013. **54**(3): p. 2393-409.
4. Weinreb, R.N. and P.T. Khaw, *Primary open-angle glaucoma.* Lancet, 2004. **363**(9422): p. 1711-20.
5. Nickells, R.W., *From ocular hypertension to ganglion cell death: a theoretical sequence of events leading to glaucoma.* Can J Ophthalmol, 2007. **42**(2): p. 278-87.
6. Feilchenfeld, Z., Y.H. Yucel, and N. Gupta, *Oxidative injury to blood vessels and glia of the pre-laminar optic nerve head in human glaucoma.* Exp Eye Res, 2008. **87**(5): p. 409-14.
7. Xiang, M., *Intrinsic control of mammalian retinogenesis.* Cell Mol Life Sci, 2013. **70**(14): p. 2519-32.
8. Marquardt, T. and P. Gruss, *Generating neuronal diversity in the retina: one for nearly all.* Trends Neurosci, 2002. **25**(1): p. 32-8.
9. Marquardt, T., et al., *Pax6 is required for the multipotent state of retinal progenitor cells.* Cell, 2001. **105**(1): p. 43-55.
10. Chow, R.L. and R.A. Lang, *Early eye development in vertebrates.* Annu Rev Cell Dev Biol, 2001. **17**: p. 255-96.

11. Swaroop, A., D. Kim, and D. Forrest, *Transcriptional regulation of photoreceptor development and homeostasis in the mammalian retina.* Nat Rev Neurosci, 2010. **11**(8): p. 563-76.

12. Ranganathan, V. and D.J. Zack, *Transcriptional Regulation of Photoreceptor Development*, in *The New Visual Neurosciences*, L.C. John S. Werner, Editor. 2013, MIT: Cambridge, Ma. p. 1468-1482.

13. Rapaport, D.H., et al., *Timing and topography of cell genesis in the rat retina.* J Comp Neurol, 2004. **474**(2): p. 304-24.

14. Young, R.W., *Cell differentiation in the retina of the mouse.* Anat Rec, 1985. **212**(2): p. 199-205.

15. Mathers, P.H., et al., *The Rx homeobox gene is essential for vertebrate eye development.* Nature, 1997. **387**(6633): p. 603-7.

16. Muranishi, Y., et al., *An essential role for RAX homeoprotein and NOTCH-HES signaling in Otx2 expression in embryonic retinal photoreceptor cell fate determination.* J Neurosci, 2011. **31**(46): p. 16792-807.

17. Nishida, A., et al., *Otx2 homeobox gene controls retinal photoreceptor cell fate and pineal gland development.* Nat Neurosci, 2003. **6**(12): p. 1255-63.

18. Montana, C.L., et al., *Transcriptional regulation of neural retina leucine zipper (Nrl), a photoreceptor cell fate determinant.* J Biol Chem, 2011. **286**(42): p. 36921-31.

19. Jia, L., et al., *Retinoid-related orphan nuclear receptor RORbeta is an early-acting factor in rod photoreceptor development.* Proc Natl Acad Sci U S A, 2009. **106**(41): p. 17534-9.

20. Mears, A.J., et al., *Nrl is required for rod photoreceptor development.* Nat Genet, 2001. **29**(4): p. 447-52.

21. Swaroop, A., et al., *A conserved retina-specific gene encodes a basic motif/leucine zipper domain.* Proc Natl Acad Sci U S A, 1992. **89**(1): p. 266-70.

22. Hennig, A.K., G.H. Peng, and S. Chen, *Regulation of photoreceptor gene expression by Crx-associated transcription factor network.* Brain Res, 2008. **1192**: p. 114-33.

23. Chen, S., et al., *Crx, a novel Otx-like paired-homeodomain protein, binds to and transactivates photoreceptor cell-specific genes.* Neuron, 1997. **19**(5): p. 1017-30.

24. Srinivas, M., et al., *Activation of the blue opsin gene in cone photoreceptor development by retinoid-related orphan receptor beta.* Mol Endocrinol, 2006. **20**(8): p. 1728-41.

25. Ng, L., et al., *A thyroid hormone receptor that is required for the development of green cone photoreceptors.* Nat Genet, 2001. **27**(1): p. 94-8.

26. Wang, D.Y., et al., *Global gene expression changes in rat retinal ganglion cells in experimental glaucoma.* Invest Ophthalmol Vis Sci, 2010. **51**(8): p. 4084-95.

27. Steele, M.R., et al., *Microarray analysis of retinal gene expression in the DBA/2J model of glaucoma.* Invest Ophthalmol Vis Sci, 2006. **47**(3): p. 977-85.

28. Schneider, M.L., D.L. Turner, and M.L. Vetter, *Notch signaling can inhibit Xath5 function in the neural plate and developing retina.* Mol Cell Neurosci, 2001. **18**(5): p. 458-72.

29. Mao, C.A., et al., *Reprogramming amacrine and photoreceptor progenitors into retinal ganglion cells by replacing Neurod1 with Atoh7.* Development, 2013. **140**(3): p. 541-51.

30. Mu, X., et al., *Gene regulation logic in retinal ganglion cell development: Isl1 defines a critical branch distinct from but overlapping with Pou4f2.* Proc Natl Acad Sci U S A, 2008. **105**(19): p. 6942-7.

31. Mu, X. and W.H. Klein, *A gene regulatory hierarchy for retinal ganglion cell specification and differentiation.* Semin Cell Dev Biol, 2004. **15**(1): p. 115-23.

32. Mu X, K.W., *Gene regulatory networks and retinal ganglion cell development*, in *Eye, Retina, and Visual System of the Mouse*, L.W. Chalupa, RW., Editor. 2008, The MIT Press: Cambridge, MA. p. 321-332.

33. Brown, N.L., et al., *Math5 encodes a murine basic helix-loop-helix transcription factor expressed during early stages of retinal neurogenesis.* Development, 1998. **125**(23): p. 4821-33.

34. Kanekar, S., et al., *Xath5 participates in a network of bHLH genes in the developing Xenopus retina.* Neuron, 1997. **19**(5): p. 981-94.

35. Mao, C.A., et al., *Neuronal transcriptional repressor REST suppresses an Atoh7-independent program for initiating retinal ganglion cell development.* Dev Biol, 2011. **349**(1): p. 90-9.

36. Kiyama, T., et al., *Overlapping spatiotemporal patterns of regulatory gene expression are required for neuronal progenitors to specify retinal ganglion cell fate.* Vision Res, 2011. **51**(2): p. 251-9.

37. Brown, N.L., et al., *Math5 is required for retinal ganglion cell and optic nerve formation.* Development, 2001. **128**(13): p. 2497-508.

38. Wang, S.W., et al., *Requirement for math5 in the development of retinal ganglion cells.* Genes Dev, 2001. **15**(1): p. 24-9.

39. Pan, L., et al., *ISL1 and BRN3B co-regulate the differentiation of murine retinal ganglion cells.* Development, 2008. **135**(11): p. 1981-90.

40. Gao, Z., et al., *Transcriptome of Atoh7 retinal progenitor cells identifies new Atoh7-dependent regulatory genes for retinal ganglion cell formation.* Dev Neurobiol, 2014. **74**(11): p. 1123-40.

41. Badea, T.C., et al., *Distinct roles of transcription factors brn3a and brn3b in controlling the development, morphology, and function of retinal ganglion cells.* Neuron, 2009. **61**(6): p. 852-64.

42. Wang, S.W., et al., *Brn3b/Brn3c double knockout mice reveal an unsuspected role for Brn3c in retinal ganglion cell axon outgrowth.* Development, 2002. **129**(2): p. 467-77.

43. Mu, X., et al., *Discrete gene sets depend on POU domain transcription factor Brn3b/Brn-3.2/POU4f2 for their expression in the mouse embryonic retina.* Development, 2004. **131**(6): p. 1197-210.

44. Sapkota, D., et al., *Onecut1 and Onecut2 redundantly regulate early retinal cell fates during development.* Proc Natl Acad Sci U S A, 2014. **111**(39): p. E4086-95.

45. Ahmed, F., et al., *Microarray analysis of changes in mRNA levels in the rat retina after experimental elevation of intraocular pressure.* Invest Ophthalmol Vis Sci, 2004. **45**(4): p. 1247-58.

46. Yang, Z., et al., *Changes in gene expression in experimental glaucoma and optic nerve transection: the equilibrium between protective and detrimental mechanisms.* Invest Ophthalmol Vis Sci, 2007. **48**(12): p. 5539-48.

47. Lambard, S., et al., *Expression of rod-derived cone viability factor: dual role of CRX in regulating promoter activity and cell-type specificity.* PLoS One, 2010. **5**(10): p. e13075.

48. Yadav, S.P., et al., *The transcription-splicing protein NonO/p54nrb and three NonO-interacting proteins bind to distal enhancer region and augment rhodopsin expression.* Hum Mol Genet, 2014. **23**(8): p. 2132-44.

49. Escher, P., D.F. Schorderet, and S. Cottet, *Altered expression of the transcription factor Mef2c during retinal degeneration in Rpe65-/- mice.* Invest Ophthalmol Vis Sci, 2011. **52**(8): p. 5933-40.

50. Swain, P., et al., *Mutations associated with retinopathies alter mitogen-activated protein kinase-induced phosphorylation of neural retina leucine-zipper.* Mol Vis, 2007. **13**: p. 1114-20.

51. Fradot, M., et al., *The loss of transcriptional inhibition by the photoreceptor-cell specific nuclear receptor (NR2E3) is not a necessary cause of enhanced S-cone syndrome.* Mol Vis, 2007. **13**: p. 594-601.

52. Shen, X., et al., *Processing of optineurin in neuronal cells.* J Biol Chem, 2011. **286**(5): p. 3618-29.

53. Tran, S., et al., *The CpG island in the murine foxl2 proximal promoter is differentially methylated in primary and immortalized cells.* PLoS One, 2013. **8**(10): p. e76642.

The transcriptional regulation of synaptotagmin 11 (*Syt11*) in retinal ganglion cells (RGCs)

Introduction

As stated earlier, transcriptional regulation allows a cell to express particular genes so it can function properly in its tissue-specific milieu. Identification of the precise regulatory DNA sequences required for RGC-specific expression would allow RGC-directed expression of potential therapeutic molecules within the retina, and perhaps even within specific subsets of RGCs. Additionally, RGC-specific reporters or reporters specific to RGC death/survival pathways can be used in screens for neuroprotective factors. We and others have been working to define the *cis*-acting elements that regulate RGC-specific transcriptional activation. Here we describe the process by which we have worked to define the regulatory elements that control expression of a model RGC-expressed gene, synaptotagmin 11 (*Syt11*).

Transcriptional regulation is often studied using immortalized cell lines, but even if originally derived from the cell type of interest, immortalized cell lines often differ significantly from the actual cell type of interest in terms of their gene expression patterns and transcription factor networks. For this reason, we chose to develop and utilize a protocol for transient transfection of primary rodent retinal ganglion cells for our promoter studies. Using this protocol, we defined some of the regulatory sequences important for *Syt11* expression in RGCs, and utilized siRNA knockdown to begin an exploration of some of the *trans*-acting transcription factors that interact with these sites.

Materials & Methods

Enrichment of Primary Rodent Retinal Ganglion Cells

All animals were treated in accordance with the ARVO statement for the care and use of animals and all procedures were approved by the Johns Hopkins University Institutional Animal Care and Use Committee. The retinal ganglion cell (RGC) enrichment procedure was adapted from Barres et al [1].

Digestion

In brief, neonatal pups (postnatal day 0-3) were euthanized on wet ice and eyes enucleated. Retinas were isolated from the globes in cold CO_2 independent media (catalog # 18045-088, Life Technologies, Carlsbad, CA) containing 2 mM L-glutamine (catalog # 25030-081, Life Technologies, Carlsbad, CA) and 50 U/mL / 50 μg/mL penicillin/streptomycin (catalog # 15070-063, Life Technologies, Carlsbad, CA). Retinas were rinsed in PBS without Ca^{2+} or Mg^{2+} (catalog # 10010-023 Life Technologies, Carlsbad, CA) and then digested in 1 mL/10 retinas of activated papain containing 250 U/mL DNase I (catalog # D4527, Sigma-Aldrich, St Louis, MO) and pH adjusted to 7.4. Papain (16.5 U/mL for pup retinas & 33 U/mL for adult retinas, catalog # LS003119 Worthington, Lakewood, NJ) was prepared in Hibernate-E without Ca^{2+}/Mg^{2+} (catalog # HE-Ca 500ml, Brainbits, Springfield, IL) activated with 0.2 mg/mL L-cysteine (catalog # C7352 Sigma-Aldrich, St Louis, MO) and the pH adjusted to 7.4 with NaOH. Retinas are digested for approximately 40 minutes, at which time the tissue has dissociated into a cell suspension. The digestion was inhibited with 0.5 mL of a soybean trypsin inhibitor solution containing 15 mg/mL soybean trypsin inhibitor (catalog # LS003587,

Worthington, Lakewood, NJ), 15 mg/mL bovine serum albumin (BSA) (catalog # 126579, Merck KGaA, Darmstadt, Germany) and 125 U/mL DNase I (catalog # D4527, Sigma-Aldrich, St Louis, MO) in Hibernate-E (catalog # A12476-01, Life Technologies, Carlsbad, CA) per 1 mL of the papain solution and the cell suspension was triturated drop-wise six times with fire polished siliconized glass pipettes to generate homogeneous single cell solution.

Macrophage depletion

Cells were spun down at 80 x *g* for 7 minutes and resuspended in 1.8 mL DPBS with glucose and pyruvate (catalog # 14287-080, Life Technologies, Carlsbad, CA) containing 0.2% BSA and then incubated with anti-CD11b antibody-coated (catalog # 554859, BD Biosciences, San Jose, CA) magnetic beads (Cellection pan mouse IgG, catalog #11531D, Life Technologies, Carlsbad, CA) with gentle rotation for 15 minutes at room temperature. The CD11b bead-bound macrophages and remaining beads were then depleted from the cell suspension using a magnet. Supernatant cells were resuspended in 13 mL DPBS with glucose and pyruvate containing 0.2% BSA and applied to a pre-made immunopanning plate.

Positive selection of RGCs using immunopanning

Immunopanning plates were created by coating a 10 cm non-cell culture treated petri dish with 70 mg of a goat anti-rat IgG for rat RGC immunopanning (catalog # 112-005-003, Jackson Immunoresearch, West Grove, PA) or a goat anti-mouse IgM for immunopanning mouse RGCs (catalog # 115-005-020, Jackson Immunoresearch, West

Grove, PA) and then 30 mg of an anti-Thy1.1 IgG for rats (catalog # MAB1406, Merck KGaA, Darmstadt, Germany) or an anti-Thy1.2 IgM for mice (catalog # MCA02R, Abd-Serotec, Raleigh, NC). The plate was gently agitated every 15 minutes during a one to two hour incubation at room temperature. The supernatant (RGC-depleted) was then removed and discarded and the plate washed 5-7 times with 5 mL of DPBS with glucose and pyruvate (total of 35 mL). The adhered RGCs were gently scraped off with a cell lifter (catalog # 83-3008, Corning, Tewksbury, MA) in 10 mL of Hibernate-E without Ca^{2+}/Mg^{2+} (catalog # HE-Ca 500ml, Brainbits, Springfield, IL) containing 10% Fetal Bovine Serum (catalog # 16140-071, Life Technologies, Carlsbad, CA). RGC enriched cells were then counted and plated at a density of 10,000 to 20,000 cells / well in 96 well poly-d-lysine-coated plates. The yield was typically 20,000 to 30,000 cells / mouse retina and 50,000 to 70,000 cells / rat retina. Cells were cultured in Neurobasal (catalog # 21103-049, Life Technologies, Carlsbad, CA) containing B27 supplement (catalog # 17504-044, Life Technologies, Carlsbad, CA) 2 mM L-glutamine , 50 U/mL / 50 μg/mL penicillin/streptomycin, forskolin (2.5 uM for rats, 5 uM for mice) (catalog # F3917, Sigma-Aldrich, St Louis, MO) and sunitinib (1 uM for rats, 0.5 uM for mice) (catalog # S-8803, LC Labs, Woburn, MA) to promote RGC survival (work of Zhiyong Yang, unpublished data). Cells were incubated at 37^{o}C in a humidified incubator containing 5% CO_2.

Promoter Reporter Creation (initial set, deletion series, binding site mutants)

Genomic DNA was isolated from Sprague-Dawley rat liver using a QIAmp DNA Mini Kit (catalog # 51304, Qiagen, Germantown, MD) and a fragment of the upstream

promoter region of solute carrier family 17 (sodium-dependent inorganic phosphate cotransporter), member 6 (*Slc17a6*), was PCR amplified and recombined in pDONR221 using the Gateway® system (BP Clonase II, catalog # 11789-020, Life Technologies, Carlsbad, CA). Promoter region fragments from published rat neurofilament medium (*Nefm*), neuritin 1 (*Nrn1*), peripherin 1 (*Prph1*), semaphorin 6b (*Sema6b*), synuclein gamma (*Sncg*) and synaptotagmin 11 (*Syt11*) were synthesized (GenScript, Piscataway, NJ) and provided in Gateway® compatible plasmids. See Table 1 for PCR primers and lengths of promoter regions. Gateway LR recombination reactions were performed to insert promoter fragments into a Gaussia luciferase gene promoter reporter Gateway® destination vector (pGluc) using the LR Clonase II from Life Technologies (catalog # 11791-019). The pGLuc vector was created by inserting the Gateway® reading frame cassette upstream of the Gaussia luciferase reporter gene in the pGLuc-Basic 2 vector (catalog # N8082S, New England Biolabs, Ipswich, MA). Insertion and proper orientation in entry and destination vectors were confirmed with colony PCR and sequencing with a forward primer within the vector upstream of the recombination site and a reverse primer within the insert.

The *Syt11* promoter deletion series was constructed by PCR amplifying fragments of the upstream region from rat genomic DNA and cloning them into pENTR (catalog # K2400-20, Life Technologies, Carlsbad, CA). Constructs were confirmed by sequencing and the insert recombined into the pGLuc destination vector using the Gateway® system. See Table 2 for primers used in the construction of the deletion series and fragment lengths. Length of insert and correct orientation within the pGLuc vector was confirmed by colony PCR.

Binding site mutants were created in the full length (-656 to +136 bp) *Syt11* promoter reporter in the pENTR vector using Life Technologies' Geneart® mutagenesis system by introducing transversions for each nucleotide within the predicted binding site. The overlapping nucleotides of the DEAF1 and SP1 binding sites were left unmutated when only the DEAF1 motif or only the SP1 motif were mutated, but mutated when the two sites were mutated together. The binding site mutations in the pENTR vector were confirmed by sequencing. See Table 3 for primers used. The DEAF1 sites were mutated in two steps because of their length and constraints of the Geneart® system. Constructs were recombined into the previously mentioned pGLuc vector using the Gateway® system (Life Technologies, Carlsbad, CA) and insert presence & orientation were confirmed via colony PCR. The full length (-656 to +136 bp), wild type *Syt11* promoter fragment was also recombined into a Cypridina luciferase (another secreted luciferase, CLuc) containing reporter plasmid which had been created by the insertion of a Gateway® site upstream of the CLuc gene (pCLuc, New England Biolabs, Ipswich, MA), which was used as a transfection control.

Plasmids were transformed into and grown in *E. coli* in batches and isolated using either Promega's PureYield Midiprep system (catalog # A2492, Madison, WI) or Life Technologies' HiPure Plasmid Filter Maxipreps (catalog # K2100, Carlsbad, CA) and resuspended and stored in tris-EDTA buffer.

Testing of Promoter Reporters

Initially (Figure 2), promoter reporters were electroporated into isolated rat RGCs using Invitrogen's Neon system. In brief, RGCs or dissociated whole retinal cells were

resuspended in the Neon electroporation buffer R and electroporated in 10 μL with 0.5 μg plasmid at 1100 V, 30 msec, 1 pulse. After electroporation, cells were gently squirted into wells already containing warmed & equilibrated growth media. There were always three or four replicate wells for each construct. Electroporation using the Neon system resulted in approximately 30-40% transfection efficiency with significant cell mortality.

Later, constructs were transfected into RGCs using NeuroMag (OZ Biosciences, San Diego, CA) (Figures 3 and 6). NeuroMag (0.2 μL) was complexed with 200 ng of plasmid in OptiMem (catalog # 31985-088, Life Technologies, Carlsbad, CA) and added to wells containing 10,000 to 15,000 RGCs/well in growth media in a 96 well plate, which was then placed on the OZ Biosciences magnet (catalog # MF14000) overnight in a cell culture incubator. Typically each well was transfected with the pGLuc construct of interest and a pCLuc construct (SV40- or CMV- CLuc or full length, wild type *Syt11*-pCLuc), which was used to normalize the transfection. Transfection efficiency using NeuroMag was lower than electroporation and was usually around 10% with less cell mortality.

Media aliquots to measure luciferase activity were collected at 48 or 72 hours post-transfection and assayed separately using Gaussia and Cypridina luciferase assay kits from New England Biolabs (Ipswich, MA). For Figures 3 and 6 the constructs' GLuc activity was normalized to the activity of a co-transfected pCLuc construct (SV40-CLuc for Figure 3, *Syt11* -656 to +136-pCLuc for RGCs and SV40-CLuc for 293 cells in Figure 6 and CMV-CLuc for Figure 8). Empty vectors (Basic-CLuc and Promoterless-GLuc [Pless-GLuc], New England Biolabs, Ipswich, MA) were used as negative controls.

RNA collection and cDNA conversion

For Figures 1 and 10, RNA was collected from dissociated whole retinal cells and immunopanned RGCs immediately after being scraped off the immunopanning plate from early post-natal Sprague-Dawley rat pups and adult rats using Qiagen's Mini RNeasy kit (catalog # 74104, Germantown, MD) including an on-the-column DNase treatment using Qiagen's RNase-free DNase set (catalog # 79254). RNA was quantified using a Nanodrop (ThermoScientific, Wilmington, DE) and 100-500 ng converted to cDNA using random primers and the Applied Biosystems High Capacity cDNA Reverse Transcription Kit (catalog # 4368814, Life Technologies, Carlsbad, CA). For siRNA knockdown experiments (Figures 7, 8B, 11, 12 and 13) RNA was collected from plated RGCs using Qiagen's Micro RNeasy kit (catalog # 74004) and all of the RNA collected was converted to cDNA without quantification using random primers using the aforementioned cDNA reverse transcription kit (catalog # 4368814, Life Technologies, Carlsbad, CA).

Quantitative Real Time-PCR (qPCR)

Sequences of primers used in qPCR assays are listed in Table 4 and came from RT Primer database (http://medgen.ugent.be/rtprimerdb/) or designed with Roche's primer design algorithm (http://lifescience.roche.com/shop/CategoryDisplay?catalogId=10001&tab=Assay+Design+Center&identifier=Universal+Probe+Library&langId=-1#tab-3). Primer pair efficiencies were determined using a standard curve of RGC cDNA and deemed adequate if they were between 90 and 110%. Samples were run in triplicate in a BioRad Cfx

C1000 384 qPCR machine in a total reaction volume of 8uL containing 0.04 μL of cDNA for gene survey (Figures 1 and 10) and 0.2 uL cDNA for siRNA KD experiments (Figures 7, 8, 11, 12 and 13), 125 nM of each primer, EvaGreen (catalog # 31000, Biotium, Hayward, CA), 0.67 U of Fermentas Hot Start *Taq* DNA polymerase (catalog # EP0603, Thermo Scientific, Wilmington, DE), 3 mM $MgCl_2$ and 0.2 mM each dNTP. The cycling parameters were: 95^{o}C for 3 min, followed by 40 cycles of 95^{o}C for 10 sec, 60^{o}C for 30 sec and 72^{o}C for 30 sec, followed by a melting curve analysis with temperature range between 60^{o}C and 95^{o}C with a 0.5^{o}C increment. Primer pair specificity was confirmed with a single sharp peak in the melting curve. Reference genes were deemed appropriate when they had CV and M values of <0.5 and 1 respectively. The geometric mean of three to four reference genes was used to normalize the target gene expression [2] using BioRad's Cfx software. Results are reported as Relative Normalized Expression based on the ΔΔ Cq calculation.

Bioinformatics

A MOPAT analysis was performed on the region of interest (-192 to -41bp) within the Syt11 5' UTR to identify predicted transcription factor binding sites [3]. The list of possible transcription factors was cross-referenced with microarray data of immunopanned mouse RGCs [4] to identify transcription factors known to be expressed in RGCs (Figure 5).

After the negative data was obtained from siRNA knockdown of *Deaf1*, *Sp1*, *Elk1*, *Hsf1* TFs, an additional bioinformatic analysis was performed on the wild type compared to the promoter mutants using TRANSFAC-database with an 80% matching

threshold to identify predicted TFs. Specifically, the changes in predicted TFBSs in the various binding site mutants compared to the wild type promoter sequence were examined to determine more relevant predicted transcription factors. These results are displayed in Figure 15.

Small interfering RNA knockdown (siRNA KD)

Immunopanned RGCs were transfected with NeuroMag (0.1uL) complexed with a total of 0.02 pmol (Figures 7 and 8) or 0.01 pmol (Figures 11, 12 and 16) of siRNA/well in 96 well plates as described earlier. Non-targeting (scrambled) siRNAs were used as a negative control. Table 5 shows the siRNAs used, their origin, product numbers and sequences. Pools of the individual siRNAs were used to obtain the data in Figures 7, 8, 11 and 16.

For dual siRNA KD and promoter reporter transfection, pools of siRNA and plasmids were complexed to Neuromag separately and then mixed together immediately before being added to the wells with RGCs.

Custom unmodified siRNAs with the 9^{th} to the 11^{th} bases complemented ("C911") [5] for *Hsf1* and *Hsf2* were ordered from Life Technologies (Silencer siRNA, Ambion, Life Technologies, Carlsbad, CA) and transfected into rat RGCs using NeuroMag as described above (0.1 pmol) (Figure 13).

Overexpression of transcription factors

ORFs of human *Deaf1* and *Hsf1* were obtained from Life Technologies (Carlsbad, CA) and inserted into an overexpression, Gateway® ready plasmid containing a chicken

beta actin promoter and a rabbit beta-globin poly T terminator (pCAG). A human *Sp1* ORF missing the initial seven amino acids was obtained from Addgene (plasmid # 12098, Cambridge, MA, deposited by Robert Tjian). The initial seven amino acids were added and the ORF amplified using PCR with the following primers (forward 5'-CACCATGAGCGACCAAGATCACTCCATGGATGAAATGACAGCTGTGG -3' and reverse 5'-CCTGATCTCAGAAGCCATTGCCACTG -3'). The full length *Sp1* ORF was inserted into the pENTR vector and then recombined into the aforementioned Gateway® ready pCAG vector as previously described.

Transfection of HEK293 cells

HEK293T cells were transfected with 0.25 μL / well of and 200 ng of plasmid total Lipofectamine 2000 (catalog #11668-019, Life Technologies, Carlsbad, CA) in 96 well plates. Aliquots of media were taken and assayed and RNA collected at 48 hrs post-transfection as described for primary cells.

Results

In order to identify an appropriate model gene to study RGC regulatory mechanisms, I first selected a set of seven genes that had already been identified as being expressed preferentially in RGCs: neurofilament medium (*Nefm*), neuritin 1 (*Nrn1*), peripherin 1 (*Prph1*), semaphorin 6b (*Sema6b*), solute carrier family 17 (sodium-dependent inorganic phosphate cotransporter), member 6 (*Slc17a6*), synuclein gamma (*Sncg*) and synaptotagmin 11 (*Syt11*) [4, 6-9]. To confirm their degree of preferential expression in primary rodent RGCs, I tested their relative levels of expression in isolated

RGCs compared to whole retina. Figure 1 shows qPCR measurement of the expression of the seven genes in rat RGCs and whole retina. The data illustrate that the genes chosen were all expressed in RGCs and that they were enriched in RGCs in the context of the retina.

In order to choose which of these seven genes to concentrate on for more detailed analysis, I generated and tested promoter reporter constructs for each of the genes. Because many genes contain important regulatory sequences within their 5'-upstream 500 bp region, I focused on this region initially. I created promoter reporter plasmid constructs with the regulatory region of interest upstream of a gene for a secreted luciferase (Gaussia, GLuc). Figure 2 shows the luciferase activity of the promoter reporters for the initial seven genes in RGCs compared to their activity in dissociated whole retinal cells, as well as the ratio of activity between the two cell populations. The promoter reporters demonstrated a range of activity in the two cell populations. Most (*Nrn1*, *Sema6b*, *Slc17a6*, *Sncg* and *Syt11*) showed higher activity in RGCs compared to whole retinal cells, though some of them had very low activity in both cell populations. The *Syt11* promoter reporter showed the highest degree of RGC-specific activity and for this reason, it was chosen for further analysis.

In order to define the active regulatory elements within the upstream region of the *Syt11* promoter, I needed to narrow down the important region. To accomplish this goal, I created a series of GLuc promoter reporters including a sequentially smaller portion of the upstream region (deletion series). The longest construct included a bit more of the upstream region that the original construct (-656 to +136 bp instead of -375 to +76 bp). I used a co-transfected CLuc reporter containing the full length *Syt11* region (-656 to +136

bp) as a transfection control. The analysis (Figure 3) showed that the longer constructs (-656, -553, -490, -373, -336, -270 and -244 bp) had similar activity to each other. However, when the regions between -192 and -101 bp and -101 to -41 bp were deleted, the promoter reporter activity dropped in a stepwise fashion to the same level as the promoter-less GLuc construct indicating the -41, -20, +11 constructs had no transcriptional activity. The -101 to +136 bp construct had an intermediate activity between that of the -192 and -41 bp constructs. Similar results were obtained when the deletion series was tested in mouse RGCs.

In order to try to determine what transcription factors might be binding within the -192 to -41 bp region, I turned to a bioinformatic analysis. Figure 4 shows the 5' upstream region of *Syt11* in the rat genome from the UCSC Genome Browser (http://genome.ucsc.edu/). The regions shown to be important from the deletion series (from -192 to -101 bp and -100 to -41 bp) are bounded by black rectangles. There are several stretches of bases that are conserved across several different species within these two regions, suggesting that there may be conserved transcription factor (TF) binding sites (BSs) (TFBSs). Figure 5 shows the results of the initial MOPAT bioinformatic analysis of the region of interest within the Syt11 promoter (-192 to -41 bp). A number of TFs had predicted binding sites BSs between -192 and -41 bp. Both DEAF1 and SP1 had a predicted BS between -192 and -101 bp and one between -101 and -41 bp, which if they were involved in *Syt11* transcriptional regulation, could explain why there was an incremental decrease in activity when those regions were excluded. One way to test their involvement was to create constructs with these specific TFBSs mutated. For this reason, the predicted binding sites for DEAF1 and SP1, alone and in various combinations, were

mutated in the full length (-656 to +136 bp) construct by introducing transversions for each nucleotide and tested in RGCs. A co-transfected full length, wild type *Syt11* (-656 to +136) CLuc construct was used as a transfection control.

Figure 6 shows the activity of the DEAF1 and SP1 binding site mutants in rat RGCs. All of the mutant constructs had a greater than 32% decrease in activity compared to the unmutated construct. When all four of the sites (both DEAF1s and both SP1s) were mutated in the promoter reporter construct, there was a 75% drop in activity and when both DEAF1 sites were mutated, there was a 71% drop in activity. These results suggested that the sequences including the predicted DEAF1 and to a lesser extent SP1 binding sites had a positive influence over the promoter-reporter activity. In order to specifically test DEAF1 and SP1's involvement in *Syt11* transcriptional regulation, siRNA knockdown (KD) of *Deaf1* and *Sp1* was pursued.

Figure 7 shows the results of *Deaf1* and *Sp1* knockdown in RGCs using pools of four different unmodified siRNA oligonucleotides (oligos). The pools of oligos were specific to their target in the small number of targets measured – in other words *Deaf1* siRNA oligos decreased the level of mRNA of *Deaf1* but not *Sp1* and the same was true of the *Sp1* oligos. However, despite a decrease in *Deaf1* and/or *Sp1* mRNA, there was no change in the *Syt11* mRNA level. Though there was no change in the endogenous *Syt11* mRNA expression with siRNA KD of *Deaf1* and *Sp1*, I wanted to test whether their KD could influence the activity of the *Syt11* promoter reporter. When siRNA KD was combined with *Syt11* promoter reporter transfection (Figure 8), there was a slight decrease in reporter activity at later time points when the pool of oligos targeting *Deaf1* was applied, but no change when the pool of oligos targeting *Sp1* was applied (Figure

8A). The KD of target in the dual transfection was not as efficient as that of siRNA KD alone (Figure 8B), so this may have softened the potential decrease in the promoter reporter activity.

Another way to test whether DEAF1 and SP1 TFs influence the transcriptional regulation of *Syt11* is to over-express them in an immortalized cell line and measure the *Syt11* promoter reporter activity. Figure 9 shows the effect of *Deaf1* and *Sp1* over-expression on the *Syt11* promoter reporter activity in HEK293 cells. The over-expression of *Deaf1* and *Sp1* alone or together, did not alter the promoter reporter activity significantly compared to empty over-expression vector.

Because these results did not support an integral part for DEAF1 or SP1 in the regulation of the transcription activity within the Syt11 promoter, the expression of additional TFs that had predicted BSs based on the original MOPAT analysis was examined with qPCR (Figure 10). These results show that most of the TFs measured had different expression in brain, retina and RGCs with some being more highly expressed in RGCs. Because ELK1, HSF1 and HSF2 all had predicted BSs that overlapped with the DEAF1 and SP1 BSs, I chose to use siRNA to knock down their expression. Pools of siRNAs targeting *Elk1*, *Hsf1* and *Hsf2* were transfected into RGCs using Neuromag. These oligo pools knocked down their target (Figure 11) and had varying effects on the expression of the other targets and *Syt11* measured via qPCR. *Elk1* KD did not affect *Syt11*; however, *Hsf1* KD decreased the expression of *Syt11*. Additionally, *Hsf2* KD decreased the expression of *Hsf1* and increased the expression of *Syt11*. *Hsf1* and *Hsf2* KD both increased the expression of *Elk1*.

To confirm the KD of *Hsf1* and *Hsf2* and the effect on *Syt11* expression, the oligos were tested in a pool and individually (Figure 12). The pools of *Hsf1* and *Hsf2* oligos decreased their target and decreased and increased *Syt11* expression respectively as before. However, individual oligos did not always decrease their target as efficiently as the pool did and those that did decrease their target did not always affect the expression of *Syt11* as the pool did. For example, the Hsf1-4 oligo decreased *Hsf1* expression the most, but had very little effect on *Syt11* expression. Hsf1-1 and Hsf1-2 both decreased *Hsf1* expression somewhat, but did not affect *Syt11* expression. The Hsf1-3 oligo both decreased *Hsf1* expression and decreased *Syt11* expression as the pool did. The Hsf2-1 oligo had a similar effect to the *Hsf2* oligo pool in that it decreased *Hsf2* expression and increased *Syt11* expression the same amount as the pool. Similar to Hsf1-4, Hsf2-2 decreased *Hsf2* expression the most, but did not change *Syt11* expression. This suggests that some of the effects seen might be due to off-target effects. To investigate possible off-target effects, custom oligos were synthesized with the 9^{th}, 10^{th} and 11^{th} bases complemented (C911 oligos) [5] and tested in RGCs.

Figure 13 shows the results of the transfection of rat RGCs with the "wild type" and their corresponding C911 siRNAs targeting *Hsf1* and *Hsf2*. The knockdown of the targets by the individual wild type siRNAs was slightly different than that in Figure 12, but they all decreased their target to varying degrees. Additionally, their effects on Syt11 were similar to that in Figure 12. The C911 oligos, however did not knock down the expression of their targets compared to the wild type siRNAs suggesting the KD of the wild type oligos' targets were all on-target effects. However, with one exception, the effect on *Syt11* expression did not differ between the wild type and its corresponding

C911 siRNA, suggesting that the effects on *Syt11* expression were all off-target. The one C911 siRNA whose effect on *Syt11* differed from that of its corresponding wild type siRNA was Hsf2-1 as the wild type siRNA increased the expression of *Syt11* but the corresponding C911 oligo did not increase *Syt11* expression as much.

As another approach to test HSF1's influence on *Syt11* transcriptional regulation, an over-expression analysis was performed in HEK293 cells. *Hsf1* over-expression in HEK293T cells did not induce endogenous *Syt11* expression as measured by qPCR (Figure 14A), nor did it increase the *Syt11* promoter reporter activity (Figure 14B). These results suggested HSF1 was not involved in *Syt11* transcriptional regulation.

Because none of the previously studied TFs seemed to strongly influence *Syt11* transcriptional regulation, at least when down-regulated in isolation, an additional bioinformatic analysis was performed using the Transfac mouse transcription factor database. An 80% matching threshold was used to compare predicted TFBSs in the DEAF1 and SP1 binding site mutants compared to the wild type construct (Figure 15). Some of these additional TFs with predicted BSs within the region of interest were knocked down with pools of siRNA oligos (Figure 16). Though some of the siRNA yielded partial knockdown (*Ets2*, *Jun* and *Nr2c2*), none of them significantly affected *Syt11* expression.

Supplemental Data

Ethanol has been reported to up-regulate *Syt1* expression through induction of *Hsf1* expression in mouse cortical neurons [10]. To test whether this was true for *Syt11* expression in rat RGCs, I treated RGCs with 0, 20, 60 and 180 mM ethanol for 2 hours

and collected RNA at 4, 8 and 24 hours post-treatment and measured gene expression via qPCR (Figure S1). *Hsf1*, *Hspa1a* and *Syt1*'s expression increased with time in culture, but not in response to ethanol treatment. *Syt11* expression did not change over time or in relation to ethanol treatment.

Clozapine and MK801 have been reported to up- and down-regulate *Syt11* expression in brain respectively [11, 12]. To test whether this was true for rat RGCs, I treated RGCs with DMSO, 0.4, 2 and 10 uM clozapine and 1.2, 6 and 30 uM MK801 and collected RNA after 48 hrs in culture and measured gene expression via qPCR. Neither clozapine nor MK801 consistently altered the expression of Syt11 (Figure S2).

Discussion

The objective of this study was to determine important *cis*-regulatory elements involved in retinal ganglion cell (RGC) gene expression. We performed transient transfection of murine primary RGC cultures using promoter reporters that contained the 5' upstream 500 bases of seven genes known to be expressed in RGCs. From an initial set of seven genes reported to be enriched in RGCs within the retina, based on its preferential activity in RGCs, we chose to concentrate on the *Syt11* promoter.

The results of the initial qPCR comparing the expression of the seven genes in RGCs compared to whole retina (Figure 1) were as expected given these genes were chosen for reportedly being enriched in RGCs within the context of the retina.

Most of the promoter reporters of the original seven genes (*Nrn1*, *Sema6b*, *Slc17a6* and *Sncg*) had overall low activity in both RGCs and whole retinal cells (Figure 2). This is likely because the promoter reporters did not include the region(s) that

conferred robust transcriptional activity or potentially the chromatin context necessary for the function of the regulatory region was not maintained when in a plasmid. Several of the promoter reporters (*Nrn1*, *Sema6b*, *Slc17a6*, *Sncg* and *Syt11*) did have higher activity in RGCs compared to whole retina even though several of them had overall low activity. The high activity of the *Nefm* promoter reporter in whole retinal cells compared to RGCs was surprising given its low expression in whole retina as measured via qPCR. This high level of activity in retina compared to RGCs could be explained by a relatively short promoter region that may not have included RGC-specific TFBSs that might be inhibitory in other retinal cells; however, this was not investigated further. The *Syt11* promoter reporter had the highest activity in RGCs of all of the promoter reporters and also had the highest RGC-specific activity indicating the promoter reporter likely included sequence required for its transcriptional promoting activity in RGCs.

Syt11 belongs to the family of synaptotagmin proteins, which are synaptic proteins involved in vesicle release and recycling [13]. To date, sixteen different synaptotagmins have been identified in the human genome [14]. Most synaptotagmins are calcium sensors and initiate vesicle fusion by interacting with SNARE proteins when calcium is present [15]; however, *Syt11* and *Syt4* both have altered calcium binding domains, which precludes their calcium binding abilities [16]. *Syt11* has specifically been studied in a neuronal context regarding schizophrenia [17] and parkinson's disease [18]; however, it has not been reported to be involved in RGC biology.

The *Syt11* promoter has a sequence with homology to a typical TATA box (TATATAAA) located at -381 to -374; however, its position is unusual. According to the accepted/published *Syt11* transcriptional start site, this likely does not fulfill the role of a

traditional TATA box, which would be typically located approximately from -31 to -26 [19]. It also has what could be considered an Initiator (CCAGTCT) located at -22 to -16, but this location is not at the typical -2 to +4 location of true Initiators. The *Syt11* promoter has three possible Downstream Promoter Elements (DPEs) as follows: GGATC from +54 to +58 bp, AGTCG from +75 to +79 bp and AGTTG from +150 to +154 bp. DPEs are typically found in promoters that lack a TATA box, however they are typically located +28 to +32 bp relative to the A_{+1} nucleotide in the Initiator motif and they typically act in concert with an Initiator sequence [19], which the *Syt11* promoter does not possess.

The results of the *Syt11* promoter deletion series (Figure 3) suggested that the region between -192 and -41 bp contained sequences that are important for the promoter activity of the promoter reporter and likely contained binding sites for important transcription factors. Conservation of promoter sequences across evolution can be helpful in defining regulatory elements. However, since there is only limited conservation of the region between -192 to -101 bp (UCSC Genome Browser) (Figure 4), this approach was not helpful in identifying the regulatory *Syt11* elements.

The initial MOPAT analysis identified DEAF1 and SP1, among others (Figure 5), as possible candidate transcription factors important for *Syt11* transcriptional regulation, which was supported by the binding site mutagenesis in which mutation of any of the DEAF1 or SP1 predicted BS sequence decreased the promoter reporter activity (Figure 6). DEAF1 is a transcription factor whose altered expression has been linked to a number of diseases and conditions including depression and suicide [20-22], intellectual disability [23], neoplasia [24, 25], neural tube defects [26] and immune disorders [27]; however,

nothing has been published about its expression in RGCs. *Sp1* is a widely expressed gene involved in the transcriptional regulation of many genes [28, 29]. *Sp1* has been shown to be expressed in RGCs and may play a role in the differential gene regulation in small *versus* large RGCs [30]. SP1's role in transcriptional regulation of *Syt11* has been investigated previously in the context of CpG methylation [31]. SP1 and DEAF1, together, have been linked in the transcriptional regulation of *Gdf5*, which is implicated in musculoskeletal development [32].

siRNA KD of *Deaf1* and *Sp1* alone or in combination did not alter *Syt11*'s expression level (Figure 7). Though the knockdown of *Deaf1* slightly decreased the *Syt11* promoter reporter activity (Figure 8), the over-expression of *Deaf1* in HEK293 cells only marginally increased the *Syt11* promoter reporter activity. The most supportive evidence of DEAF1 and SP1 playing a role in *Syt11*'s transcriptional regulation came from the mutagenesis assay, which implicated a role for their putative binding sites; however, because it is possible that the mutation of the predicted DEAF1 and SP1 binding sites in the promoter reporter construct affected important sequences for other transcription factor binding, the siRNA KD of additional predicted TFs was pursued.

TFs that had predicted binding sites that overlapped with the DEAF1 and SP1 sites that were mutated included HSF1, HSF2, ELK1, GATA1 and ETF (Figure 5). HSF1 and HSF2 (heat shock factors) are transcription factors involved in the transcriptional regulation of heat shock proteins, which are chaperone proteins involved in cellular stress responses[33, 34]. Both *Hsf1* and *Hsf2* are expressed in RGCs and have been implicated in the response to various induced cellular stresses [35, 36]. However, in drosophila, HSF1 binding sites are more often than not located in genes that are not involved in heat

shock response [37]. ELK1 is a member of the ternary complex factor subfamily and is involved in the c-fos pathway among others [38-41].

Knockdown of *Hsf1*, *Hsf2* and *Elk1* was successful, however only KD of *Hsf1* and *Hsf2* altered the expression of *Syt11* (Figure 11). When tested separately, however, the individual siRNAs targeting *Hsf1* and *Hsf2* did not always act as the pool did (Figure 12). This suggests that off-target effects may have played a role in producing the observed effects on *Syt11* expression. For this reason, an attempt to tease out the possible off-target effects was done by testing the ability of siRNAs for *Hsf1* and *Hsf2* that had the 9^{th}, 10^{th} and 11^{th} bases complemented [5] to decrease *Syt11*'s expression (Figure 13).

The results of the C911 analysis overall suggest that the knockdown effect of the individual wild type siRNAs on their specific target (*Hsf1* or *Hsf2*) were, in fact, on-target effects because the C911 oligos did not affect their targets as the wild type siRNAs did. However, with one exception (Hsf2-1), the effect on *Syt11* expression did not differ between the wild type and its corresponding C911 siRNA, which overall suggests that the effects on *Syt11* expression are off-target effects. HSF1 is likely not involved in the transcriptional regulation of *Syt11* evidenced by the fact that only one of the four siRNA oligos decreased its expression when tested individually and the mutated C911 oligos had the same effect on *Syt11*'s expression as the wild type ones did. HSF2's involvement is unclear since only one of the two oligos tested influenced *Syt11*'s expression and one of the C911 oligos did not increase *Syt11*'s expression to the same degree as its corresponding wild type oligo.

Two other attempts to find supporting evidence that HSF1 influences the transcription of *Syt11* included over-expression of *Hsf1* in HEK293 cells (Figure 14) and

ethanol treatment of RGCs (Figure S1). The over-expression of *Hsf1* did not cause higher activity of the *Syt11* promoter reporter, nor did it induce the endogenous expression of *Hsf1* measured via qPCR in HEK293 cells (Figure 14). Additionally, time in culture but not ethanol treatment increased *Hsf1* expression, but *Syt11* expression was unaffected in the experiment by any parameter, suggesting HSF1 is not involved in the transcriptional regulation of *Syt11*.

Syt11 was reported to be up-regulated in brain with systemic treatment of clozapine and down regulated when treated with MK801 [11, 12]. Clozapine at 0.4 and 2 μM did up-regulate *Syt11* compared to both DMSO and untreated and 1.2 μM MK801 treatment did down-regulate *Syt11* expression, but the higher doses either had no effect, or increased it compared to the DMSO-treated and untreated RGCs (Figure S2). These results could be a reflection of a truncated dosage response curve with some doses having the predicted effect. Additionally, these results may reflect similarities between RGCs and cortical neurons.

An additional bioinformatic analysis of the *Syt11* promoter region suggested that GABPAa and other TFs might be involved in the transcriptional regulation of *Syt11* (Figure 15). However, KD of *Gabpa* was unsuccessful so its influence on *Syt11*'s expression could not be elucidated. The siRNA KD of the other potentially involved TFs (ETS2, JUN and NR2C2), though variably successful, did not influence *Syt11* expression, suggesting they are not involved in *Syt11* transcriptional regulation (Figure 16).

Though these results are interesting and suggest that the sequence from -192 to -41 bp contains important sequence for *Syt11*'s promoter activity, our siRNA experiments were inconclusive in identifying the specific TFs that regulate *Syt11* transcription in

RGCs. It is possible that some of the identified TFs could work in concert to affect *Syt11*'s expression and when examined individually, these effects were not apparent. Future studies to further investigate the transcriptional regulation of *Syt11* include additional bioinformatic analyses to identify potentially involved transcription factors. An unbiased scanning mutagenesis assay of the entire region of interest could help to identify subregions that convey promoter activity, which would allow a more detailed bioinformatic analysis. Use of CRISPR-mediated knockdown of candidate TFs could provide another experimental approach that might be more powerful and more specific than the siRNA approach that we employed.

References

1. Barres, B.A., et al., *Immunological, morphological, and electrophysiological variation among retinal ganglion cells purified by panning.* Neuron, 1988. **1**(9): p. 791-803.
2. Vandesompele, J., et al., *Accurate normalization of real-time quantitative RT-PCR data by geometric averaging of multiple internal control genes.* Genome Biol, 2002. **3**(7): p. Research0034.
3. Hu, J., H. Hu, and X. Li, *MOPAT: a graph-based method to predict recurrent cis-regulatory modules from known motifs.* Nucleic Acids Res, 2008. **36**(13): p. 4488-97.
4. Yang, Z., et al., *Changes in gene expression in experimental glaucoma and optic nerve transection: the equilibrium between protective and detrimental mechanisms.* Invest Ophthalmol Vis Sci, 2007. **48**(12): p. 5539-48.
5. Buehler, E., Y.C. Chen, and S. Martin, *C911: A bench-level control for sequence specific siRNA off-target effects.* PLoS One, 2012. **7**(12): p. e51942.
6. Kim, C.Y., et al., *Gene expression profile of the adult human retinal ganglion cell layer.* Mol Vis, 2006. **12**: p. 1640-8.
7. Ivanov, D., et al., *Microarray analysis of gene expression in adult retinal ganglion cells.* FEBS Lett, 2006. **580**(1): p. 331-5.
8. Ahmed, F., et al., *Microarray analysis of changes in mRNA levels in the rat retina after experimental elevation of intraocular pressure.* Invest Ophthalmol Vis Sci, 2004. **45**(4): p. 1247-58.

9. Wang, D.Y., et al., *Global gene expression changes in rat retinal ganglion cells in experimental glaucoma.* Invest Ophthalmol Vis Sci, 2010. **51**(8): p. 4084-95.

10. Varodayan, F.P., L. Pignataro, and N.L. Harrison, *Alcohol induces synaptotagmin 1 expression in neurons via activation of heat shock factor 1.* Neuroscience, 2011. **193**: p. 63-71.

11. Kontkanen, O., et al., *Antipsychotic drug treatment induces differential gene expression in the rat cortex.* J Neurochem, 2002. **83**(5): p. 1043-53.

12. Paulson, L., et al., *Comparative genome- and proteome analysis of cerebral cortex from MK-801-treated rats.* J Neurosci Res, 2003. **71**(4): p. 526-33.

13. Schwarz, T.L., *Synaptotagmin promotes both vesicle fusion and recycling.* Proc Natl Acad Sci U S A, 2004. **101**(47): p. 16401-2.

14. Craxton, M., *Synaptotagmin gene content of the sequenced genomes.* BMC Genomics, 2004. **5**(1): p. 43.

15. Sudhof, T.C., *Calcium control of neurotransmitter release.* Cold Spring Harb Perspect Biol, 2012. **4**(1): p. a011353.

16. von Poser, C., et al., *The evolutionary pressure to inactivate. A subclass of synaptotagmins with an amino acid substitution that abolishes Ca2+ binding.* J Biol Chem, 1997. **272**(22): p. 14314-9.

17. Inoue, S., et al., *Synaptotagmin XI as a candidate gene for susceptibility to schizophrenia.* Am J Med Genet B Neuropsychiatr Genet, 2007. **144b**(3): p. 332-40.

18. Huynh, D.P., et al., *The autosomal recessive juvenile Parkinson disease gene product, parkin, interacts with and ubiquitinates synaptotagmin XI.* Hum Mol Genet, 2003. **12**(20): p. 2587-97.

19. Smale, S.T. and J.T. Kadonaga, *The RNA polymerase II core promoter.* Annu Rev Biochem, 2003. **72**: p. 449-79.

20. Albert, P.R., F. Vahid-Ansari, and C. Luckhart, *Serotonin-prefrontal cortical circuitry in anxiety and depression phenotypes: pivotal role of pre- and post-synaptic 5-HT1A receptor expression.* Front Behav Neurosci, 2014. **8**: p. 199.

21. Lemonde, S., et al., *Impaired repression at a 5-hydroxytryptamine 1A receptor gene polymorphism associated with major depression and suicide.* J Neurosci, 2003. **23**(25): p. 8788-99.

22. Szewczyk, B., et al., *Gender-specific decrease in NUDR and 5-HT1A receptor proteins in the prefrontal cortex of subjects with major depressive disorder.* Int J Neuropsychopharmacol, 2009. **12**(2): p. 155-68.

23. Vulto-van Silfhout, A.T., et al., *Mutations affecting the SAND domain of DEAF1 cause intellectual disability with severe speech impairment and behavioral problems.* Am J Hum Genet, 2014. **94**(5): p. 649-61.

24. Barker, H.E., et al., *Deaf-1 regulates epithelial cell proliferation and side-branching in the mammary gland.* BMC Dev Biol, 2008. **8**: p. 94.

25. Manne, U., et al., *Altered subcellular localization of suppressin, a novel inhibitor of cell-cycle entry, is an independent prognostic factor in colorectal adenocarcinomas.* Clin Cancer Res, 2001. **7**(11): p. 3495-503.

26. Hahm, K., et al., *Defective neural tube closure and anteroposterior patterning in mice lacking the LIM protein LMO4 or its interacting partner Deaf-1.* Mol Cell Biol, 2004. **24**(5): p. 2074-82.

27. Yip, L., et al., *Deaf1 isoforms control the expression of genes encoding peripheral tissue antigens in the pancreatic lymph nodes during type 1 diabetes.* Nat Immunol, 2009. **10**(9): p. 1026-33.

28. Li, L., et al., *Gene regulation by Sp1 and Sp3.* Biochem Cell Biol, 2004. **82**(4): p. 460-71.

29. Suske, G., *The Sp-family of transcription factors.* Gene, 1999. **238**(2): p. 291-300.

30. Ivanov, D., et al., *Differential gene expression profiling of large and small retinal ganglion cells.* J Neurosci Methods, 2008. **174**(1): p. 10-7.

31. Inoue, S. and M. Oishi, *Effects of methylation of non-CpG sequence in the promoter region on the expression of human synaptotagmin XI (syt11).* Gene, 2005. **348**: p. 123-34.

32. Reynard, L.N., et al., *CpG methylation regulates allelic expression of GDF5 by modulating binding of SP1 and SP3 repressor proteins to the osteoarthritis susceptibility SNP rs143383.* Hum Genet, 2014. **133**(8): p. 1059-73.

33. Vihervaara, A. and L. Sistonen, *HSF1 at a glance.* J Cell Sci, 2014. **127**(Pt 2): p. 261-6.

34. Fujimoto, M. and A. Nakai, *The heat shock factor family and adaptation to proteotoxic stress.* Febs j, 2010. **277**(20): p. 4112-25.

35. Kwong, J.M., et al., *Co-expression of heat shock transcription factors 1 and 2 in rat retinal ganglion cells.* Neurosci Lett, 2006. **405**(3): p. 191-5.

36. Ahn, J., et al., *Expression of heat shock transcription factors and heat shock protein 72 in rat retina after intravitreal injection of low dose N-methyl-D-aspartate.* Neurosci Lett, 2008. **433**(1): p. 11-6.

37. Gonsalves, S.E., et al., *Whole-genome analysis reveals that active heat shock factor binding sites are mostly associated with non-heat shock genes in Drosophila melanogaster.* PLoS One, 2011. **6**(1): p. e15934.

38. Cohen-Armon, M., *PARP-1 activation in the ERK signaling pathway.* Trends Pharmacol Sci, 2007. **28**(11): p. 556-60.

39. Shaw, P.E. and J. Saxton, *Ternary complex factors: prime nuclear targets for mitogen-activated protein kinases.* Int J Biochem Cell Biol, 2003. **35**(8): p. 1210-26.

40. Odrowaz, Z. and A.D. Sharrocks, *ELK1 uses different DNA binding modes to regulate functionally distinct classes of target genes.* PLoS Genet, 2012. **8**(5): p. e1002694.

41. Sharrocks, A.D., *Complexities in ETS-domain transcription factor function and regulation: lessons from the TCF (ternary complex factor) subfamily. The Colworth Medal Lecture.* Biochem Soc Trans, 2002. **30**(2): p. 1-9.

Figures

Gene	Forward Primer	Reverse Primer	Regions included	Length (# bases)
Nefm	Synthesized by GenScript		-424 to +76	450
Nrn1	Synthesized by GenScript		-473 to +76	450
Prph1	Synthesized by GenScript		-423 to +27	450
Sema6b	Synthesized by GenScript		-473 to +76	450
Slc17a6	GGGGACAAGTTTG TACAAAAAAGCAG GCTTCTGTCCGTGG TGCTGAAATGCTA	AGGCGAGTTCTGC GCATAGTCTTAGGG GACCACTTTGTACA AGAAAGCTGGGT	-312 to +408	720
Sncg	Synthesized by GenScript		-404 to +45	450
Syt11	Synthesized by GenScript		-375 to +76	450

Table 1. Construction of initial seven promoter reporters. Most of the promoter reporters were created with synthesized fragments of the promoter region (*Nefm*, *Nrn1*, *Prph1*, *Sema6b*, *Sncg*, *Syt11*) and included 450 bases of the upstream region. The sequences submitted for synthesis were obtained from the UCSC Genome Browser for each of the genes. The promoter reporter for *Slc17a6* was created by amplifying a region upstream of the *Slc17a6* gene from genomic DNA from a Sprague-Dawley rat with PCR using the primer sequences listed above.

Deletion mutant	Forward Primer	Reverse primer	Region included (bp)	# bases
Syt11 del 1	CACCAACATGGACCA ACACTGCCCAGAA	TTGGAAATCTCGAT CAGTACCGAGGC	-656 to +136	792
Syt11 del 2	CACCAATCGTCATGC TTCTGCCCAGGAT	TTGGAAATCTCGAT CAGTACCGAGGC	-553 to +136	689
Syt11 del 3	CACCTCCCTTTACTGT TTCAGGAGTGCT	TTGGAAATCTCGAT CAGTACCGAGGC	-490 to +136	626
Syt11 del 4	CACCCCCAGGCAACA AGAATTACAGCTTC	TTGGAAATCTCGAT CAGTACCGAGGC	-373 to +136	509
Syt11 del 5	CACCAGCGACTATCT TCCTCCCTTCTGT	TTGGAAATCTCGAT CAGTACCGAGGC	-336 to +136	472
Syt11 del 6	CACCACCCACTCGAC TGCTATAGTCACA	TTGGAAATCTCGAT CAGTACCGAGGC	-270 to +136	406
Syt11 del 7	CACCGGAATGTGTGA CTGAGCTAGCAGT	TTGGAAATCTCGAT CAGTACCGAGGC	-244 to +136	380
Syt11 del 8	CACCAATTCTAGCCA CAAACGCCCACAG	TTGGAAATCTCGAT CAGTACCGAGGC	-192 to +136	328
Syt11 del 9	CACCTTCCGGAATCTT TCGGGCAGA	TTGGAAATCTCGAT CAGTACCGAGGC	-101 to +136	237
Syt11 del 10	CACCAGCCTATGTCTC ATCAGGACCAGT	TTGGAAATCTCGAT CAGTACCGAGGC	-41 to +136	177
Syt11 del 11	CACCAGTCTGACTGC ACCTGCATCCTTA	TTGGAAATCTCGAT CAGTACCGAGGC	-20 to +136	56
Syt11 del 12	CACCAGCATCCCTGG AGCATCTAAGAGA	TTGGAAATCTCGAT CAGTACCGAGGC	+11 to +136	25

Table 2. Primers used to amplify *Syt11* promoter fragments for the creation of the deletion series. A series of 12 deletion mutants were created by amplifying progressively smaller regions of the promoter series from genomic DNA from a Sprague-Dawley rat. Forward primers include CACC- overhang necessary for directional cloning into pENTR. The same reverse primer was used for all constructs.

Forward Primer	Reverse Primer	Site Mutated
GGGAATGGGCGGAGCCTC TGAGGATTTCAAACTCGG CAGTGGG	CCCACTGCCGAGTTTGAAA TCCTCAGAGGCTCCGCCCA TTCCC	1st half of 1st DEAF1
AGCCTCTGAGGATTTCCC CAGATTACTTGGGAGGGG TCTTCTC	GAGAAGACCCCTCCCAAG TAATCTGGGGAAATCCTCA GAGGCT	2nd half of 1st DEAF1
TTCCCCAGATTACTTGGG CTTTTGCTTCTCTCGAAGA GCTTCC	GGAAGCTCTTCGAGAGAA GCAAAAGCCCAAGTAATC TGGGGAA	1st SP1 with 1st DEAF1
GGCTTTTGCTTCTCTCGAA TCTAGGAATTCATCTTTCG GGCAGAGGCG	CGCCTCTGCCCGAAAGAT GAATTCCTAGATTCGAGA GAAGCAAAAGCC	1st half of 2nd DEAF1 with 1st DEAF1 and 1st SP1
TCGAATCTAGGAATTCCG AGGGATTTAAGAGGCGGA GTCTTCT	AGAAGACTCCGCCTCTTAA ATCCCTCGGAATTCCTAGA TTCGA	2nd half of 2nd DEAF1 with 1st DEAF1 and 1st SP1
CCGAATGGCCCTCGGCAG ACTCAGAATAATCTTAAA TCCCTCGGAATTCC	GGAATTCCGAGGGATTTA AGATTATTCTGAGTCTGCC GAGGGCCATTCGG	2nd SP1 with 2nd DEAF1, 1st SP1 and 1st DEAF1
GGGGTCTTCTCTCGAATCT AGGAATTCATCTTTCGGG CAGAGG	CCTCTGCCCGAAAGATGA ATTCCTAGATTCGAGAGA AGACCCC	1st half of 2nd DEAF1
TCGAATCTAGGAATTCCG AGGGATTTAAGAGGCGGA GTCTTCT	AGAAGACTCCGCCTCTTAA ATCCCTCGGAATTCCTAGA TTCGA	2nd half of 2nd DEAF1
CTCGGCAGTGGGCTTTTG CTTCTCTCGAAGAGC	GCTCTTCGAGAGAAGCAA AAGCCCACTGCCGAG	1st SP1 alone
GGAATCTTTCGGGCAGAT TATTCTGAGTCTGCCGAG GGCCATT	AATGGCCCTCGGCAGACT CAGAATAATCTGCCCGAA AGATTCC	2nd SP1 alone
TCCGAGGGATTTAAGATT ATTCTGAGTCTGCCGAGG GCCATTC	GAATGGCCCTCGGCAGAC TCAGAATAATCTTAAATCC CTCGGA	2nd SP1 with 2nd DEAF1

Table 3. Primers for site directed mutagenesis of *Syt11* promoter reporter.

Transcription factor binding site mutants were created for DEAF1 and SP1 within the upstream region of *Syt11* using site directed mutagenesis within the full length construct

created for the deletion series (-656 to + 136 bp). Because of the length of some the DEAF1 binding sites, they were mutated in two steps.

Table 4: qPCR primers		
Species & Gene	**Forward Primer**	**Reverse Primer**
Rat *Gapdh*	ATGATTCTACCCACGGCAAG	CTGGAAGATGGTGATGGGTT
Rat *Hprt1*	GCGAAAGTGGAAAAGCCAAGT	GCCACATCAACAGGACTCTTGTAG
Rat *Hmbs*	TCTAGATGGCTCAGATAGCATGCA	TGGACCATCTTCTTGCTGAACA
Rat *Nefm*	ACCTCTGCAAAAGTGTTTCTATCA	CCGCTACTGGTGACACATCA
Rat *Nrn1*	CGTCATTTGCGAGAATACCA	TCTTCACCCTCCAGTAGTTTCC
Rat *Prph1*	GCCGGAAGATGGTTCTGAT	GCTGCTCCTTCTGAGACTCTGT
Rat *Sema6b*	GGTCACCCATGGCCTTTT	TAGTCCCTGGGAGCCACA
Rat *Slc17a6*	GATTCCGGGCGGATACAT	TATGGCAGCCCCAAAGAC
Rat *Sncg*	CACCACCGGGGTAGTACG	CGCCCTCCTCTTGCTCTT
Rat *Syt11*	ACCTCTGCAAAAGTGTTTCTATCA	CCGCTACTGGTGACACATCA
Rat *Deaf1*	GTGACCCAGGCGAGAATG	GCCGCAGTTGACACATGA
Rat *Sp1*	GCTATAGCAAACACCCCAGGT	CAGGGCTGTTCTCTCCTTCTT
Rat *Hsf1*	GAAAGATCCCTCTGATGTTGAG	CTGGAGATGGAGCTGAGTAT
Rat *Hsf2*	TGCTCTCAGGAAGACAGTTTAGC	GGTAGCTTCTAATCCCTTATTCTCAG
Rat *Elk1*	CACCAGTCCAAACCCCTTAG	TCAACTCTTCAGATTTCTGGTTTG
Rat *Gabpa*	GGTTGCCCACATTCCCAAAC	TCCTGCCAAACTTGCTCCAT
Rat *Creb*	GACGGAGGAGCTTGTACCAC	GCATCTCCACTCTGCTGGTT
Rat *Ebf1*	CAGCTGCCAACTCACCCTA	GGGGAGGCTTGTAGATGAGG
Rat *Gata1*	TGCTGAACCTTCTGCATCAA	GGGCAAGGGTTCTGAGGT
Rat *Hnf4a*	AGCAATGGACAGATGTGTGAGT	AGATCCAGAGCCACTTGGTG
Rat *Jun*	GCCACCGAGACCGTAAAG	CTGTGCGAGCTGGTATGAGT
Rat *NfkB*	ACTGCTCAGGCCCACTTG	TGTCATTATCTCGGAGCTCATCT
Rat *Nfyc*	TGAAACTGGATGAAGATGTGAAG	CAGGCTCGAAGAGTCAGCTC
Rat *Pbx1*	GCCAGACAGGAGGATACAGTG	CTGCCAACCTCCATTAGCAC
Rat *Rreb1*	ACCTCACACGGCACATGA	CGCAGGTCTGACACTTGTATG
Rat *Sf1*	CGTAAACTGCGCACAGGA	GATTGGCTCAGGGGAAGG
Rat *Tcf4*	AAAAGTTCCTCCAGGCTTGC	TCCCTGTTGTAGTCGGCAGT
Rat *Tp53*	AGAGAGCACTGCCCACCA	AACATCTCGAAGCGCTCAC
Rat *Zfp384*	CCAAGCCCTACAACTGTTCC	TTGTATGGTCTATCGCCAGTGT
Rat *Hmga1*	TGAAGTGCCAACCCCGAA	CTCCTCTTCCTCCTTCTCC
Rat *Nr2c2*	CACCTCAGCGCATTCAGA	TGCTGTTTAGAGGATCCAGAGG
Rat *Ets2*	CACAATCGTTGTGGCTATTTG	GTTTGTGTATCCACCACATGCT
Rat *Tcfcp2*	GAATCCGGCTCTTCAACG	CGTCCTCCTGCTTCTGCT
Mouse *Deaf1*	GCCACTGCTGTCATCTCTGA	CACACCTGCCTCTTGCACT

Mouse *Sp1*	ATGCCCCTATTGCAAAGACA	TGGATGTGACAAATGTGCTGT
Mouse *Syt11*	AGTGTTTCTATCAACAGCCTC TGA	CCGCTACCGGTGACACAT
Mouse *Gapdh*	CTCCCACTCTTCCACCTTCG	CCACCACCCTGTTGCTGTAG
Mouse *Hprt*	CCTCCTCAGACCGCTTTTT	AACCTGGTTCATCATCGCTAA
Mouse *Hmbs*	TCCCTGAAGGATGTGCCTAC	AAGGGTTTTCCCGTTTGC
Mouse *Actb*	CTAAGGCCAACCGTGAAAAG	ACCAGAGGCATACAGGGACA
Human *SYT11*	ACCAATATCCGACCTAGCTTT G	GACACACACCACCAGCACA
Human *HSF1* (endogenous)	CAAGCTGTGGACCCTCGT	TCGAACACGTGGAAGCTGT
Human *HSF1* (exogenous)	CTCGGAGCCTCCCAAAG	ATTCACTCCTCAGGTGCA
Human *GAPDH*	TGCACCACCAACTGCTTAGC	GGCATGGACTGTGGTCATGAG
Human *HPRT1*	TGACACTGGCAAAACAATGCA	GGTCCTTTTCACCAGCAAGCT
Human *HMBS*	GGCAATGCGGCTGCAA	GGGTACCCACGCGAATCAC

Table 4. qPCR primers. Primers sequences came from RT Primer database (http://medgen.ugent.be/rtprimerdb/) or designed with Roche's primer design algorithm (http://lifescience.roche.com/shop/CategoryDisplay?catalogId=10001&tab=Assay+Design+Center&identifier=Universal+Probe+Library&langId=-1#tab-3).

Gene & Species	Company	Product	Product #	Modified or unmodified	Sequence
Deaf1 Rat	Dharmacon	siGENOME	D09674201	Unmodified	GUACAGCCCAA CCGAGUUU
Deaf1 Rat	Dharmacon	siGENOME	D09674202	Unmodified	GCGAUGACAUG ACUCUAAG
Deaf1 Rat	Dharmacon	siGENOME	D09674203	Unmodified	AGAAAGGUGGU ACCAAGUA
Deaf1 Rat	Dharmacon	siGENOME	D09674204	Unmodified	CAGAUAACGUC UUCACAAC
Sp1 Rat	Dharmacon	siGENOME	D09001201	Unmodified	GCAAGGGUCUG AUUCUCUA
Sp1 Rat	Dharmacon	siGENOME	D09001202	Unmodified	GAGGAGCGAUC AUCUGUCA
Sp1 Rat	Dharmacon	siGENOME	D09001203	Unmodified	GAUCAUACCAG GUGCAAAU
Sp1 Rat	Dharmacon	siGENOME	D09001204	Unmodified	CCAAGGAUGCG GCAAAGUA
Deaf1 Mouse	Dharmacon	siGENOME	D04394701	Unmodified	GCAGAUAACGU CUUCACAA
Deaf1 Mouse	Dharmacon	siGENOME	D04394702	Unmodified	CAACUCCAGUG AAGAAGGA
Deaf1 Mouse	Dharmacon	siGENOME	D04394703	Unmodified	GGCAAACGCAG CAUCGAUA
Deaf1 Mouse	Dharmacon	siGENOME	D04394704	Unmodified	GGAUAUGGGUA CCGAGGCU
Sp1 Mouse	Dharmacon	siGENOME	D04063305	Unmodified	GAACAGAGUGG CAACAGUA
Sp1 Mouse	Dharmacon	siGENOME	D04063306	Unmodified	GGAUGGUUCUG GUCAAAUA
Sp1 Mouse	Dharmacon	siGENOME	D04063307	Unmodified	GAAUAGCUCUG AUCUCCAA
Sp1 Mouse	Dharmacon	siGENOME	D04063308	Unmodified	GCAAGGAAGUC AGCAGAAA
Elk1 Rat	Dharmacon	ONTARGE Tplus	J09542209	Modified	CCAAGGUGGCU UAGCACGA
Elk1 Rat	Dharmacon	ONTARGE Tplus	J09542210	Modified	CCAGGGAGCAC UUGUACGA
Elk1 Rat	Dharmacon	ONTARGE Tplus	J09542211	Modified	CCAAGGACCCG AACGGACU
Elk1 Rat	Dharmacon	ONTARGE Tplus	J09542212	Modified	GGAAUGAAUAC AUGCGCUC
Hsf1 Rat	Dharmacon	ONTARGE Tplus	J08101013	Modified	CCUCAUAGCCC UCGGGUAC
Hsf1 Rat	Dharmacon	ONTARGE Tplus	J08101014	Modified	GAGAAGUGCCU CAGCGUAG
Hsf1 Rat	Dharmacon	ONTARGE Tplus	J08101015	Modified	GAAUAGUAACG CCGACUCA
Hsf1 Rat	Dharmacon	ONTARGE Tplus	J08101016	Modified	GGCCCAUAAUC UCCGAUAU

Hsf2 Rat	Ambion	Silencer	62257	Unmodified	GGAAAGAGAUG GCCCUGUUtt
Hsf2 Rat	Ambion	Silencer	158144	Unmodified	CGAGUUCAUCA CCUGGAGUtt
Hsf1 Rat C911	Ambion	Silencer	Custom	Unmodified	CCTCATAGGGG TCGGGTACtt
Hsf1 Rat C911	Ambion	Silencer	Custom	Unmodified	GAGAAGTGGGA CAGCGTAGtt
Hsf1 Rat C911	Ambion	Silencer	Custom	Unmodified	GAATAGTATGC CCGACTCAtt
Hsf1 Rat C911	Ambion	Silencer	Custom	Unmodified	GGCCCATATAG TCCGATATtt
Hsf2 Rat C911	Ambion	Silencer	Custom	Unmodified	CGAGTTCAAGT CCTGGAGTtt
Hsf2 Rat C911	Ambion	Silencer	Custom	Unmodified	GGAAAGAGTAC GCCCTGTTtt
Gabpa Rat	Ambion	Silencer	61785	Unmodified	GGUAAUUUCUU ACCAAGGAtt
Gabpa Rat	Ambion	Silencer	61700	Unmodified	GGAGUGAAAAC AGAUGGGAtt
Gabpa Rat	Ambion	Silencer	61610	Unmodified	GGCCAUAGACA UCAAUGAAtt
Gabpa Rat	Ambion	Silencer	157638	Unmodified	GCAUUGUGGAA CAAACCUAtt
Nr2c2 Rat	Ambion	Silencer	261089	Unmodified	GGAGGGAGUAU CCAUGUCAtt
Nr2c2 Rat	Ambion	Silencer	261088	Unmodified	GCGCAUUCAGA UUGUAACAtt
Nr2c2 Rat	Ambion	Silencer	261087	Unmodified	GCUAUAGUUCU CUUUAGUCtt
Ets2 Rat	Ambion	Silencer	70249	Unmodified	GGCUCCAUAUG GAAUGCAGtt
Tcfcp2 Rat	Ambion	Silencer	85381	Unmodified	GGACAUCUGUG UUUAUUCAtt
Tcfcp2 Rat	Ambion	Silencer	85191	Unmodified	GGACAGUCUUA UGAAAUCCtt
Jun Rat	Ambion	Silencer	155944	Unmodified	CGAUGGACUUU UCGUUAACtt
Jun Rat	Ambion	Silencer	67634	Unmodified	GGAAAAAGUGA AAACCUUGtt
Jun Rat	Ambion	Silencer	67730	Unmodified	GGGUACACAAG AUGGACUGtt

Table 5. siRNAs used to knockdown the expression of specific transcripts in mouse and rat RGCs. Multiple siRNA oligos for each transcript were used when available.

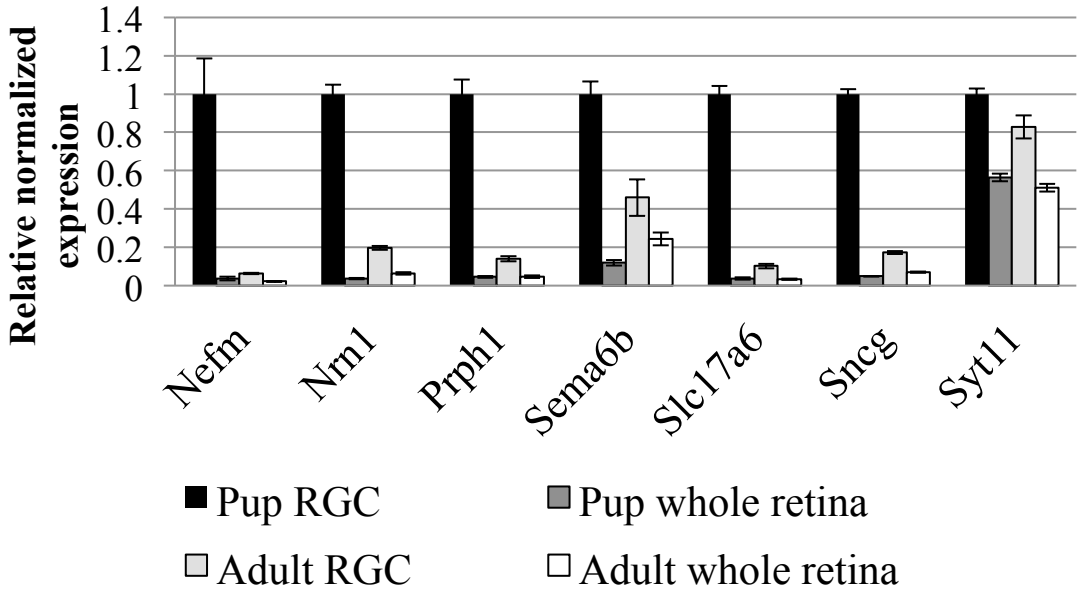

Figure 1. Expression of original 7 genes in adult and rat pup retina and RGCs. The originally chosen seven genes have higher expression in rat RGCs compared to rat whole retina and were higher in RGCs from pups than adult RGCs. The seven genes chosen for initial promoter analysis were measured via qPCR in immunopanned rat RGCs and dissociated whole retinal cells. Expression of target genes was normalized to the geometric mean of three reference genes: *Gapdh*, *Hprt1* and *Hmbs* and then to the Pup RGC sample. Bars represent the average of technical triplicates with standard errors of the mean.

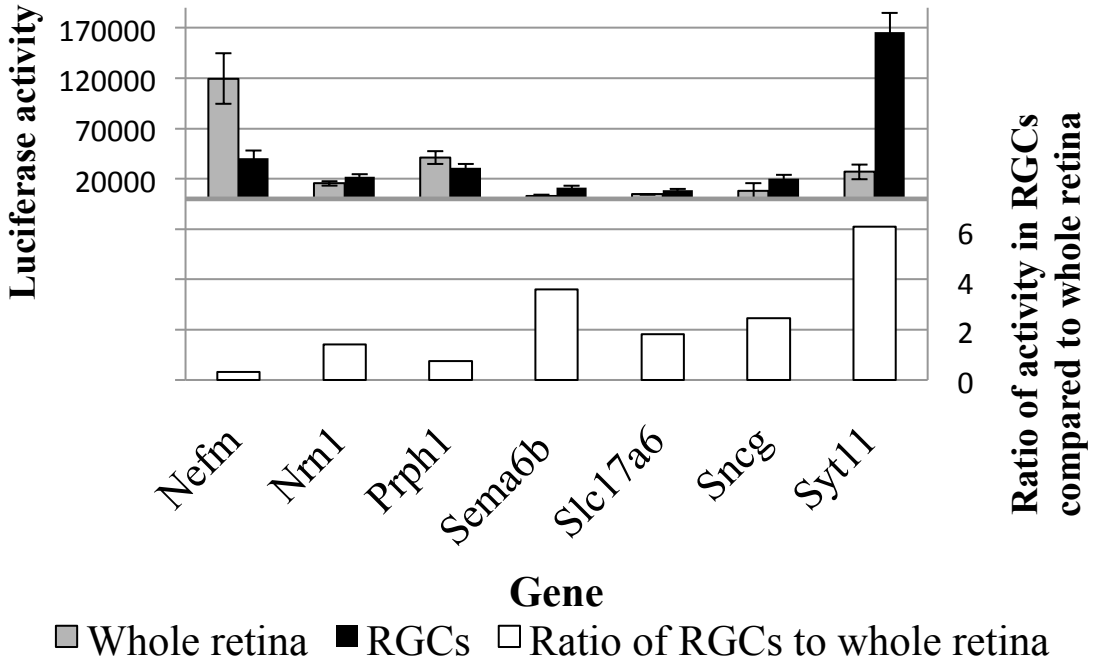

Figure 2. Activities of initial promoter reporters. The initial set of promoter reporters have different activity in RGCs compared to whole retina. Most promoter reporters have higher activity in RGCs, though most have low activity overall. The Nefm promoter reporter has higher activity in whole retina compared to RGCs. The *Syt11* promoter reporter has higher activity in RGCs compared to whole retina. Error bars display the standard deviations. Length of constructs: *Nefm* (-424 to +76 bp), *Nrn1* (-473 to +76 bp), *Prph1* (-423 to +23 bp), *Sema6b* (-473 to +76 bp), *Slc17a6* (-312 to +408 bp), *Sncg* (-404 to +45 bp) and *Syt11* (-375 to +76 bp).

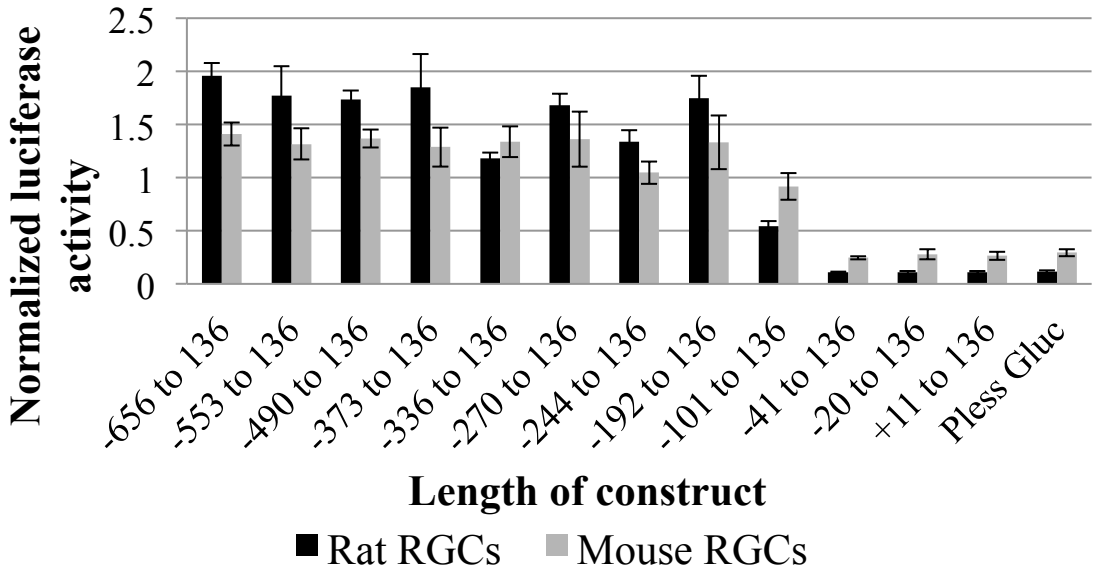

Figure 3. *Syt11* promoter deletion series. The deletion series demonstrates critical sequence between -192 and -41 bp for promoter activity in rat and mouse RGCs. A series of deletion mutants of the *Syt11* promoter region showed a similar level of activity when -656 to -192 bp was included and a step-wise decrease in activity when -192 to -101 bp and -100 to -42 bp were excluded. Promoter region from -41 to +11 bp did not confer any transcriptional activity. Error bars display the standard deviations. Gaussia luciferase values (of the deletion mutant constructs) were normalized to a co-transfected SV40-driven Cypridina luciferase. Error bars display the standard deviations.

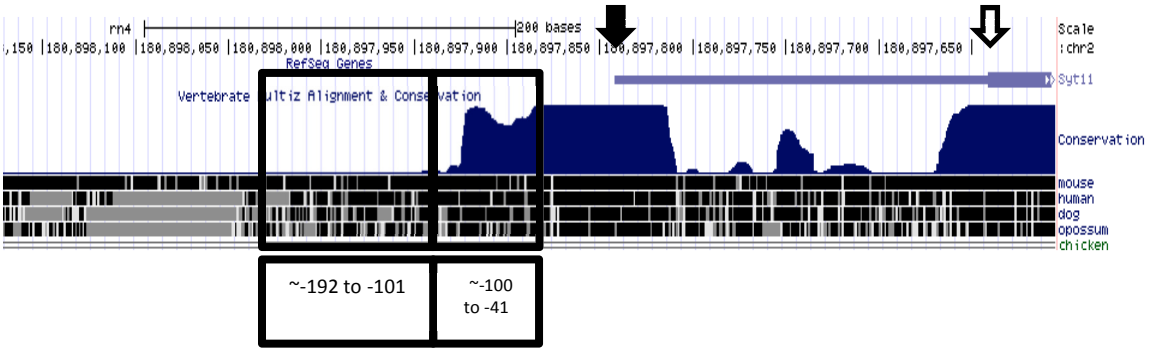

Figure 4. *Syt11* upstream region shows areas of sequence conservation. The two critical regions identified in the promoter deletion series are outlined in black boxes. Areas of conserved sequence suggest areas where important transcription factors might bind. This image was taken from the UCSC Genome Browser (http://genome.ucsc.edu/). Black vertical arrow indicates the *Syt11* transcriptional start site. White arrow indicates the *Syt11* start codon.

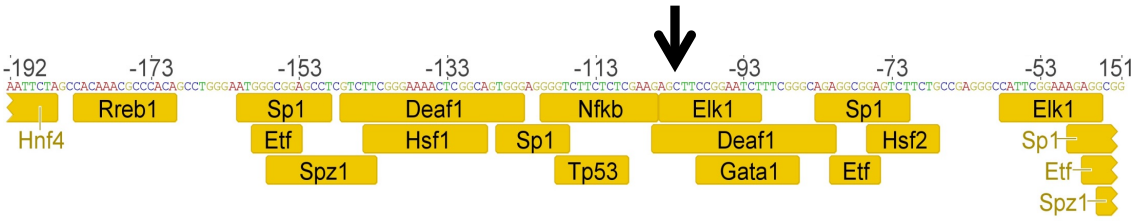

Figure 5. Predicted transcription factor binding sites (TFBSs) in the region of interest (-192 and -41 bp) in the *Syt11* upstream region. Predictions are from a MOPAT analysis (Hu 2007), which was then cross-referenced to immunopanned mouse RGC microarray data to determine which predicted TFBSs were most relevant. Of particular interest because of their location within the two sub regions, were the binding sites of DEAF1 and SP1. Vertical black arrow indicates ~-101, the boundary between the two deletion mutants that had a stepwise drop in activity. This figure prepared in and created by Geneious software.

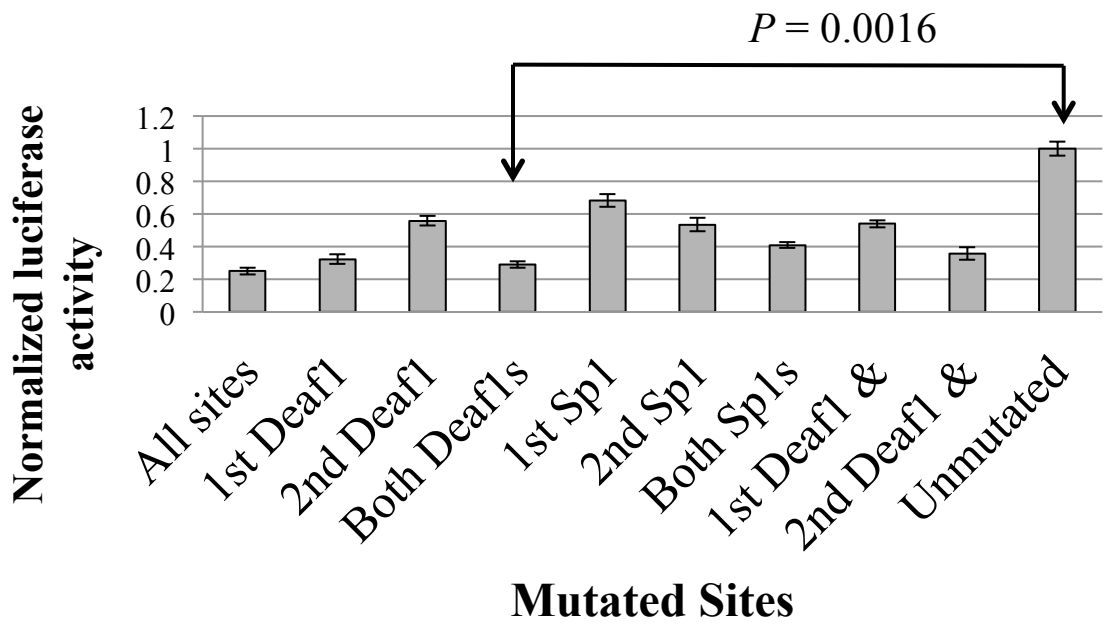

Figure 6. Activities of DEAF1 and SP1 binding site mutant promoter reporters. Mutation of all sites and DEAF1 sites decreased the *Syt11* promoter reporter activity in rat RGCs the most. All mutants were significantly lower than the unmutated construct, suggesting that all of the mutated sequenced plays a positive role in the transcriptional activity of the *Syt11* promoter reporter. Gaussia luciferase values (of the binding site mutant constructs) were normalized to a co-transfected full length, wild type reporter expressing Cypridina luciferase. Error bars display the standard deviations.

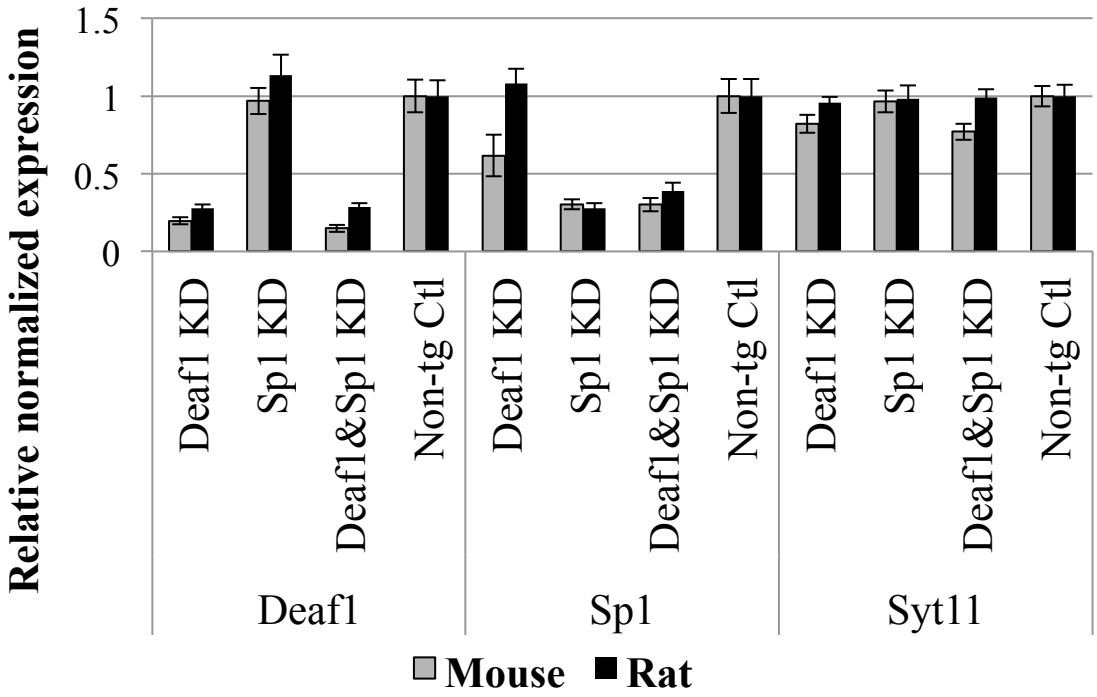

Figure 7. Knockdown of *Deaf1* and *Sp1* using siRNA. Greater than 75% knockdown of *Deaf1* and *Sp1* in rat and mouse RGCs did not alter *Syt11* expression. Pools of four different siRNAs to *Deaf1* and *Sp1* alone and together decreased the expression of their target but did not change *Syt11* expression. Target gene expression was normalized to the geometric mean of three reference genes: *Gapdh*, *Hprt1* and *Hmbs*. Bars represent the average of technical triplicates of biological triplicates with standard errors of the mean.

A

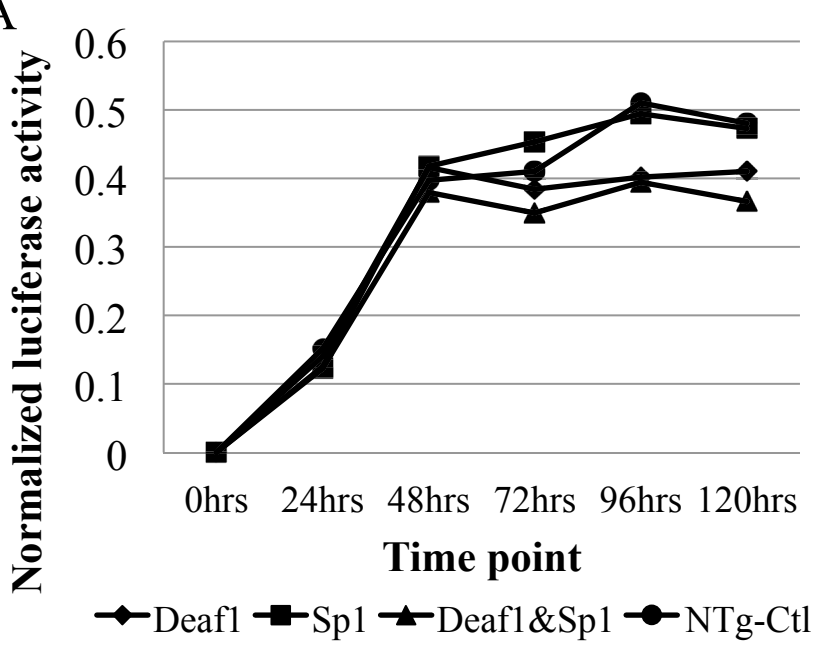
Normalized luciferase activity
0.6
0.5
0.4
0.3
0.2
0.1
0
0hrs
24hrs
48hrs
72hrs
96hrs
120hrs
Time point
Deaf1
Sp1
Deaf1&Sp1
NTg-Ctl

B

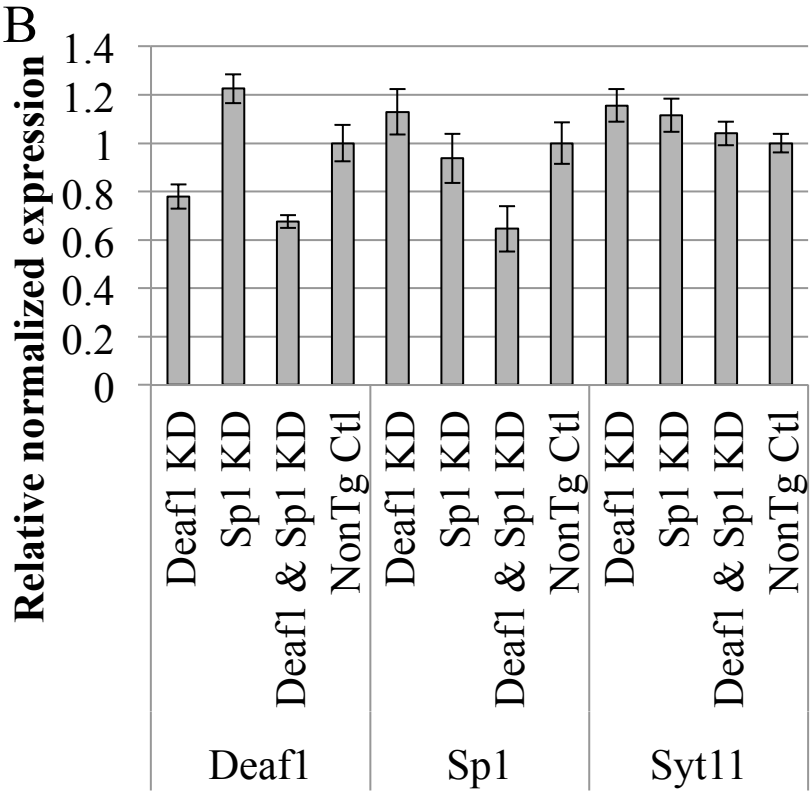
Relative normalized expression
1.4
1.2
1
0.8
0.6
0.4
0.2
0
Deaf1 KD
Sp1 KD
Deaf1 & Sp1 KD
NonTg Ctl
Deaf1 KD
Sp1 KD
Deaf1 & Sp1 KD
NonTg Ctl
Deaf1 KD
Sp1 KD
Deaf1 & Sp1 KD
NonTg Ctl
Deaf1
Sp1
Syt11

Figure 8. Activity of *Syt11* promoter reporter with knockdown of *Deaf1* and *Sp1*. siRNA KD of *Deaf1* but not *Sp1* decreased the activity of the Syt11 promoter reporter. **A**. Luciferase data demonstrating that when *Deaf1* was knocked down, either alone or in combination with *Sp1*, the promoter reporter activity decreased indicating DEAF1 has a positive influence over the *Syt11* promoter reporter's activity. **B**. qPCR data showing that the siRNA KD was not as efficient in this dual plasmid/siRNA transfection experiment. *Deaf1* expression was decreased by 22% (alone) and 32% (with *Sp1*) and *Sp1* expression was decreased by 6% (alone) and 35% (with *Deaf1*). *Syt11* expression was unaffected by the siRNA KD of *Deaf1* and *Sp1*. Bars represent the average of technical triplicates of a single biological replicate with standard errors of the mean. Target gene expression was normalized to the geometric mean of three reference genes: *Gapdh*, *Hprt1* and *Hmbs*. NTg-Ctl = non-targeting control siNA oligos.

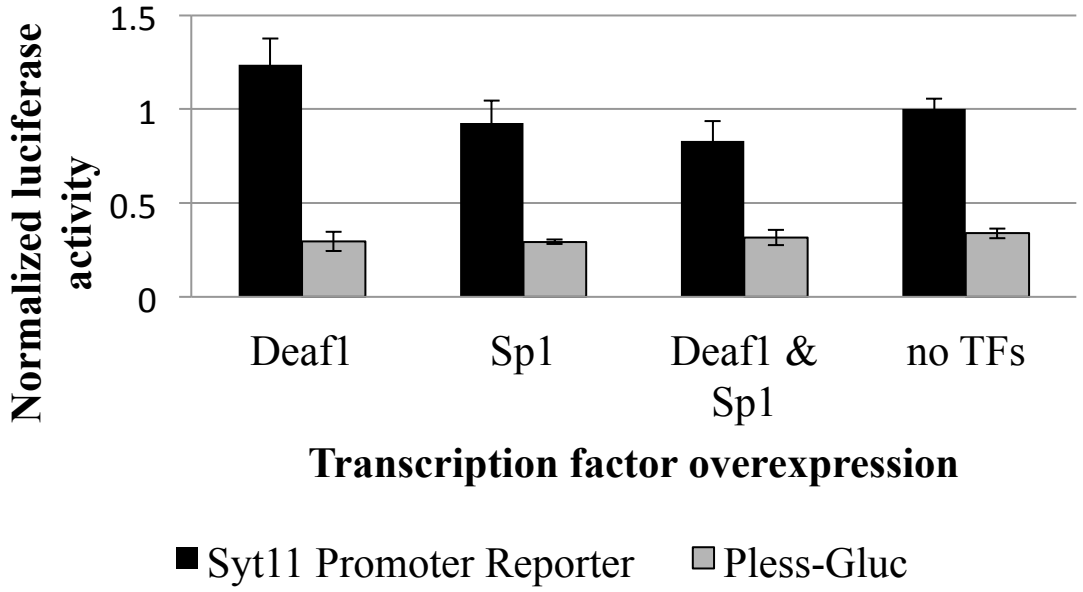

Figure 9. *Deaf1* and *Sp1* over-expression in HEK293 cells. *Deaf1* & *Sp1* over-expression alone or together in HEK293 cells did not significantly alter the activity of the *Syt11* promoter reporter. An empty over-expression vector was used to standardize the amount of plasmid when *Deaf1* and *Sp1* were over-expressed alone and was used in the "no TFs" sample. Gaussia luciferase values (of the *Syt11* promoter reporter and Pless-Gluc) were normalized to a co-transfected full length, wild type *Syt11* reporter expressing Cypridina luciferase. Bars represent the average of biological triplicates with standard deviations.

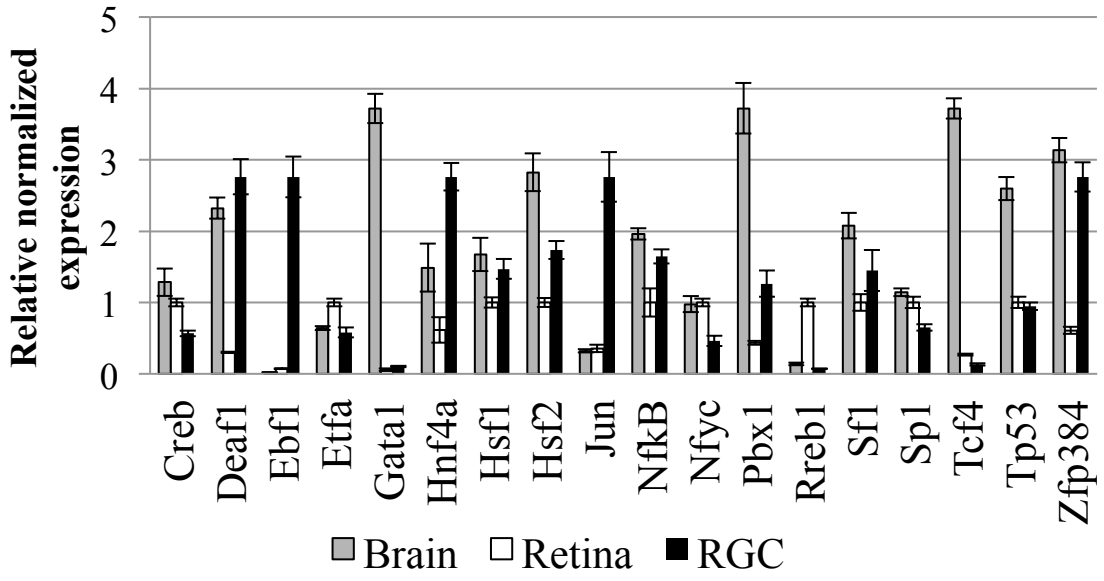

Figure 10. Expression of different TFs with predicted BSs within the *Syt11* upstream region of interest (-192 to -42 bp) in RGCs, retina & brain from rat pup. Some TFs are more highly expressed in RGCs than in retina or brain. Target gene expression was normalized to the geometric mean of three reference genes: *Gapdh*, *Hprt1* and *Hmbs*. Bars represent the average of technical triplicates with standard errors of the mean.

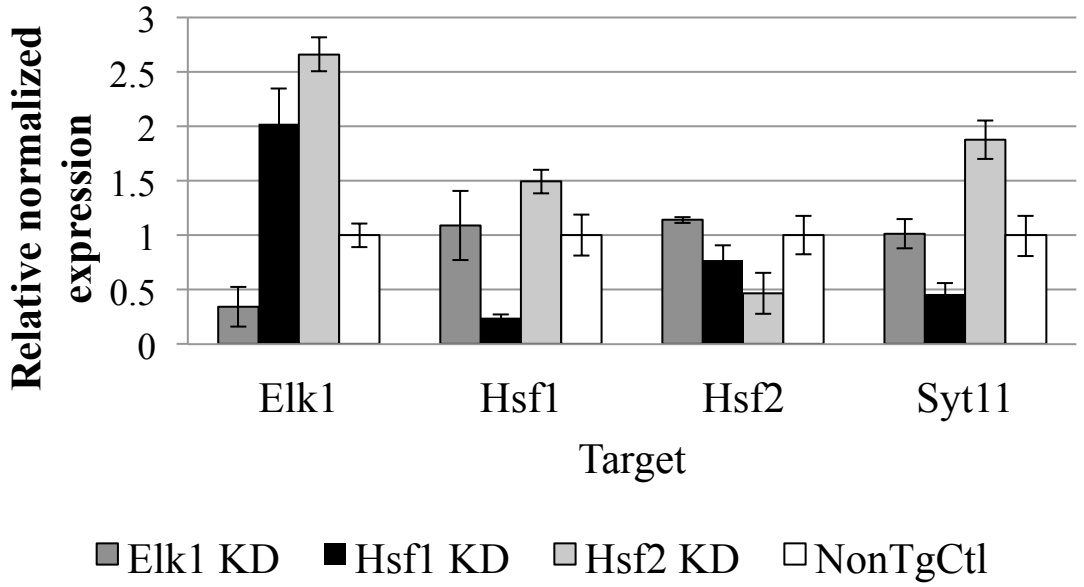

Figure 11. siRNA KD of *Hsf1* and *Hsf2* but not *Elk1* altered *Syt11* expression in rat RGCs. *Hsf1* KD of 75% decreased *Syt11* expression by 54%. *Hsf2* KD of 53% increased *Hsf1* expression by 49% and increased *Syt11* expression by 88%. *Elk1* KD of 66% did not alter *Syt11* expression. *Hsf1* and *Hsf2* KD both increased *Elk1* expression. siRNA KD was accomplished with pools of several different oligos for each target. Bars represent the average of technical triplicates of biological triplicates with the standard errors of the mean. Target gene expression was normalized to the geometric mean of three reference genes: *Gapdh, Hprt1* and *Hmbs*.

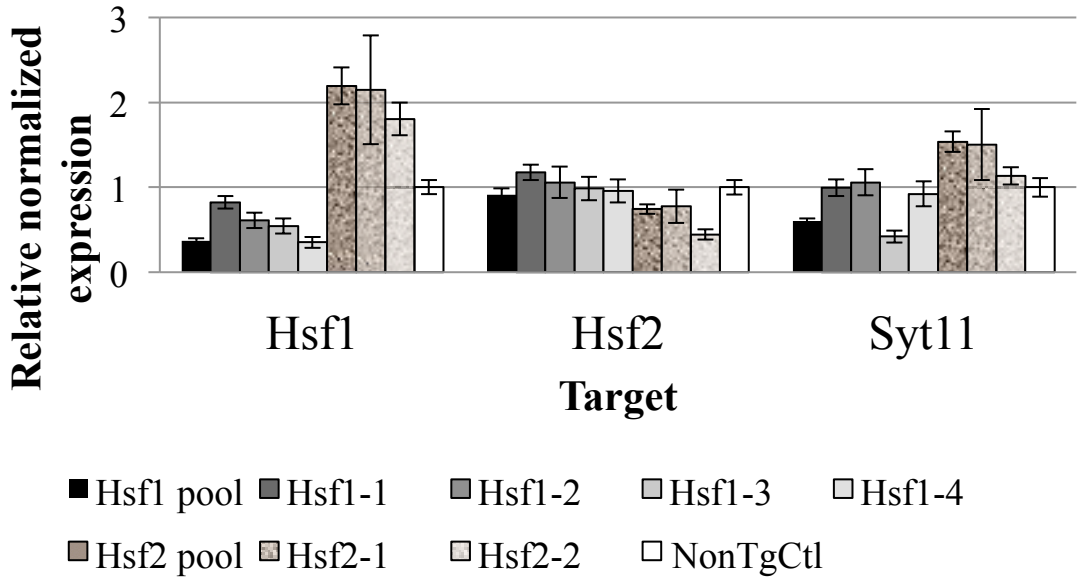

Figure 12. Individual *Hsf1* and *Hsf2* siRNAs did not always recapitulate the effect of the pool of siRNAs. Though all of the individual siRNAs did decrease their target, many of them were not as efficient at decreasing the expression of their target or the expression of *Syt11*. Some siRNAs that decreased the expression of their target the best did not alter *Syt11* expression much if at all (*i.e.* Hsf1-4 and Hsf2-2). Bars represent the average of technical triplicates of biological triplicates. Target gene expression was normalized to the geometric mean of three reference genes: *Gapdh, Hprt1* and *Hmbs*. Error bars display the standard errors of the mean.

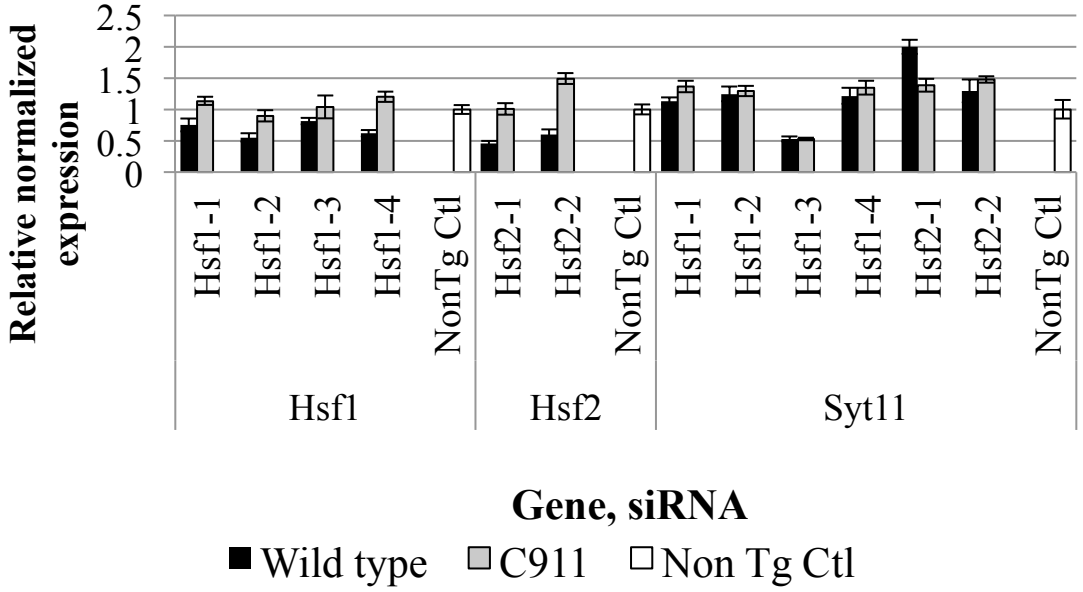

Figure 13. siRNA knockdown (KD) of *Hsf1* and *Hsf2* using "wild type" siRNAs and C911 mutant oligos in which the 9th, 10th and 11th bases were complemented [5]. Wild type siRNAs decreased their target to varying degrees and C911 mutant siRNAs were not as efficient as decreasing their targets suggesting the wild type effects were on-target. However, only Hsf1-3 decreased *Syt11* expression and both the wild type and C911 siRNA affected *Syt11* equally, suggesting the effect on *Syt11* was an off-target effect. Bars represent the average of technical triplicates from a single well. An additional well was analyzed and had similar results. Target gene expression was normalized to the geometric mean of three reference genes: *Gapdh, Hprt1* and *Hmbs*. Error bars display the standard errors of the mean.

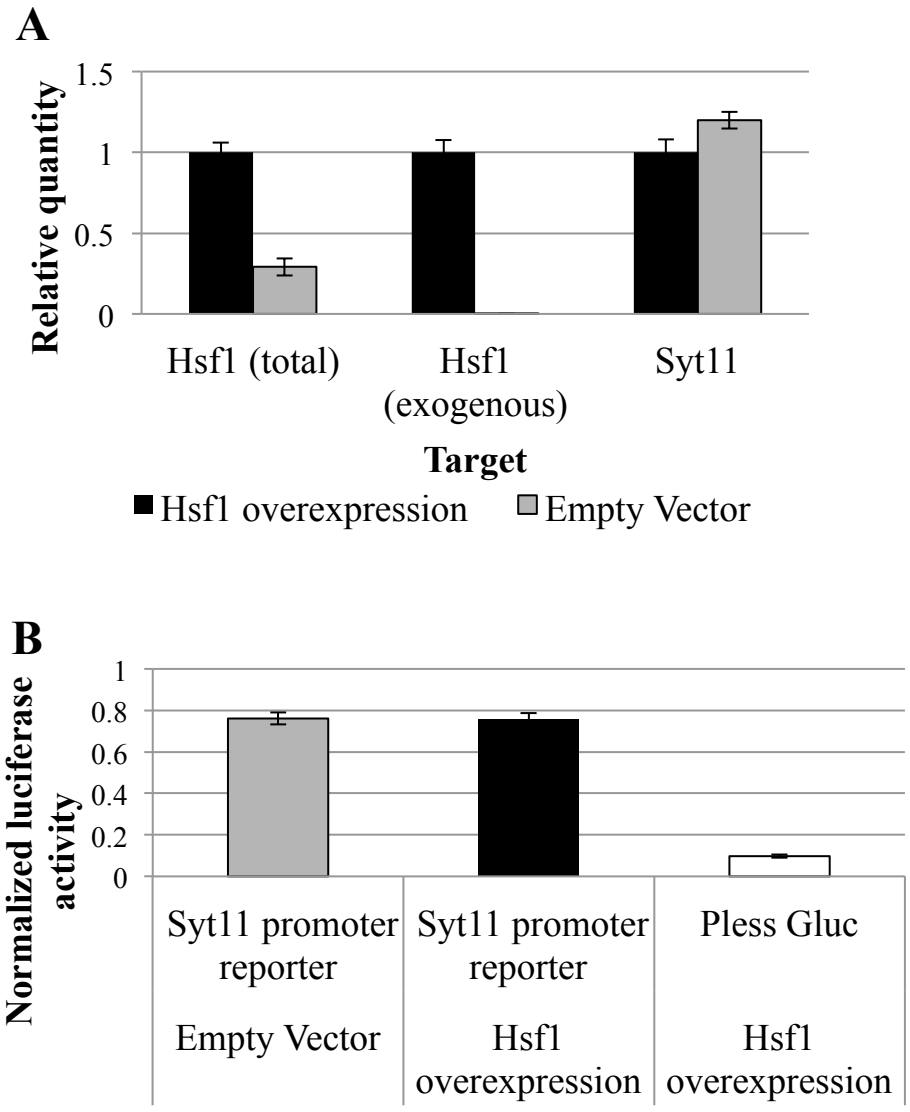

Figure 14. *Hsf1* overexpression in HEK293 cells did not affect *Syt11* promoter reporter activity or induce endogenous expression of *Syt11*. A. qPCR data confirms that over-expression was successful but that *Syt11* expression remained relatively unchanged. Target gene expression was normalized to the geometric mean of three reference genes: *Gapdh, Hprt1* and *Hmbs*. Error bars display the standard errors of the mean. **B.** Luciferase data showing that *Hsf1* over-expression did not change the *Syt11* promoter reporter activity. Error bars display the standard deviations.

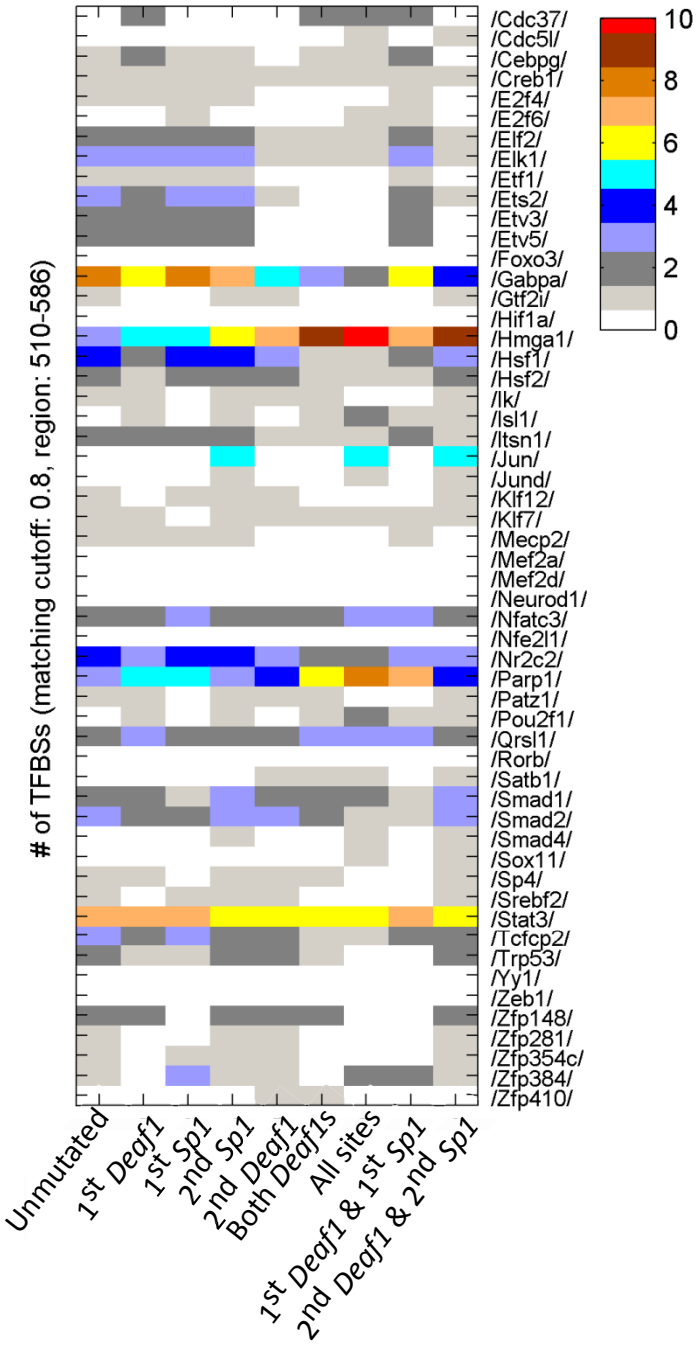

Figure 15. TRANSFAC analysis of *Syt11* -192 to -42 bp focusing on the change in predictions between the various binding site mutants. Of particular interest is GABPA because there are 8 predicted sites in the unmutated construct and only 2 in the All Sites mutated construct. NR2C2, ETS2 and TCFCP2 all had fewer sites in the All Sites

construct compared to the unmutated. Other potentially interesting TFs include HMGA1, JUN and PARP1 which have more predicted sites in the All Sites mutated construct compared to the unmutated construct.

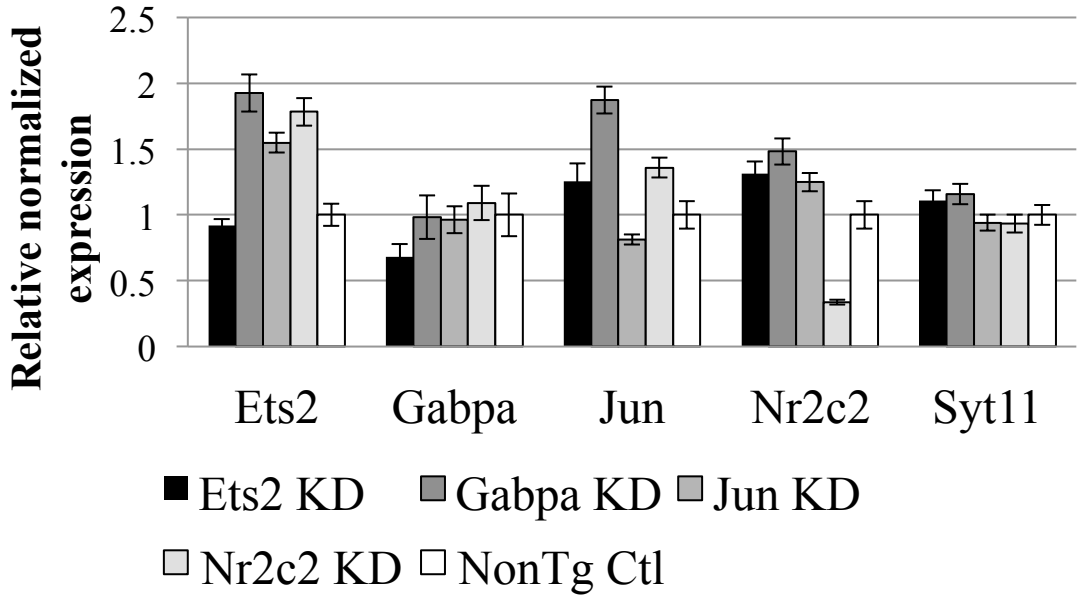

Figure 16. siRNA knockdown of additional transcription factors predicted to bind within the *Syt11* promoter region of interest. Though the expression of some of the TFs was decreased, there was no difference in *Syt11* expression. Bars represent the average of technical triplicates of biological triplicates with standard errors of the mean. Target gene expression was normalized to the geometric mean of three reference genes: *Gapdh, Hprt1* and *Hmbs*.

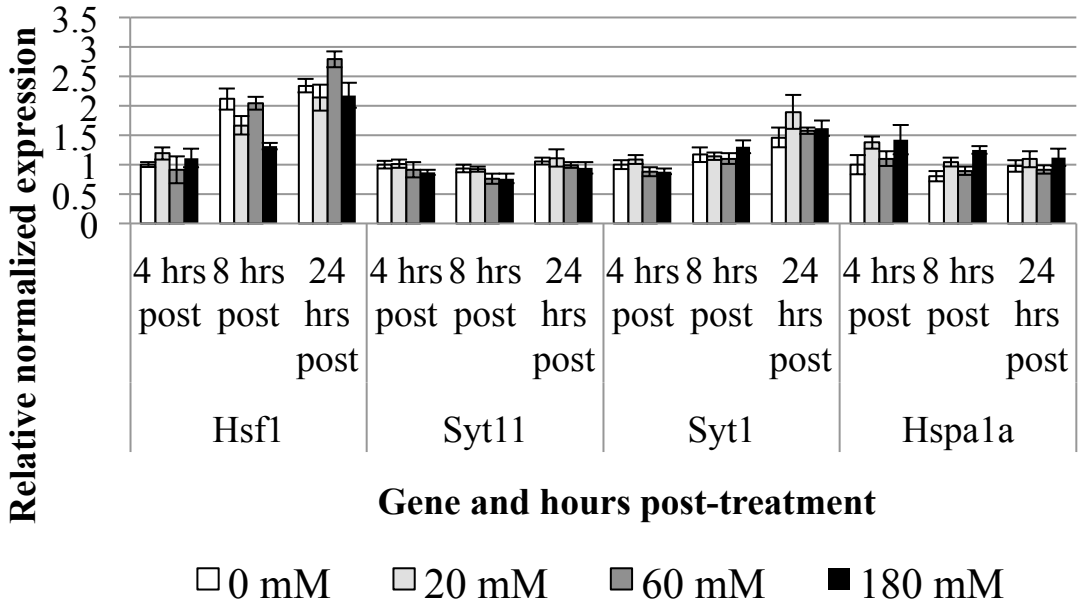

Figure S1. Ethanol treatment of RGCs did not alter *Syt11* expression. *Hsf1* and *Syt1* expression increased over time in culture, but not due to ethanol treatment. *Hspa1a* expression was slightly increased with ethanol treatment. Lack of change of *Syt11* expression with an increase of *Hsf1* expression suggests HSF1 is not involved in the transcriptional regulation of *Syt11*. Bars represent the averages of triplicates of biological duplicates. Target gene expression was normalized to the geometric mean of three reference genes: *Gapdh, Hprt1* and *Hmbs*. Error bars display the standard errors of the mean.

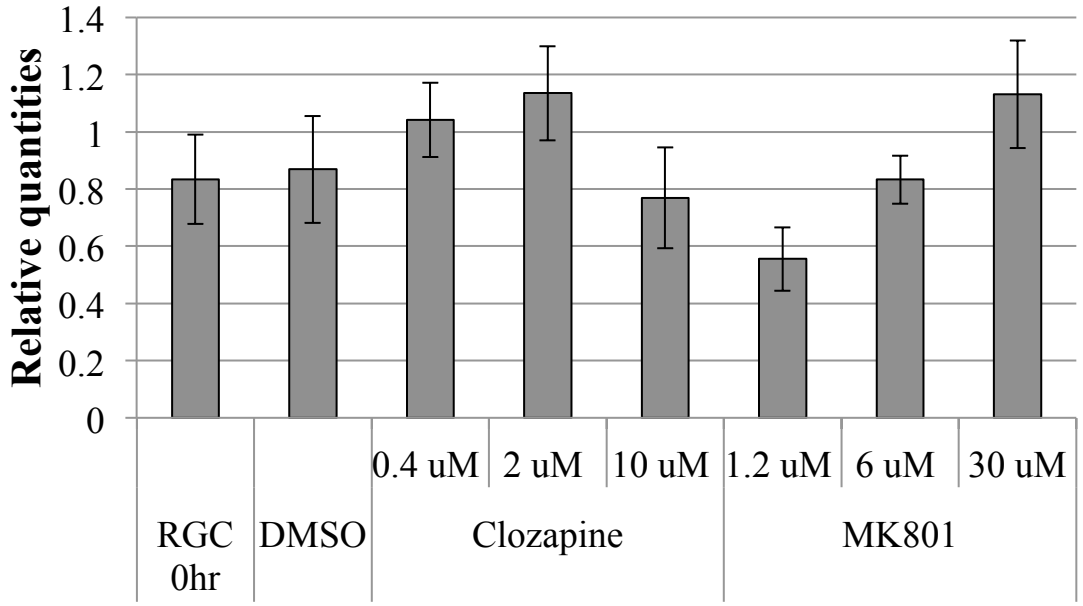

Figure S2. Clozapine & MK801 treatment of RGCs did not consistently alter *Syt11* expression. Rat RGCs were cultured with clozapine and MK801 and *Syt11* expression was measured by qPCR after 48 hrs of treatment. Bars represent technical triplicates with standard errors of the mean. Target gene expression was normalized to the geometric mean of three reference genes: *Gapdh, Hprt1* and *Hmbs*.

Chapter 2: Transcriptional Control of S-antigen (*Sag*) expression in photoreceptors (PRs)

Introduction

Identification of the precise regulatory DNA sequences required for photoreceptor (PR) specific expression would not only further our knowledge of transcriptional regulation and networks in the retina and PRs, but would also allow controlled PR-directed expression of potential therapeutic molecules within the retina. Additionally, PR-specific reporters or reporters specific to PR death/survival pathways could be used in screens for neuroprotective factors. We and others have been working to define the *cis*-acting elements that regulate PR-specific transcriptional activation. Here we describe the process by which we have worked to define the regulatory elements that control expression of a model PR-expressed gene, S-antigen (*Sag*). Like the study of *Syt11* in RGCs, we used primary rodent retinal cells for this study as well, since analyses with such cells are more likely to accurately reflect endogenous cell-type specific regulatory mechanisms.

In order to decide which promoter to concentrate on, we performed an initial analysis comparing the transcriptional activity of the 5'-upstream regions from sixteen genes whose expression pattern had previously been reported to be photoreceptor specific within the retina [1, 2]. The set of sixteen genes consisted of opsin 1 medium wavelength sensitive (green) cone opsin (*Opn1mw*), phosphodiesterase 6H (*Pde6h*), phosphodiesterase 6C (*Pde6c*), guanine nucleotide binding protein, gamma transducing activity polypeptide 2 (*Gngt2*), olfactomedin 1 (*Olfm1*), solute family carrier 24

(Na/K/Ca exchanger) member 2 (*Slc24a2*), rod transducin alpha subunit (*Gnat1*), guanine nucleotide binding protein beta 1 (*Gnb1*), guanylate cyclase 2d (*Gucy2d*), retinal S-antigen (rod arrestin, *Sag*), phosphodiesterase 6G (*Pde6g*), guanine nucleotide binding protein gamma transducing activity polypeptide 1 (*Gngt1*), phosducin (*Pdc*), retinoschisis 1 homolog (*Rs1*), rod outer segment membrane protein 1 (*Rom1*), ATP binding cassette subfamily A member 4 (*Abca4*) (Table 1). Promoter reporters for each gene were constructed using PCR. The promoter reporter for *Sag* had the highest activity amongst the promoter reporters tested, and hence was thus chosen for further analysis. A *Sag* promoter deletion series identified a region of interest (-279 to -182 bp) that when deleted led to a significant decrease in promoter activity. Bioinformatic analysis identified several candidate transcription factors (TFs) that had predicted binding sites within this region of interest. To evaluate the potential role of these candidate transcription factors in *Sag* gene regulation, the expression of several of the TFs was knocked down using siRNAs and the consequence of the knockdown on endogenous *Sag* was assessed.

Materials & Methods

Primary mouse retinal cells

All animals were treated in accordance with the ARVO statement for the care and use of animals and all procedures were approved by the Johns Hopkins University Institutional Animal Care and Use Committee.

Eyes were removed from mouse pups (postnatal days 1-4 [P1-4]) and retinas were isolated from the globes in CO_2 independent media (catalog # 18045-088, Life Technologies, Carlsbad, CA) containing 2 mM L-glutamine (catalog # 25030-081, Life

Technologies, Carlsbad, CA) and 50 U/mL / 50 μg/mL penicillin/streptomycin (catalog # 15070-063, Life Technologies, Carlsbad, CA). Retinas were rinsed in PBS without Ca^{2+} or Mg^{2+} (catalog # 10010-023 Life Technologies, Carlsbad, CA) and then digested for 40 minutes at 37 ^{o}C in papain (16.5 U/mL, catalog # LS003119 Worthington, Lakewood, NJ) activated in Hibernate-E without Ca^{2+}/Mg^{2+} (catalog # HE-Ca 500ml, Brainbits, Springfield, IL) with 0.2 mg/mL L-cysteine [catalog # C7352 Sigma-Aldrich, St Louis, MO] and 250 U/mL DNase I (catalog # D4527, Sigma-Aldrich, St Louis, MO) and pH adjusted to 7.4. One mL of activated papain was use per 10 retinas to be dissociated. After 40 minutes in papain, the tissue was dissociated into a homogenous single cell suspension and the digestion was inhibited with 0.5 mL of a soybean trypsin inhibitor solution (15 mg/mL soybean trypsin inhibitor [catalog # LS003587, Worthington, Lakewood, NJ], 15 mg/mL bovine serum albumin [BSA] [catalog # 126579, Merck KGaA, Darmstadt, Germany] and 125 U/mL DNase I [catalog # D4527, Sigma-Aldrich, St Louis, MO] in Hibernate-E [catalog # A12476-01, Life Technologies, Carlsbad, CA]) per 1 mL of the cell suspension. The cell suspension was triturated six times with fire polished siliconized glass pipettes, then centrifuged for 7 min at 80 x *g*. Then the supernatant was removed and cells resuspended and counted.

Transfection of primary retinal cells

The dissociated retinal cells were resuspended in electroporation buffer at 2,000,000 cells/mL (RPMI [catalog # 11875-119, Life Technologies, Carlsbad, CA] with 10 mM HEPES [catalog # 15630-080, Life Technologies, Carlsbad, CA] and 50 U/mL / 50 μg/mL penicillin/streptomycin [catalog # 15070-063, Life Technologies, Carlsbad,

CA]). Cells were mixed with DNA construct at a final concentration of 0.03 mg/mL and DMSO was added to a final concentration of 1.25%. For promoter reporter experiments, generally the photoreceptor promoter reporter of interest would be mixed with a plasmid containing Cypridina luciferase (CLuc, another secreted luciferase) driven by the rhodopsin promoter in a two to one ratio. Expression of CLuc would be used to normalize photoreceptor transfection. One hundred uL of the cell/DNA mix would then be loaded into the wells of a 96 well electroporation plate (model # HT-P96-2, catalog # 45-0450 BTX Harvard Apparatus, Holliston, MA). Cells were electroporated with a single square pulse of 350 V with 900 μs duration using a BTX Harvard Apparatus HT100 plate electroporator (catalog # 45-0400) with an ECM 830 Square Wave Electroporator (model # 45-0052, BTX Harvard Apparatus, Holliston, MA).After sitting for 5 minutes at room temperature, the 100 uL cell suspension was transferred to a PDL-coated 96 well plate containing 100 μL of growth media (Neurobasal [catalog # 21103-049, Life Technologies, Carlsbad, CA], B27 supplement [catalog # 17504-044, Life Technologies, Carlsbad, CA], 2 mM L-glutamine, 50 U/mL / 50 μg/mL penicillin/streptomycin) per well and cultured 37^{o}C with 5% CO_2 in a cell culture incubator. 150 μL of media was changed after 3-4 hours.

Construction of promoter reporters

Genomic mouse DNA was isolated from the liver of a C57Bl/6 mouse using the QIAmp DNA Mini Kit (catalog # 51304, Qiagen, Germantown, MD). For each construct, primers designed to target 500-1000 bases of the upstream promoter region of the genes of interest (Table 2) or for specific regions within the *Sag* promoter region (Table 3),

were used to amplify these sequences using PCR, which were then cloned into pENTR (catalog # K2400-20, Life Technologies, Carlsbad, CA) by TOPO cloning. The insert was then recombined into a Gaussia luciferase (GLuc) promoter reporter Gateway® destination vector (pGLuc) using LR Clonase II from Life Technologies (catalog # 11791-019). Insertion and proper orientation in entry and destination vectors were determined by colony PCR with a forward primer within the vector upstream of the recombination site and a reverse primer within the insert and final constructs sequenced.

As mentioned above, for a photoreceptor transfection normalization control, we used a rhodopsin promoter-driven CLuc. This construct was made by amplifying a sequence 225 base pairs upstream from the transcriptional start site (TSS) to 70 base pairs downstream of the TSS (bRho225, from -225 to +70 bp) from a previously created bRho225-GLuc reporter construct and using the same cloning strategy described above, introduced this sequence into a pENTR plasmid and finally into a CLuc destination vector (New England BIolabs, Ipswich, MA). Similarly, as a transfection control for the *Sag* mutations created in GLuc, a "full length" *Sag* promoter reporter (*Sag*-429 to +71 bp) was constructed in the CLuc vector.

Scanning mutagenesis was done in the -429 to +71 bp *Sag* promoter construct in the pENTR vector using Life Technologies' Geneart® mutagenesis system by introducing transversions for each nucleotide in 10 to 11 bp stretches from -279 to -158 bp (Table 4). As described above, after sequence confirmation these mutations were introduced into the GLuc reporter construct.

Plasmids were isolated using Promega's PureYield Midiprep system (catalog # A2492, Madison, WI) or Life Technologies' HiPure Plasmid Filter Maxipreps (catalog #

K2100, Carlsbad, CA) and resuspended and stored in TE buffer (10mM Tris-HCl, 1mM EDTA, pH 8.0).

Promoter reporter assay

GLuc promoter reporter plasmids were co-transfected with the bRho225-CLuc plasmid into dissociated retinal cells (Figure 1) as described above. Expression of CLuc was used to normalize for variation in photoreceptor transfection efficiency. For the *Sag* promoter mutations created in the GLuc vector, we used the -429 to +71 bp *Sag* CLuc construct for normalization (Figures 2 and 4 respectively).

To assay promoter activity, two 20 uL aliquots of culture media were collected seven days after cells were electroporated and luciferase activity was measured using the Gaussia and Cypridina luciferase assay kits (separately) from New England Biolabs (Ipswich, MA). The GLuc activity was normalized to the CLuc activity within the same well by dividing the measured relative light units (RLU) in the GLuc assay by the RLU in the CLuc assay as a means to control for transfection efficiency. Empty vectors ([pCLuc-Basic 2, catalog # N0317S] and promoterless-GLuc [pless-GLuc, pGLuc-Basic 2, catalog # N8082S], New England Biolabs, Ipswich, MA) were used as negative controls and promoter activity values were expressed as fold change over the GLuc/CLuc RLU values measured in these controls.

Small interfering RNA knockdown (siRNA KD)

siRNAs targeting various transcription factors (Table 5) with predicted binding sites in the *Sag* promoter region were transfected into dissociated retinal cells. siRNAs

were pooled and 12 pmol/96 well reaction were complexed with TrueFect-Lipo (catalog # TF1101-2, United Biosystems, Herndon, VA) for 30 minutes in Optimem (catalog # 31985-070, Life Technologies, Carlsbad, CA) in PDL-coated 96 well plates. Retinal cells suspended in growth media (50,000 cells/100 uL) were added to the wells with complexed siRNA and cultured. After 48 hours, RNA was collected from each well using Qiagen's Micro RNeasy kit (catalog # 74004) and then all of the RNA collected was converted to cDNA using the Applied Biosystems High Capacity Reverse Transcription kit.

Quantitative Real Time-PCR (qPCR)

Sequences of the primers used in qPCR assays are listed in Table 6. Primer sequences were chosen through the RT Primer database (http://medgen.ugent.be/rtprimerdb/) or designed with Roche's primer design algorithm (http://lifescience.roche.com/shop/CategoryDisplay?catalogId=10001&tab=Assay+Design+Center&identifier=Universal+Probe+Library&langId=-1#tab-3). Primer pair efficiencies were determined using a standard curve of cDNA from whole retina and deemed adequate if they were between 90 and 110%. Samples were run in triplicate in a BioRad Cfx C1000 384 qPCR machine in a total reaction volume of 8uL; 0.2 uL cDNA, 125 nM of each primer, EvaGreen (catalog # 31000, Biotium, Hayward, CA), 0.67 U of Fermentas Hot Start *Taq* DNA polymerase (catalog # EP0603, Thermo Scientific, Wilmington, DE), 3 mM MgCl2 and 0.2 mM each dNTP. The cycling parameters were: 95^{o}C for 3 min, followed by 40 cycles of 95^{o}C for 10 sec, 60^{o}C for 30 sec and 72^{o}C for 30 sec, followed by a melting curve analysis with temperature range between 60^{o}C and

95^{o}C with a 0.5^{o}C increment. Primer pair specificity was suggested by a single sharp peak in the melting curve. Expression of a single reference gene (beta-actin) was used to normalize the target gene expression and results were reported as Relative Normalized Expression based on the ΔΔ Cq calculation performed by the Cfx software.

Bioinformatics

A motif pair tree (MOPAT) analysis was performed on the region of interest (-279 to -182 bp) within the *Sag* 5' UTR to identify *cis*-regulatory modules (CRMs) that may be binding sites [3] of known mammalian transcription factors (Figure 3).

We also compared the potential transcription factor (TF) binding sites (BSs) in the wild type *Sag* 5' UTR to the sequences generated by the scanning mutagenesis. Using the TRANSFAC-database with an 80% matching threshold to identify TFs with predicted BSs (Figure 6), we identified a set of mouse TFs that potentially interact with these sequences.

Statistical Tests

Student's *t* tests were performed in Microsoft Excel with $P < 0.05$ being considered significant.

Results

With the goal of discovering novel *cis*-regulatory elements and trans-acting factors involved in photoreceptor gene regulation, we evaluated published studies on PR expression studies to assemble a set of genes on which to focus. Since in most cases the

major DNA elements regulating promoter activity are located in the 5′ 500-1000 upstream bases of a given gene [4-7], we cloned the 500-1000 upstream regions of the genes to be evaluated into a set of promoter reporter constructs. As we are interested in regulatory elements in the context of the photoreceptor rather than assessing expression of the reporters in a cell line, we transfected primary murine retinal cultures, which are made up of approximately 50-60% rod photoreceptor cells. Retinal cultures were co-transfected with the CLuc containing reporter constructs for each of the candidate genes, and the resulting GLuc activity values of the promoter constructs were normalized to the CLuc construct.

An initial set of promoter reporters was constructed and tested in dissociated whole retina cell cultures (Figure 1). Normalized luciferase activity (Figure 1) showed that whereas the promoter activity of the -225 to +70 bp upstream bovine rhodopsin gene construct was nearly 6-fold higher than that of the pless-GLuc reporter, the majority of the promoter reporters showed activity that was approximately two-fold or lower compared to the pless-GLuc reporter. This result indicated the majority of the upstream fragments tested had only modest promoter activity in our cell culture system. However, the *Pdc* and *Pde6c* constructs demonstrated activity that was almost as strong as the bRho225-GLuc construct, and both the longer (-859 to +71 bp) and shorter (-494 to +71 bp) *Sag* constructs showed activity that was higher than that of the bRho225-GLuc construct. Based on these results, the upstream promoter region of *Sag* was chosen for further analysis.

We next dissected the -859 to +71 bp region of *Sag* to define the important the biologically active regulatory sequences within this region. This was accomplished by

performing a deletion series, creating a series of GLuc promoter reporters with a sequentially smaller portion of the upstream region. The GLuc activity of these constructs were normalized to the activity of a co-transfected CLuc full length *Sag* (-859 to +71 bp) promoter construct.

Figure 2 shows the normalized luciferase activity of the *Sag* promoter series of deletion mutants. The five longest constructs, -859, -494, -429, -340 and -279 to +71 bp, all had similar luciferase activities (between eight and 12 times higher than the promoter-less GLuc [pless-GLuc] construct). Then there was a sharp, and statistically significant ($P = 0.0145$), decrease in activity from the -181 to +71 bp construct, and smaller decreases in the activity from the shortest two constructs (-138 and -37 to +71 bp), neither of which had activity that was statistically different from the pless-GLuc construct ($P > 0.05$). These results suggest that the region between -279 and -182 bp contained sequences important for the activity of the *Sag* promoter.

In order to try to determine what transcription factors might be binding within the -279 to -182 bp region, I turned to bioinformatic analysis. Figure 3 shows the transcription factor binding sites within the -279 to -182 bp sequence that are predicted by the bioinformatic tool MOPAT. Several of these predicted TFs, including COUP1, COUP2, PPARA and RORA, have been studied in the context of the eye [8-10] and were therefore thought to be likely candidate TFs involved in *Sag* transcriptional regulation. siRNA KD of these four TFs was attempted. Figure 4 shows the level of *Sag* expression after transfection with siRNAs targeting *Coup1, Coup2, Ppara* and *Rora*. There was greater than 40% knockdown of *Coup1, Coup2* and *Ppara*. The siRNA KD of *Rora* was unsuccessful. However, regardless of whether or not the siRNA KD of the TF was

successful, *Sag* expression was increased 1.5 to 2.5 times compared to the non-targeting control siRNA.

In addition to the siRNA KD, an additional analysis of *Sag*'s promoter region of interest was undertaken. An unbiased mutagenesis approach was taken to identify important sub-regions within the 97 bp region of interest. Transversions were introduced for each nucleotide in 10 bp stretches within this region of interest and construct activity was tested using the dissociated retinal cell assay (Figure 5). The GLuc activity of the mutant constructs was once again normalized to the CLuc activity of a wild type construct (*Sag*, -429 to +71 bp). Some of the mutants had higher activity than the wild type construct, some had similar activity and some had lower activity. Mutants with similar activity included -269 to -260 bp and -239 to -230 bp. Those with higher activity included -279 to -270 bp, -259 to -250 bp, -249 to -240 bp and -199 to -190 bp. The construct with -199 to -190 bp mutated had the highest activity overall and was approximately three times as high as the wild type construct. Those with decreased activity included -229 to -220 bp, -219 to -210 bp, -209 to -200 bp, -189 to -180 bp, -179 to -170 bp and -169 to -158 bp. The constructs with -219 to -210 bp, -209 to -210 bp, -189 to -180 bp, -179 to -170 bp and -169 to -160 bp mutated had the lowest activity, approximately half the activity of the wild type construct. The lower activities of some of the mutants suggest their region contains binding sites for transcription promoting factors.

Because of the variable activities of the scanning mutagenesis constructs, an additional bioinformatic analysis using the TRANSFAC database was performed to identify binding sites that were added or removed with the various mutations (Figure 6).

This bioinformatic prediction identified a number of transcription factors that might be important for the transcriptional regulation of *Sag* that could be pursued further in the future.

Discussion

The objective of this study was to identify and characterize important *cis*-regulatory elements involved in photoreceptor (PR) gene expression. We performed transient transfection of murine primary retinal cultures using promoter reporters that contained the 5' upstream 500-1000 bases of 16 genes known to be expressed in PRs. Most of the regulatory sequences tested had marginal promoter activity suggesting that either the complete region necessary for promoting robust PR gene expression was not contained in the sequences used to create the reporter or potentially that the transfected promoter sequences require aspects of chromatin structure that are not present in transfected plasmids.

Additionally, some of the regulatory sequences tested in the study lie in the promoter region of cone specific genes (*Opn1mw*, *Pde6h*, *Pde6c*, *Gngt2*, *Olfm1* and *Slc24a2*), and since cones make up only a small percentage of the mixed retinal cultures used for this study (approximately 1-2%), even promoter fragments that are active in cones, if they are cone-specific, would be expected to show minimal activity compared to background when tested in whole retina cultures. Interestingly though, the *Pde6c* reporter containing 763 upstream bases had 2.75 times more activity than the construct containing 443 bases, suggesting that the sequences necessary for transcriptional activity lie within the additional 320 bases contained in the longer construct. Since the activity of this

putatively cone-specific promoter is relatively robust in our assay, it is not clear whether the sequence being assessed maintains all the elements necessary to restrict its activity solely to cone cells. The assay, since it is population-based, does not distinguish between a small percentage of cells having a very high expression level (as would be the case if the construct maintained cone-specificity) or a large percentage of cells expressing the reporter at a moderate level, which may suggest that the sequence we are examining may not maintain cone-specific regulatory elements. Further studies in which reporters can be analyzed at the cell level, and potentially multiplexed with cone-specific markers, will allow us to distinguish between these possibilities and hone in on cone-specific regulatory elements.

The regulatory element that had the highest expression in our assay was the -429 to +71 bp *Sag* fragment. The expression of this reporter was 1.22 times higher than our rhodopsin promoter construct. Rhodopsin is expressed at a very high level in PRs, and if the bRho225 promoter reporter accurately reflects the level of rhodopsin expression in these cultures, then the fact that the *Sag* promoter reporter has higher activity than the rhodopsin promoter reporter could be explained several different ways. It is possible that *Sag* is more highly expressed than rhodopsin either in general, or at this stage of development. Another possibility is that the promoter reporter included transcription-promoting sequence but lacked transcription-inhibiting sequence. Last but not least, 1.22 times greater than rhodopsin is possibly within the realm of random variation in the assay and may not reflect a true difference in activity between the two genes' promoter reporters. Because the *Sag* promoter reporter had the highest activity of all of the 16 PR genes of interest, it was chosen for further analysis.

Both of the *Sag* constructs had similar activity even though one contained 365 bp more of the promoter region. This would indicate that the sequence between -859 and -494 bp did not contain binding sites for transcription factors important to the promoter reporter's activity, at least in our *in vitro* assay system.

The next step in evaluating the *Sag* promoter region was to make a deletion series. The results of the deletion series indicated the region between -279 and -182 bp likely contains binding sites for transcription factors that are important for positively regulating *Sag* promoter activity. The initial bioinformatic analysis (MOPAT analysis, [3]) predicted that a number of transcription factors had binding sites within this region, several of which have been studied within the context of the retina including COUP, RORA, PPARA, MEF2, AP2G and TBX5 [8-14]. Of initial interest were the COUP transcription factor binding sites because the COUP TFs are involved in eye and specifically retinal development [9]. RORA, which also has a predicted binding site within this region, is also known to be involved in photoreceptor gene regulation, though primarily in cones [8, 11]. PPARA is expressed in the retina and exerts protective effects in retinal ischemia and in diabetic retinopathy [10, 15]. The siRNA KD of these four transcription factors within whole retinal cells was then pursued.

To explore whether these candidate TFs were indeed positive regulators of *Sag* expression, we attempted to knock down their expression using siRNA technology. siRNA knockdown in dissociated retinal cultures is difficult and the technique is still not optimized. TrueFect-Lipo transfection reagent, used in this study, is one of the reagents shown to have some efficacy in transfecting retinal cells with siRNAs (Zack lab, unpublished data). siRNAs targeting *Coup1, Coup2, Ppara* and *Rora* were transfected

into dissociated retinal cells and then knockdown was evaluated by qPCR. Knockdown of *Coup1, Coup2* and *Ppara* was somewhat successful; however, the *Rora* knockdown did not work. Interestingly the *Sag* expression was not decreased by the knockdowns, but instead all of the targeting siRNAs (even the ones that targeted but did not affect *Rora* expression) increased *Sag* expression. Given the high reported rate of off-target effects of siRNAs [16], it is somewhat likely that the effect on *Sag* expression in this experiment may be due to these undesired off-target effects either directly, or through the change in expression of the target genes themselves. One way to investigate this possibility is to test each siRNA oligo individually and see if, as individuals, they are able to recapitulate the effects of the pool [16]. Another way to investigate this further would be to mutate the seed sequence, which should decrease on-target but not off-target effects [17]. Overall, our siRNA experiments did not implicate any of the identified candidate TFs as being important positive regulators of *Sag* expression.

As a complementary approach to further define the regulatory regions identified by our deletion analysis, we performed a scanning mutagenesis study to identify at a higher resolution regulatory sequences within the *Sag* -279 to -182 bp region of interest. The various mutants showed a range of activities compared to the unmutated construct. Those that had similar activity indicate that the mutated stretch of bases is not likely to play a role in the promoter's activity. Those with increased activity (-279 to -270 bp, -259 to -250 bp, -249 to -240 bp and -199 to -190 bp) may indicate a region where an inhibitory transcription factor binds, or they may have created a new binding site for a transcription-promoting factor. Those with decreased activity (-229 to -220 bp, -219 to -210 bp, -209 to -200 bp, -189 to -180 bp, -179 to -170 bp and -169 to -158 bp) may have

disrupted a binding site of a transcription-promoting factor or created a binding site of an inhibitory factor. According to the initial MOPAT analysis, the mutants that had the lowest activity overlapped with the binding sites for PPAR, COUP, RORA, MEF2, and TBP. siRNA KD results did not strongly support the involvement of COUP or PPAR, leaving MEF2 and TBP as potentially interesting TFs to investigate in the future.

The additional bioinformatic analysis of the region of interest in the context of the scanning mutagenesis suggested a number of additional transcription factors that might play a role in *Sag* transcriptional regulation. TFs with a decreased number of predicted sites within mutants with lower activity included HMGA1, PARP1, RARA, SAFB1, SF1 and TBP. HMGA1 is a potentially interesting transcription factor as it is highly expressed in adult mouse photoreceptors and influences the expression of rhodopsin, another gene that is highly expressed in rod photoreceptors [18]. Another potentially generally interesting transcription factor is TBP. Though there appears to be a TATA box in the region of interest within the *Sag* promoter, it is further away from the transcriptional start site than TATA boxes are generally considered to be located [19]. The construct with the highest activity is potentially due to the creation of a NEUROD1 binding site. NEUROD1 is known to be involved in photoreceptor maturation and development [20] and it is possible though unconfirmed that in creating a NEUROD1 binding site, the mutant promoter reporter gained increased activity.

In summary, the 5'-upstream region of a number of photoreceptor-specific genes were analyzed for promoter activity in primary retinal cell cultures, and several of them were found to have detectable promoter activity. Further investigation of *Sag*'s 5'-upstream region defined a 97-bp region that was important for *Sag*'s promoter activity. ,

Bioinformatic analysis of this region and siRNA KD of candidate TFs were pursued. Though the exact *trans*-acting factors influencing *Sag* expression in the retina were not identified in this study, a number of potentially involved transcription factors were identified. Future work will hopefully define the putative role of these factors in regulating *Sag* gene expression.

References

1. Corbo, J.C., et al., *A typology of photoreceptor gene expression patterns in the mouse.* Proc Natl Acad Sci U S A, 2007. **104**(29): p. 12069-74.
2. Blackshaw, S., et al., *Genomic analysis of mouse retinal development.* PLoS Biol, 2004. **2**(9): p. E247.
3. Hu, J., H. Hu, and X. Li, *MOPAT: a graph-based method to predict recurrent cis-regulatory modules from known motifs.* Nucleic Acids Res, 2008. **36**(13): p. 4488-97.
4. Fujimaki, T., et al., *Truncation and mutagenesis analysis of the human X-arrestin gene promoter.* Gene, 2004. **339**: p. 139-47.
5. Mohamed, M.K., et al., *Structure and upstream region characterization of the human gene encoding rod photoreceptor cGMP phosphodiesterase alpha-subunit.* J Mol Neurosci, 1998. **10**(3): p. 235-50.
6. Pittler, S.J., et al., *Functional analysis of the rod photoreceptor cGMP phosphodiesterase alpha-subunit gene promoter: Nrl and Crx are required for full transcriptional activity.* J Biol Chem, 2004. **279**(19): p. 19800-7.
7. Young, J.E., et al., *A short, highly active photoreceptor-specific enhancer/promoter region upstream of the human rhodopsin kinase gene.* Invest Ophthalmol Vis Sci, 2003. **44**(9): p. 4076-85.
8. Fujieda, H., et al., *Retinoic acid receptor-related orphan receptor alpha regulates a subset of cone genes during mouse retinal development.* J Neurochem, 2009. **108**(1): p. 91-101.
9. Tang, K., et al., *COUP-TFs regulate eye development by controlling factors essential for optic vesicle morphogenesis.* Development, 2010. **137**(5): p. 725-34.

10. Hu, Y., et al., *Pathogenic role of diabetes-induced PPAR-alpha down-regulation in microvascular dysfunction.* Proc Natl Acad Sci U S A, 2013. **110**(38): p. 15401-6.

11. Jetten, A.M., *Retinoid-related orphan receptors (RORs): critical roles in development, immunity, circadian rhythm, and cellular metabolism.* Nucl Recept Signal, 2009. **7**: p. e003.

12. Escher, P., D.F. Schorderet, and S. Cottet, *Altered expression of the transcription factor Mef2c during retinal degeneration in Rpe65-/- mice.* Invest Ophthalmol Vis Sci, 2011. **52**(8): p. 5933-40.

13. Bassett, E.A., et al., *Overlapping expression patterns and redundant roles for AP-2 transcription factors in the developing mammalian retina.* Dev Dyn, 2012. **241**(4): p. 814-29.

14. Golz, S., et al., *Regulation of RALDH-1, RALDH-3 and CYP26A1 by transcription factors cVax/Vax2 and Tbx5 in the embryonic chick retina.* Int J Dev Neurosci, 2008. **26**(5): p. 435-45.

15. Moran, E., et al., *Protective and antioxidant effects of PPARalpha in the ischemic retina.* Invest Ophthalmol Vis Sci, 2014. **55**(7): p. 4568-76.

16. Sigoillot, F.D. and R.W. King, *Vigilance and validation: Keys to success in RNAi screening.* ACS Chem Biol, 2011. **6**(1): p. 47-60.

17. Buehler, E., Y.C. Chen, and S. Martin, *C911: A bench-level control for sequence specific siRNA off-target effects.* PLoS One, 2012. **7**(12): p. e51942.

18. Chau, K.Y., et al., *The architectural transcription factor high mobility group I(Y) participates in photoreceptor-specific gene expression.* J Neurosci, 2000. **20**(19): p. 7317-24.

19. Smale, S.T. and J.T. Kadonaga, *The RNA polymerase II core promoter.* Annu Rev Biochem, 2003. **72**: p. 449-79.

20. Pennesi, M.E., et al., *BETA2/NeuroD1 null mice: a new model for transcription factor-dependent photoreceptor degeneration.* J Neurosci, 2003. **23**(2): p. 453-61.

Figures

Gene	Cell type	Name
*Opn1mw**	Cone	Opsin 1, medium wavelength sensitive (green) cone opsin
*Pde6h**	Cone	Phosphodiesterase 6H, cGMP-specific
*Pde6c**	Cone	Phosphodiesterase 6C, cGMP specific
Gngt2	Cone	Guanine nucleotide binding protein, gamma transducing activity polypeptide 2
Olfm1	Cone	Olfactomedin 1
Slc24a2	Cone	Solute family carrier 24 (Na/K/Ca exchanger) member 2
*Gnat1**	Rod	Rod transducin alpha subunit
Gnb1	Rod	Guanine nucleotide binding protein, beta 1
*Gucy2d**	Rod	Guanylate cyclase 2d
*Sag**	Both	Retinal S-antigen (rod arrestin)
*Pde6g**	Both	Phosphodiesterase 6G, cGMP-specific
Gngt1	Both	Guanine nucleotide binding protein, gamma transducing activity polypeptide 1
Pdc	Both	Phosducin
*Rs1**	Both	Retinoschisis 1 homolog
*Rom1**	Both	Rod outer segment membrane protein 1
*Abca4**	Both	ATP binding cassette, subfamily A, member 4

Table 1. Initial set of photoreceptor-specific genes chosen to examine. Asterisks indicate genes in which disease causing mutations have been found for various human retinopathies. “Both” means the gene is reported to be expressed in rods and cones.

Gene	Forward Primer	Reverse Primer	Region included
Gnb3	CACCTTGTCAGGGAAATCTCAGC CACCT	ATAAGAGCATCAGCCCAC GGATCA	-675 to -16
Cnga3	CACCAGCCCAAACTTTGACAGGG TAAGG	TTTCCCACTTCCTAGCTCC ACAGT	-837 to +61
Cnga3	CACCAACCAAACAGAAAGAGCT GGGCTG	TTTCCCACTTCCTAGCTCC ACAGT	-532 to +61
Cngb1	CACCGGCCTTGGGTTAAGGTTAG TGGTT	TTTCTAGCTGGCACTCGTC CACAT	-512 to +59
Cngb3	CACCGCCCTGGGTGAGGAGTTTA ACAAT	TGACCCTGTATCTCGAAGA GGAGA	-554 to +47
Gnat1	CACCAAATGAGCACACACACAC ACCCGT	CCCAAAGCCAACAATCAA CTGGCT	-936 to -23
Gnat1	CACCGGAACAGAAAGACACACA TGGGCT	CCCAAAGCCAACAATCAA CTGGCT	-678 to -23
Gnb1	CACCGTTCCTCACTTCTACCCATC CACT	GAGAGGCTTAAAGGACCC GTGATT	-678 to -100
Gngt1	CACCTGTTCAATGTGCTGCAGCG GTTAC	TGCTCACACTGCATACCAG GCTTA	-495 to +1
Gngt2	CACCTTTCCCGTGAGTGGGAAGT GTTCT	TCTGACTTCCTCTTGTCCC GGAAT	-572 to +24
Olfm1	CACCTACAAGTCTTGGCACAGAT ACTGC	CGACGCAATCTGCCCAGG AAAT	-896 to -97
Olfm1	CACCTGTTTAAACCTGCTCCCAC AAGCC	CGACGCAATCTGCCCAGG AAAT	-614 to -97
Opn1mw	CACCAGCAGGAGTCTTTGCTTGG AAGTG	TGGAACCTGTCAGACTTG GCACAT	-839 to +22
Opn1mw	CACCTGGGAGCAATCCTGCTAAC ACACA	TGGAACCTGTCAGACTTG GCACAT	-500 to +22
Pdc	CACCAGCAGACACAATCGGAGA GCTGTA	AGTTTGGGTCTCTGTTCCT GGTGT	-500 to +72
Pde6c	CACCTGGCAGGAATCCTAGCAAC AGAAG	ACCCTGAGCACCATACCA AGGAAA	-760 to +111
Pde6c	CACCAACATGAAGGCCACTGAG AAGGGA	ACCCTGAGCACCATACCA AGGAAA	-443 to +111
Pde6g	CACCAGGCACAGGAAATGGGAC TACACA	TCAGCAGAACACTGGCCT AGGAAT	-425 to +17
Pde6h	CACCTCCTTCCTTATCTGCATGGC TAGG	AGAGCCGAATGTGTTCCC GTAAGT	-921 to +38
Sag	CACCAGACTGGATGGAAAGCCA GCAGAT	TGCCCACTTCAGCAGTTCT AGCAT	-859 to +71
Sag	CACCTGTCTCCATGCAAGAGTGA CAGGA	TGCCCACTTCAGCAGTTCT AGCAT	-494 to +71
Rs1	CACCATGGTGGGAACAGAGAAC TAACCG	ACCTTGAACAGGTTCCTGC TGAGT	-1031 to -13
Rs1	CACCACTGAAACTCGACGTCCAA TGACC	ACCTTGAACAGGTTCCTGC TGAGT	-705 to -13
Rom1	CACCTGTGACACAGTGGTCAGGG AAACT	AATAACCCTCTGCAGGCTC CGATT	-853 to +36
Rom1	CACCACTAGACAGCGGTCCAGCA CTA	AATAACCCTCTGCAGGCTC CGATT	-682 to +36

Abca4	CACCAGCCAGGACCGGTTGATTAGACTT	CCCGCTGTGTCCTTCTGGTGATTAAA	-459 to -5
Slc24a2	CACCGACTCTGGGAAAGCAGGCAAGTAT	CAGGCAAGGGCACAAAGGAGAAAT	-963 to -64
Slc24a2	CACCCGTCTGATGGACTGTAGAGCCAAA	CAGGCAAGGGCACAAAGGAGAAAT	-664 to -64
Gucy2d	CACCACAGCTGGCTCTGTTAACTCCACA	GTTGCCAAGACAACGGCAACCATA	-1167 to -46

Table 2. Primers for initial promoter reporter construction. A series of promoter reporters were created by amplifying upstream regions of genes from genomic DNA from a C57Bl/6 mouse. Forward primers include CACC- overhang necessary for directional cloning into pENTR. Promoter reporters of two different lengths were constructed for some of the genes.

Deletion mutant	Forward Primer	Reverse Primer	Region included
Sag Del 1	CACCTCTGTACTGGGTATAGAGAAGGGC	TGCCCACTTCAGCAGTTCTAGCAT	-429 to + 71
Sag Del 2	CACCCGTGTAGACCCATACTGAACGTGT	TGCCCACTTCAGCAGTTCTAGCAT	-340 to +71
Sag Del 3	CACCTTGGTGTGTAGGGTGAAGGTAAGG	TGCCCACTTCAGCAGTTCTAGCAT	-279 to +71
Sag Del 4	CACCGCTTAATCAGGCCTGTCAGTCGAA	TGCCCACTTCAGCAGTTCTAGCAT	-181 to +71
Sag Del 5	CACCGGTGAAGAGCGAAAGGATAAGCCA	TGCCCACTTCAGCAGTTCTAGCAT	-138 to +71
Sag Del 6	CACCATTCCTCTCTTTGCACCTTGCCCA	TGCCCACTTCAGCAGTTCTAGCAT	-37 to + 71

Table 3. PCR primers for *Sag* deletion series construction. A series of 6 deletion mutants were created by amplifying progressively smaller regions of the promoter series from genomic DNA from a C57Bl/6 mouse. Forward primers include CACC- overhang necessary for directional cloning into pENTR. The same reverse primer was used for all constructs.

Forward Primer	Reverse Primer	Region mutated
GAGGGCCCAACAGAACTCGGTTGTG TGCGGGTGAAGGTAAGGGCC	GGCCCTTACCTTCACCCGCACACA ACCGAGTTCTGTTGGGCCCTC	-279 to -270
CAGAACTCTTGGTGTGTATTTGTCCT TGAAGGGCCACGTGCAGCC	GGCTGCACGTGGCCCTTCAAGGAC AAATACACACCAAGAGTTCTG	-269 to -260
GGTGTGTAGGGTGAAGGTCCTTTAA CATTGCAGCCCAGCCCTGGG	CCCAGGGCTGGGCTGCAATGTTAA AGGACCTTCACCCTACACACC	-259 to -250
TGAAGGTAAGGGCCACGGTACTAAA CTCCCTGGGCTGACCTTTC	GAAAGGTCAGCCCAGGGAGTTTAG TACCGTGGCCCTTACCTTCAC	-249 to -240
GGGCCACGTGCAGCCCAGAAAGTTT AGTACCTTTCTCCTTGACCT	AAGGTCAAGGAGAAAGGTACTAAA CTTTCTGGGCTGCACGTGGCC	-239 to -230
CAGCCCAGCCCTGGGCTGCAAGGGA GAATTGACCTTTTTCTTTAT	ATAAAGAAAAAGGTCAATTCTCCC TTGCAGCCCAGGGCTGGGCTG	-229 to -220
CTGGGCTGACCTTTCTCCGGTCAAG GGGTCTTTATATAACACCCT	AGGGTGTTATATAAAGACCCCTTG ACCGGAGAAAGGTCAGCCCAG	-219 to -210
CTTTCTCCTTGACCTTTTGAGGGCGC GCACACCCTAATGCTGCTG	CAGCAGCATTAGGGTGTGCGCGCC CTCAAAAGGTCAAGGAGAAAG	-209 to -200
GACCTTTTTCTTTATATACACAAAGC CGGCTGCTGAGCTTAATCA	TGATTAAGCTCAGCAGCCGGCTTT GTGTATATAAAGAAAAAGGTC	-199 to -190
TTTATATAACACCCTAATTAGTAGTC TATTAATCAGGCCTGTCAG	CTGACAGGCCTGATTAATAGACTA CTAATTAGGGTGTTATATAAA	-189 to -180

Table 4. PCR primers for scanning mutagenesis of *Sag* promoter -279 to -158 bp. A series of mutants were made using site directed mutagenesis within the full length construct created for the deletion series (-429 to + 71). Ten to 11 bases were mutated at a time within the construct.

Gene	Company	Product	Product #	Modified or unmodified	RNA Oligo Sequence
Coup1	Ambion	Silencer Select	s14020	Modified	UCUCAUCCGCGAUAUG UUAtt
Coup1	Ambion	Silencer Select	s224723	Modified	GCGGUUCAGCGAGGAA GAAtt
Coup1	Ambion	Silencer Select	s14018	Modified	ACAUUAUGGGCAUCGA GAAtt
Coup2	Ambion	Silencer Select	s14021	Modified	GCUUUGGAAGAAUACG UUAtt
Coup2	Ambion	Silencer Select	s14022	Modified	CGCCUUUAUGGACCAC AUAtt
Coup2	Ambion	Silencer Select	s14023	Modified	CCUCCUCAGUCAUAGA GCAtt
Coup1	Ambion	Silencer	66695	Unmodified	GGCCAGUAUGCACUCA CAAtt
Coup1	Ambion	Silencer	66605	Unmodified	GGAACUUAACUUACAC AUGtt
Coup1	Ambion	Silencer	66781	Unmodified	GGACCAUGAGAAAUUU AAUtt
Coup2	Ambion	Silencer	65809	Unmodified	GGAAAAGUCCCAGUGU GCUtt
Coup2	Ambion	Silencer	282808	Unmodified	GGCAAAAGACUGGUUU UGUtt
Coup2	Ambion	Silencer	282809	Unmodified	GCUUGCAGGAAAAGUC CCAtt
Ppara	Ambion	Silencer	151210	Unmodified	CGACCUGAAAGAUUCG GAAtt
Ppara	Ambion	Silencer	151211	Unmodified	GGCUAAUAGGAUUCAG ACAtt
Rora	Ambion	Silencer	151977	Unmodified	GGUGGUGUUUAUUAGG AUGtt
Rora	Ambion	Silencer	151978	Unmodified	GCCAUGCAAAUCGAUG GGUtt
Rora	Ambion	Silencer	71274	Unmodified	GGUAUCUCAGUCACGA AGAtt

Table 5. siRNAs used to knockdown transcription factors in primary mouse retinal cells. Multiple siRNA oligos for each transcript were used.

Gene	Forward Primer	Reverse Primer
Beta-actin	CTAAGGCCAACCGTGAAAAG	ACCAGAGGCATACAGGGACA
Coup1	CCTCAAAGCCATCGTGCTATTCAC	GATTTCTCCTGCAGGCTTTCGATG
Coup2	ACTCTTCCAAAGCACACTGGGACT	TCCAAGAGCAAGTGGAGAAGCTCA
Ppara	ATGCCAGTACTGCCGTTTTC	GGCCTTGACCTTGTTCATGT
Rora	GTGGAGACAAATCGTCAGGAAT	TGGTCCGATCAATCAAACAGTTC
Sag	TGAAGCCTCCTGGCAGTTCTTCAT	CACAACCTTGTCGGTGTTGTTGGT

Table 6. qPCR primers. All primers were designed to amplify mouse sequence. Primers sequences came from RT Primer database (http://medgen.ugent.be/rtprimerdb/) or designed with Roche's primer design algorithm (http://lifescience.roche.com/shop/CategoryDisplay?catalogId=10001&tab=Assay+Design+Center&identifier=Universal+Probe+Library&langId=-1#tab-3).

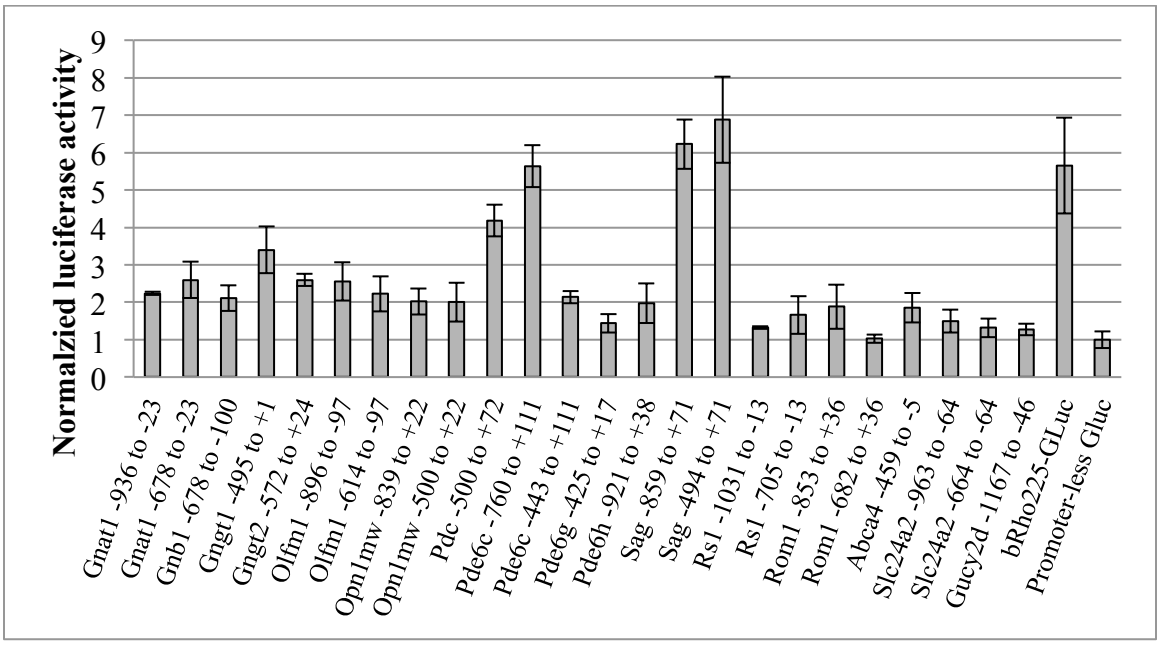

Figure 1. Normalized luciferase activity of photoreceptor gene promoter reporters in whole retinal cells. Data demonstrate that both *Sag* promoter reporters have the highest activity. Numbers indicate 5' upstream region that was included in relation to the transcriptional start site (TSS = +1). Luciferase activity was assayed in aliquots of media taken seven days post-electroporation. Promoter reporters expressed Gaussia luciferase, which was normalized to a co-transfected bovine rhodopsin promoter reporter expressing Cypridina luciferase (bRho225-Cluc). Bars represent the averages (with standard deviations) of four replicates.

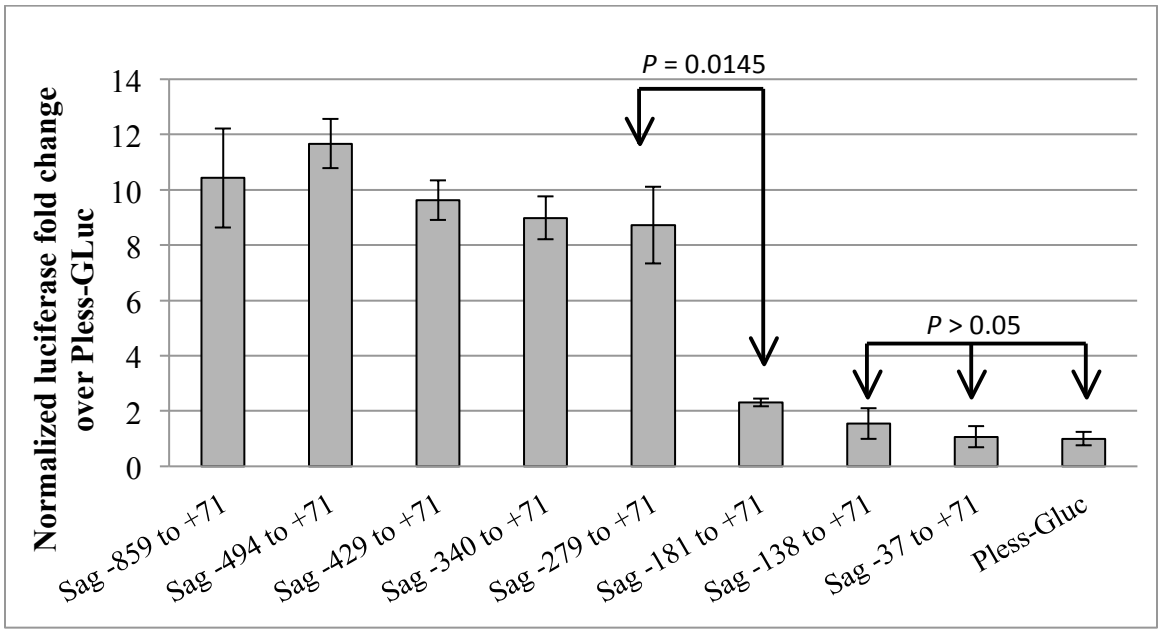

Figure 2. Sag deletion series. Data demonstrate the normalized luciferase activity of a series of deletion mutants of the S-antigen promoter region in dissociated early post-natal mouse whole retinal cells. Aliquots of media were taken at seven days post-electroporation and assayed for luciferase activity. The activity of the Gaussia luciferase expressed by the deletion mutants was normalized to a co-transfected Cypridina luciferase expressing full length Sag promoter reporter and then normalized to a promoterless-Gaussia luciferase construct (Pless-Gluc). The activity of the deletion mutants dropped significantly when -278 to -182 (and beyond) was not included. Bars represent the average (with standard deviations) of triplicates. *P* values from Student's *t* test.

Figure 3. Predicted transcription factor binding sites within the region of interest (-279 to -180 bp) within the *Sag* promoter according to a MOPAT analysis. The figure was prepared with Geneious software.

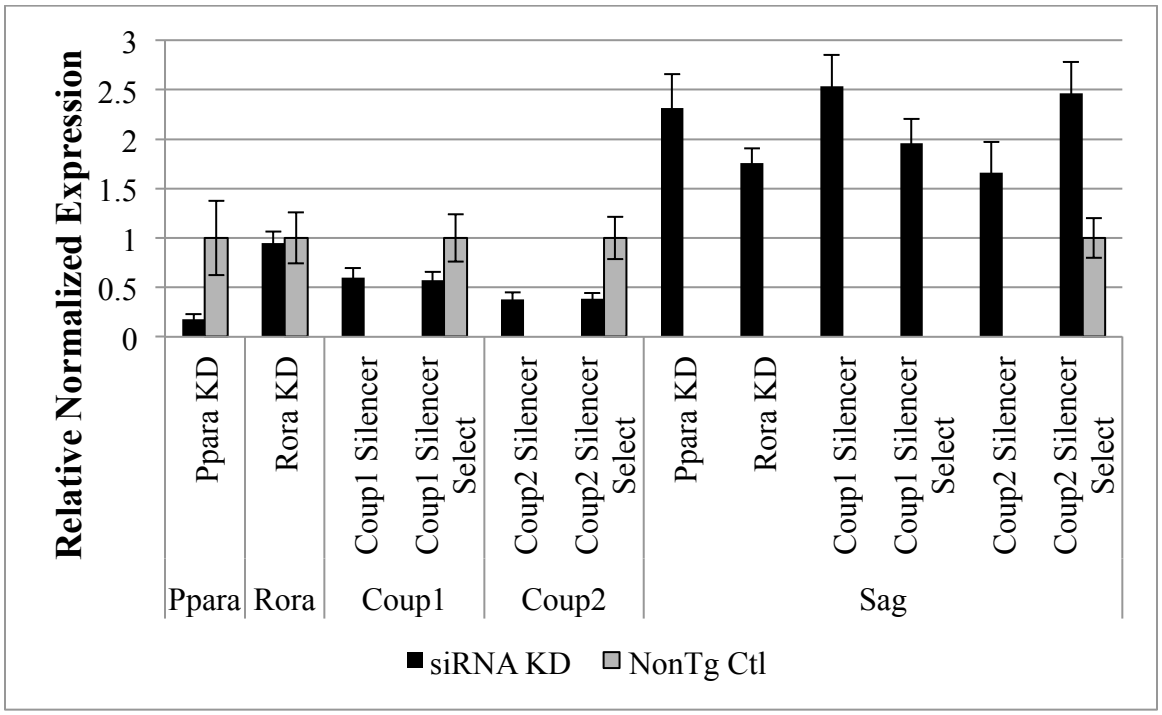

Figure 4. siRNA KD of *Ppara, Rora, Coup1* and *Coup2* did not decrease *Sag* expression in dissociated mouse retinal cells. siRNA KD was accomplished with pools of several different oligos for each target and was successful at decreasing the expression of *Ppara, Coup1* and *Coup2*. Bars represent the average of technical triplicates from pools of biological triplicates with the standard errors of the mean. Target gene expression was normalized to the expression of *beta-actin*.

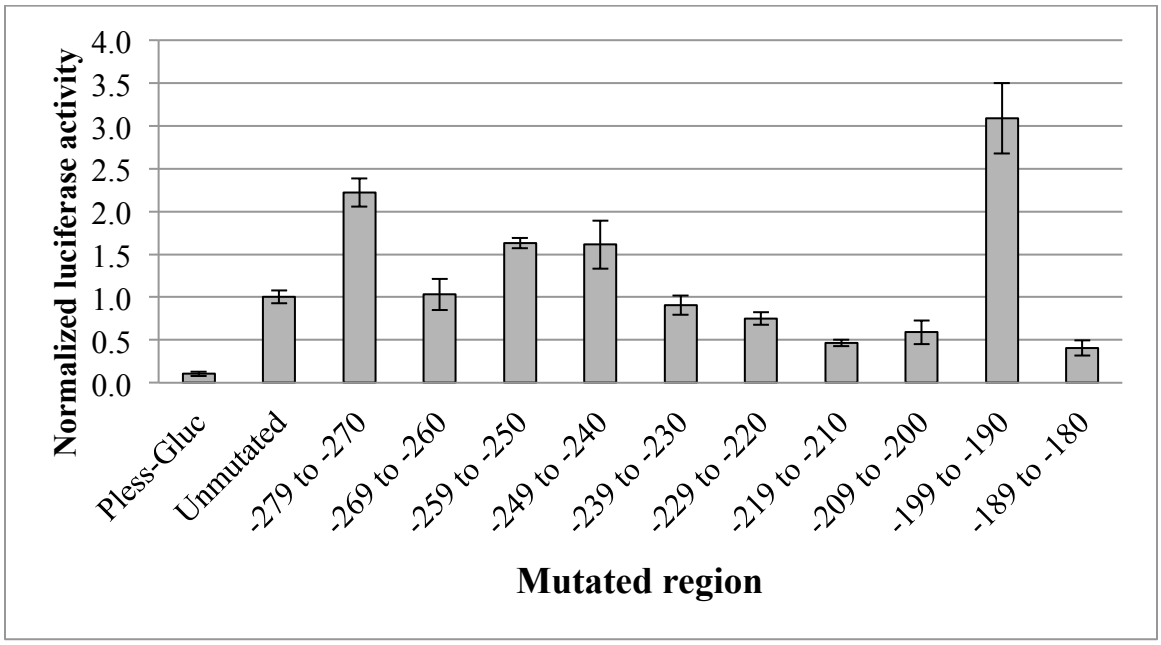

Figure 5. Scanning mutagenesis of the *Sag* region of interest (-279 to -180 bp). Data demonstrate the normalized luciferase activity of *Sag* promoter mutants created by scanning mutagenesis of 10 bp stretches within the area of interest (-279 to -180 bp), which was identified in the deletion series. Transversions were introduced into each nucleotide position within the 10 bp region. Some mutations were activating and some were repressing compared to the unmutated construct. The bars represent the average of triplicate wells with standard deviations.

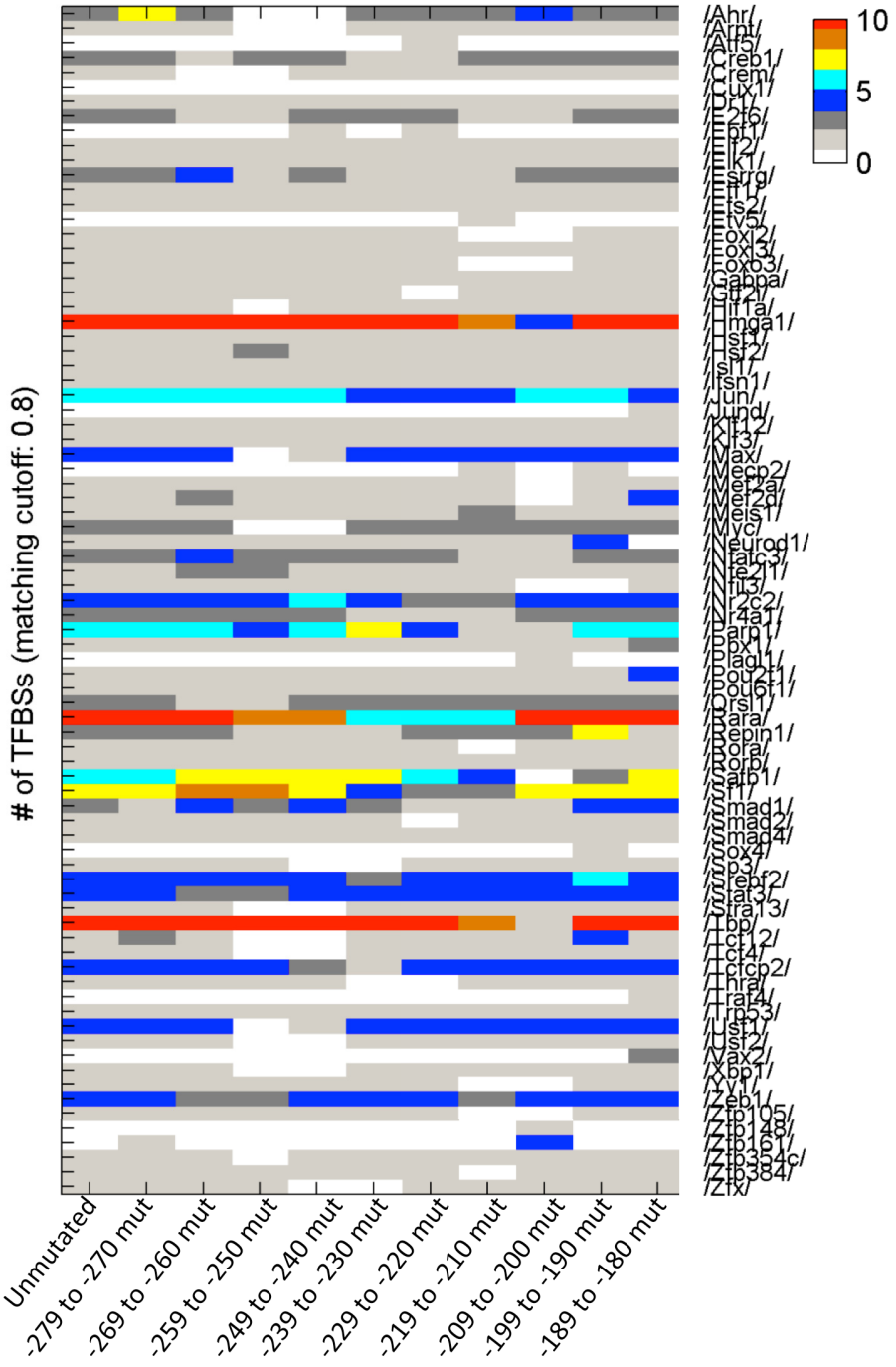

Figure 6. Predicted binding sites of transcription factors in the various binding site mutants from a TRANSFAC analysis. Specifically, this analysis examines the change

in predicted TFBSs in the various mutants, which might help explain the activities of the various mutants.

Part II: Neuroprotection of Photoreceptors

Introduction

Retinal degeneration (RD) encompasses a group of genetically and clinically heterogeneous disorders that primarily affect photoreceptor (PR) and/or retinal pigment epithelial (RPE) cells and lead to progressive vision loss. The age of clinical onset and degree of disease severity varies significantly, ranging from severe symptoms at birth to only mild symptoms in the sixth and seventh decades of life. Two major types of RD are Leber congenital amaurosis (LCA), in which infants can demonstrate profound vision loss, and retinitis pigmentosa (RP), which is generally not clinically evident until later in childhood or in early adulthood. To date, 212 genes have been identified as having causative mutations in the various forms of RD with 40 additional loci being linked to RD (https://sph.uth.edu/RetNet/). LCA and RP are orphan diseases, affecting 1 in 81,000 and 1 in 4,000 individuals, respectively [1, 2]. In general, with a few exceptions, the RDs are untreatable.

Age-related macular degeneration (AMD) and diabetic retinopathy are two other important diseases that affect photoreceptors. Both diseases have an increased prevalence in older adults compared to the general population [3]. Much of the resulting vision loss in these two diseases is due to abnormal vascular growth. While there are treatments to slow and even reverse the abnormal vessel growth, including most importantly anti-VEGF therapy, no specific treatment exists to support the photoreceptors.

Vision loss and blindness from the aforementioned diseases is ultimately a result of dysfunction and death of retinal PRs, which are the cells responsible for the remarkable conversion of light energy into an electrochemical signal (recently reviewed by Sung & Chuang [4]). A complex, but very well characterized, signal transduction

pathway with many components is responsible for this light to electrochemical energy conversion. Mutations in many of the genes encoding components of this pathway have been implicated in RP and LCA. RPE cells are involved in the recycling of the vitamin A derivative, retinal, and its shuttling back to the photoreceptors (the visual cycle); thus, mutations in genes encoding important RPE proteins can also cause RD.

Though the vision-threatening end result of the RDs and other non-specific retinal degenerative diseases is all the same (death of PRs), there is much debate over the exact mechanisms leading to PR death. A number of different and often opposing mechanisms for photoreceptor cell death in retinal degenerative diseases have been proposed and studied. One of the challenges in this field is that there are a large number of diverse diseases, caused by mutations in an even larger number of genes that affect photoreceptors that are modeled by a large number of different animal models. Therefore, findings of one model can rarely be generalized to all forms of retinal degeneration and there are often very different findings in the various models suggesting very different mechanisms of cell death. Initial morphologic studies into photoreceptor cell death in retinal degenerations concluded that apoptosis was the final common pathway causing cell death [5]. Since then, photoreceptor death in retinal degenerative diseases has been further studied molecularly and a number of distinct apoptotic and non-apoptotic mechanisms have been identified (reviewed by Sancho-Pelluz et al [6] and Marigo [7]). One of the pathways leading to photoreceptor apoptosis is endoplasmic reticulum stress and the unfolded protein response (UPR) (reviewed by Jing et al [8] and Wang [9]). Parthanatos, in which an over-activation of poly-ADP ribose polymerase (PARP) leads to photoreceptor death, is another recently proposed mechanism [10].

The vast majority of the RDs are untreatable, though advances in various treatment modalities have recently made successful therapy a possibility. Gene therapy has made the most recent progress in improving vision [11]. Several canine and human gene therapy trials have been completed or are underway to treat LCA due to mutations in Rpe65, a gene expressed in RPE cells, and they have shown encouraging results [12-14]. However, since gene therapy is generally designed to target a specific mutated gene, most existing and planned gene therapy approaches for the RDs will only be useful for a small number of patients.

Other potential treatments for RD patients include the use of trophic factors and small molecules as neuroprotective agents directed at increasing PR cell survival. For example, both brain-derived and ciliary neurotropic factors (BDNF & CNTF) have been shown to support photoreceptors in retinal degeneration models [15, 16], and CNTF has been tested in human clinical trials and has shown some possible success [17]. One example of a small molecule showing suggestive efficacy is rasagiline treatment in a mouse model of RD, which was shown to delay outer nuclear layer (photoreceptor cell bodies) degeneration [18]. In an effort to further develop small molecule-based neuroprotective therapies for the RDs, I have been testing protein kinase inhibitors and PARP inhibition in animal RD models.

References

1. Berson, E.L., *Retinitis pigmentosa. The Friedenwald Lecture.* Invest Ophthalmol Vis Sci, 1993. **34**(5): p. 1659-76.
2. Stone, E.M., *Leber congenital amaurosis - a model for efficient genetic testing of heterogeneous disorders: LXIV Edward Jackson Memorial Lecture.* Am J Ophthalmol, 2007. **144**(6): p. 791-811.
3. Klein, R. and B.E. Klein, *The prevalence of age-related eye diseases and visual impairment in aging: current estimates.* Invest Ophthalmol Vis Sci, 2013. **54**(14): p. Orsf5-orsf13.
4. Sung, C.H. and J.Z. Chuang, *The cell biology of vision.* J Cell Biol, 2010. **190**(6): p. 953-63.
5. Chang, G.Q., Y. Hao, and F. Wong, *Apoptosis: final common pathway of photoreceptor death in rd, rds, and rhodopsin mutant mice.* Neuron, 1993. **11**(4): p. 595-605.
6. Sancho-Pelluz, J., et al., *Photoreceptor cell death mechanisms in inherited retinal degeneration.* Mol Neurobiol, 2008. **38**(3): p. 253-69.
7. Marigo, V., *Programmed cell death in retinal degeneration: targeting apoptosis in photoreceptors as potential therapy for retinal degeneration.* Cell Cycle, 2007. **6**(6): p. 652-5.
8. Jing, G., J.J. Wang, and S.X. Zhang, *ER stress and apoptosis: a new mechanism for retinal cell death.* Exp Diabetes Res, 2012. **2012**: p. 589589.
9. Wang, T. and J. Chen, *Induction of the Unfolded-Protein Response by Constitutive G-protein Signaling in Rod Photoreceptor Cells.* J Biol Chem, 2014.

10. Paquet-Durand, F., et al., *Excessive activation of poly(ADP-ribose) polymerase contributes to inherited photoreceptor degeneration in the retinal degeneration 1 mouse.* J Neurosci, 2007. **27**(38): p. 10311-9.

11. Petrs-Silva, H. and R. Linden, *Advances in gene therapy technologies to treat retinitis pigmentosa.* Clin Ophthalmol, 2014. **8**: p. 127-136.

12. Jacobson, S.G., et al., *Gene therapy for leber congenital amaurosis caused by RPE65 mutations: safety and efficacy in 15 children and adults followed up to 3 years.* Arch Ophthalmol, 2012. **130**(1): p. 9-24.

13. Testa, F., et al., *Three-year follow-up after unilateral subretinal delivery of adeno-associated virus in patients with Leber congenital Amaurosis type 2.* Ophthalmology, 2013. **120**(6): p. 1283-91.

14. Annear, M.J., et al., *Successful gene therapy in older Rpe65-deficient dogs following subretinal injection of an adeno-associated vector expressing RPE65.* Hum Gene Ther, 2013. **24**(10): p. 883-93.

15. LaVail, M.M., et al., *Protection of mouse photoreceptors by survival factors in retinal degenerations.* Invest Ophthalmol Vis Sci, 1998. **39**(3): p. 592-602.

16. Azadi, S., et al., *CNTF+BDNF treatment and neuroprotective pathways in the rd1 mouse retina.* Brain Res, 2007. **1129**(1): p. 116-29.

17. Birch, D.G., et al., *Randomized trial of ciliary neurotrophic factor delivered by encapsulated cell intraocular implants for retinitis pigmentosa.* Am J Ophthalmol, 2013. **156**(2): p. 283-292.e1.

18. Eigeldinger-Berthou, S., et al., *Rasagiline interferes with neurodegeneration in the Prph2/rds mouse.* Retina, 2012. **32**(3): p. 617-28.

Chapter 1: Exploration of the ability of protein kinase inhibitors to promote photoreceptor survival in murine models of retinal degeneration

Introduction

Previous work in the Zack lab using phenotypic screens of primary rodent retinal ganglion cells (RGCs) to identify neuroprotective compounds identified a number of promising small molecules. One of the identified molecules, sunitinib, is a multiple protein kinase inhibitor that is an FDA approved cancer chemotherapeutic agent. Sunitinib has been shown to promote RGC survival both *in vitro* and in rodent optic nerve injury and glaucoma models (Zhiyong Yang, unpublished data).

Although sunitinib had very clear RGC survival promoting effects, it was unknown which of the many kinases it inhibits accounted for its neuroprotective activity. A study by Welsbie et al. using a kinome-wide small interfering RNAs (siRNAs) screen with primary mouse RGCs identified DLK (MAP3K12) as an important mediator of RGC death [1]. The c-Jun N-terminal kinase (JNK) has been shown to be involved in the death of RGCs in several studies [2-5], and there is evidence that DLK activates JNK after RGC injury, which promotes apoptosis [1, 6]. JNK activation has also been implicated in photoreceptor apoptosis [7, 8]. DLK is a sunitinib target [9] and it was indirectly implicated to be one of sunitinib's neuroprotective targets (Zhiyong Yang, unpublished data).

The goal of this project was to evaluate sunitinib's ability to protect photoreceptors in models of photoreceptor injury and to determine whether DLK is involved in photoreceptor degeneration.

Materials & Methods

All animals used in this research were treated in accordance with the ARVO statement for the use of animals in vision research and all protocols were approved by Johns Hopkins' institutional animal care and use committee.

Kinase inhibitor intravitreal injections

Rodent – sunitinib

A collaboration was established with Matthew LaVail at University of California in San Francisco where sunitinib was tested intravitreally in two rat models of autosomal dominant retinal degeneration (Rho S334ter and Rho P23H mutants). All animal husbandry, handling, treatments, tissue processing and morphological evaluation were performed at that institution. Rat pups were anesthetized with isoflurane and injected intravitreally with a Hamilton syringe (catalog #80337, Hamilton, Reno, NV) either once at p9 or twice at p9 and p12 (for Rho S334ter rats) and at p15 (for Rho P23H rats) with 2 μL of sunitinib solution (see doses below). Animals were sacrificed at p19 and eyes were enucleated and fixed in a mixture of 2.5% glutaraldehyde and 2% paraformaldehyde. Globes were embedded in epoxy resin, and 1 μm thick sections were made along the vertical axis.

At Johns Hopkins University, hemizygous Rho Q344ter mouse [10] pups and homozygous *rd1* mouse pups between 10 and 11 days of age were anesthetized with a 20% isoflurane/propylene glycol mixture and their eyelids were gently opened with curved forceps. The globe was proptosed and a hole made 0.5 to 1 mm behind the limbus with the tip of a 30 gauge needle in the upper temporal quadrant. The tip of a pulled glass

pipette containing drug solution was inserted into the hole and 1 μL of solution was injected using a pneumatic injector. Then the globe was replaced and triple antibiotic ophthalmic ointment was applied to the eyelids. Either uninjected or vehicle injected eyes served as untreated controls. The pups were allowed to recover in a heated box until they were mobile and then returned to the cage with their mothers, which was usually within 15 minutes. At 17 or 18 days of age, the pups were anesthetized with isoflurane and then cervically dislocated. Globes were removed and fixed in either Bouin's fixative overnight at room temperature or 4% PFA overnight at 4 ^{o}C. Globes were processed routinely, paraffin embedded, sectioned at 5 μm and stained with hematoxylin and eosin stain (H&E).

Rodent – DLK inhibitor

Rho S334ter rat pups were injected with the DLK inhibitor at UCSF by Matt LaVail at p8 and sacrificed at p19.

Hemizygous Rho Q344ter and homozygous *rd1* mouse pups were injected with the DLK inhibitor at JHU at p11 and sacrificed at p17. There were only enough *rd1* pups to test one dose.

Pigs

In collaboration with Henry Kaplan at University of Louisville in Kentucky, a slow-release formulation of sunitinib was tested intravitreally in a transgenic minipig model of an autosomal dominant retinitis pigmentosa (RhoP23H) [11]. All animal housing, handling, dosing and testing was done at the University of Louisville. The piglets were either injected twice at p3 and p17 (five transgenic and three wild type) or injected once at p14 (six transgenic) and then all were sacrificed at p30. The left eye was

injected with sunitinib-containing microspheres at three different concentrations (1.056 μg sunitinib/μL, 0.264 μg sunitinib/μL, 0.066 μg sunitinib/μL) and the right eye was injected with solutions containing the same amount of microspheres as the sunitinib loaded solutions. P3 animals received 50 μL of microsphere solutions and p14 and p17 animals received 75 μL to adjust for eye growth. After euthanasia and enucleation, corneas were incised to allow for better fixation and globes submersion fixed in 4% PFA at 4 ^{o}C. Globes were processed routinely, paraffin embedded, sectioned at 5 μm and stained with H&E stain.

Systemic treatment

Rho Q344ter and rd1 pups

Intraperitoneal injections of sunitinib or vehicle (DMSO in PBS) were administered daily to pups from age p6 to p14. Pups were weighed daily to monitor growth and to dose them appropriately. Doses of sunitinib were 0, 5, 10, 15 (once daily) and 30 (every other day), 30 and 50 (daily) mg/kg. Pups were euthanized with isoflurane followed by cervical dislocation, enucleated and globes were fixed in 4% PFA overnight at 4 ^{o}C. Globes were processed routinely for paraffin embedding. Only one eye from each animal was embedded, sectioned at 5 μm and stained with H&E for morphological analysis.

Retinal analysis

Slides were imaged at 100x with a Zeiss Axioplan 2 imaging system (Carl Zeiss Microscopy LLC, Thornwood, NY) and layer thicknesses were measured using Image J

(Abramoff 2004) for the sunitinib dosing. For the new DLK inhibitor evaluation, layers of nuclei in the ONL were counted manually in the retinas.

Rats

The mean ONL thickness was obtained by taking an average of a total of 54 measurements from the superior and inferior hemispheres (27 per hemisphere) using the Bioquant Morphometry System (R&M Biometrics, Nashville, TN).

Mice

Three points between the optic nerve head (ONH) and the limbus were measured and averaged on both sides of the ONH for a total of six measurements per eye. For each point, the thickness of the outer nuclear layer (ONL) and the thickness of the outer border of the ONL from the inner border of the inner nuclear layer (INL) were measured. To avoid artifacts of a distorted retinal section, the ratio of the ONL to the ONL-INL measurement was reported.

Pigs

Generally, twenty-four images were taken of each retina, two images from each of six points above and below the optic nerve head. Within each image, the retinal layers were measured (ONL and ONL-INL) at five points. Thus each location was measured ten times and then averaged. Some retinas could not be measured at all points due to artifact, which typically affected the more peripheral locations.

Drug formulations

Sunitinib malate (catalog # S-8803, LC Laboratories, Woburn, MA) was dissolved in DMSO and then further diluted in sterile PBS for injection. Intravitreal

injections in rats were 2 μL of 2, 10 and 20 mg/mL in 50% DMSO. Intravitreal injections in mice were 1 μL of either 0.156, 0.625, 2.5 or 10 mg/mL or 5, 10 and 20 mg/mL in 50% DMSO.

Sunitinib malate was formulated with PLGA (poly(lactic-co-glycolic acid)) into slow release microspheres (collaboration with Justin Hanes), which were used in the minipig injections.

A new potent DLK inhibitor was developed and the information was released as a publicly available patent. Colleagues synthesized it and it was tested intravitreally at UCSF and JHU. Two doses were tested in rats (2 mM and 0.4 mM) and 3 in mice (0.5, 5 and 50 μg).

DLK western blotting

Mice of various ages were euthanized via isoflurane followed by cervical dislocation, enucleated and retinas dissected in PBS. Individual retinas were homogenized in PBS and then an equal volume of Laemmli buffer (catalog # 1610737, BioRad Laboratories, Hercules, CA) with β-mercaptoethanol was added and homogenized and vortexed. Homogenates were stored at -80 ^{o}C and thawed when needed, heated to 100 ^{o}C for 5 minutes and then quantified using the EZQ™ Protein Quantitation Kit (catalog # R33200, Life Technologies, Carlsbad, CA). Samples were diluted to be approximately the same concentration, run in precast polyacrylamide gels (catalog # 345-0027, BioRad Laboratories, Hercules, CA) and transferred to a nitrocellulose membrane (catalog # RPN203D, GE Healthcare, Pittsburgh, PA) using a

Criterion™ Cell/Plate Blotter System (catalog #165-6024, BioRad Laboratories, Hercules, CA). Each lane represents a retina from a single individual.

Blots were blocked in TBST (TBS with 0.1% Triton X-100 (catalog # 11332481001, Roche, Indianapolis, IN)) with 5% milk, washed and then individual primary antibodies were diluted in TBST with 5% milk and applied overnight at 4 ^{o}C. Primary antibody was washed in TBST, and then secondary antibody diluted in TBST with 5% milk was applied for one hour at room temperature and then washed in TBST. Blots were developed with SuperSignal Femto West Substrate (catalog # 34095, ThermoScientific, Waltham, MA) and imaged with an ImageQuant LAS4000 system (GE Healthcare, Pittsburgh, PA). Band densities were measured with Image J (Abramoff 2004). Blots were stripped with Restore™ Western Blot Stripping Buffer (catalog # 21059, ThermoScientific, Waltham, MA). Antibodies included: anti-Map3k12 (catalog # NBP2-17218, Novus Biologicals, Littleton, CO), anti-Gapdh (catalog # ab8245, Abcam, Cambridge, MA) and HRP-linked anti-mouse and HRP-linked anti-rabbit (catalog #s 7076 & 7074 respectively, Cell Signaling Technology, Danvers, MA).

Statistical tests

Rat retinal thicknesses were analyzed with paired T tests.

Mouse retinal thickness measurements were analyzed by multilevel linear mixed effects models with a random intercept for the animal to account for the correlations among the repeated measures from the same animal.

Results

Based upon sunitinib's neuroprotective effect on RGCs, we wanted to test the hypothesis that sunitinib might also promote photoreceptor survival. In collaboration with Dr. Matt LaVail (UCSF), sunitinib was tested in the rat transgenic autosomal dominant rhodopsin mutation (Rho S334ter) retinal degeneration model, which mimics the mutation in a form of human retinitis pigmentosa. The retinas of Rho S334ter rats are morphologically normal from birth to p10, at which point they begin to degenerate [12]. Wild-type and Rho S334ter rats were injected intravitreally with sunitinib, either once at P9 or at both P9 and P12. The highest dose of sunitinib (20 mg/mL) showed neuroprotective effects evidenced by a slowing of the rate of degeneration in the treated rats (Figure 1). The protective effect was more pronounced when rats received two injections (p9 and p12). Figure 1 shows retinal sections from representative rats and demonstrates that untreated retinas (A) only have one to two rows of nuclei in the ONL whereas twice-injected retinas (B) have three to four rows remaining. Some treated retinas had up to six rows of nuclei in the ONL (data not shown). A spider plot showing ONL thickness measurements at 21 points across the retina demonstrates that the twice-injected retinas have a thicker ONL at all points measured. With all of the treated and untreated retinas combined, there was an overall statistically significant difference in ONL thicknesses between the two sets of retinas (Table 1) for both the once and twice injected eyes. Some sunitinib-treated and DMSO injected control eyes developed rosette-like structures in the outer nuclear layer (Figure 1 D).

Given the data demonstrating that sunitinib is neuroprotective for both RGCs and photoreceptors, that DLK inhibition promotes RGC survival, and that sunitinib is a potent

DLK inhibitor, it seemed reasonable to hypothesize that inhibition of DLK might also be neuroprotective for photoreceptor cells. To explore this hypothesis, I measured DLK expression in degenerating retinas. Figure 2 shows a western blot and the densitometric quantification of the amount of DLK protein in a time course of degenerating retinas from *rd1* and hemizygous Rho Q344ter and age matched wild type mice. The results demonstrate that in both of the older ages in both RD models, there is increased DLK protein in the degenerating retinas compared to the age matched normal control retinas. It also demonstrates that at a point when very few rods remain in the *rd1* retina (p20), there is still an elevated amount of DLK present, suggesting that DLK is being expressed by cells in addition to or other than rod photoreceptors. Additional western blots of degenerating retinal lysates run with 24 hours-in-culture RGC lysates as a positive control showed that the DLK present in whole retinal lysates ran slightly faster than the DLK present in RGCs (Figure 3).

Given the elevation of DLK protein in degenerating mouse retinas and the evidence of neuroprotection of intravitreal sunitinib in the Rho S334ter rats, we designed and carried-out a number of experiments to test for neuroprotection in mouse models of retinal degeneration. Initially, we tested systemic drug administration. Sunitinib was administered intraperitoneally to homozygous *rd1* and hemizygous Rho Q344ter mice. The first experiment used relatively high drug doses (30 and 50 mg/kg daily) and the pups did not survive long enough to evaluate their retinas at a point when neuroprotection could be evaluated (data not shown). The next attempt included lower doses (5, 10, 15 mg/kg daily and 30 mg/kg every other day). Figure 4 shows the ratio of the ONL to ONL-INL measurement in one eye from each pup. There were no statistically significant

differences in any of the treatment groups, though there appeared to be a slight trend toward increased ONL thickness in the treatment group.

Given that lack of sufficient drug delivery to the retina when administered systemically was one possible explanation as to why no neuroprotection was observed, we next pursued intravitreal injection. Figures 5 and 6 show the ratios of ONL to ONL-INL layer thicknesses from two different experiments in which sunitinib was injected intravitreally. There were no significant differences in the means of any of the treatment groups in either experiment. Multiple eyes from those reported in Figure 5 had injection artifacts including cataract, debris and inflammatory cells in the vitreous, pre-retinal fibrovascular membrane, focal retinal thinning and occasional retinal rosettes. The eyes reported in Figure 6 had no artifacts attributed to the injections, but also did not show any protective effect with any of the tested doses of sunitinib. A possible explanation for the lack of observed neuroprotection in these experiments is that due to pharmacokinetic issues, even thought a single injection was protective in the rat Rho S334ter model, a single injection may not provide sufficient sustained levels of drug over time in the mouse eye.

An opportunity arose to try a slow-release formulation of sunitinib (sunitinib loaded PLGA microspheres, collaboration with Dr. Justin Hanes) in a mini-pig model of autosomal dominant rhodopsin mutation (Rho P23H) in collaboration with Henry Kaplan at the University of Louisville [11]. When the pigs were evaluated with spectral domain optical coherence tomography (SD-OCT) the injected bolus of microspheres was visualized as a focal opaque accumulation of material in the vitreous in the pigs that received the highest dose of microspheres. These accumulations of microspheres were

still visible when the eyes were hemisected for processing. Though some regions of the retinas (mostly peripheral) showed significant differences between right (blank microspheres) and left (sunitinib-containing microspheres), there were no consistent differences across the entire retina of any individual. Figure 7 shows representative data from two pigs (one wildtype and one transgenic) that received the highest dose of sunitinib.

Because of the interest in DLK as a neuroprotective agent, additional DLK inhibitors have been developed. A new potent DLK inhibitor was synthesized at JHU based upon a published patent application and tested in both Rho S334ter rats (through the collaboration with Dr. LaVail) and in the Rho Q344ter mice at JHU. There was a small but significant difference in the rat eyes that received the 2 mM dose compared to the uninjected eyes ($P = 0.0460$), but not the 0.4 mM dose (Table 2 and Figure 8). There was no significant difference in any of the doses compared to the uninjected eyes in the Rho Q344ter mice ($P > 0.05$); however, there was a significant difference in the *rd1* eyes that received 5 μg compared to those that were uninjected ($P = 0.033$) (Figure 9).

Discussion

Sunitinib is a multiple kinase inhibitor that showed promising neuroprotective effects in retinal ganglion cells (RGCs) both *in vitro* and *in vivo* (Zhiyong Yang unpublished data). This led to a collaboration with Dr. Matthew LaVail, which showed that sunitinib also exhibited promising and statistically significant PR survival promoting activity in the context of photoreceptor degeneration in the Rho S334ter rat, a model of autosomal dominant retinitis pigmentosa (Table 1 and Figure 1). As the function of the

photoreceptors was not evaluated in this study, it is unknown if there was any rescue of photoreceptor function. The dose that had neuroprotective effects (2 μL of 20 mg/mL) was extremely high, and given that it was not administered as a slow release formulation, its success is surprising. There were some signs of possible toxicity evidenced by retinal rosette formation in some of the rats, although at least some of this rosette forming activity appeared to be related to the DMSO vehicle.

Because of the recent discovery of DLK's involvement in the death of injured neurons including RGCs [1, 6, 13, 14], DLK protein levels were measured in retinas undergoing photoreceptor degeneration. An elevation of DLK protein was confirmed in degenerating retinas at several time points; however, its elevation was also present after a point at which very few photoreceptors remained, suggesting that the DLK was present in another retinal cell (perhaps in addition to photoreceptors) (Figure 2). Because DLK was measured in whole retinal lysates, it was not possible to determine which cell type was accumulating DLK protein. Future studies could utilize flow sorting of various subpopulations of retinal cells from degenerating retinas to determine from where the elevation in DLK originates. Even if the DLK is present in a cell type other than PRs, it is possible that DLK inhibition could still promote PR survival.

Of potential interest, the RGC positive control DLK runs slightly more slowly than that of the degenerating retinal lysates (Figure 3). Though the reason for this is unknown, it is possibly due to the phosphorylation of DLK in injured RGCs similar to that reported in dorsal root ganglia (DRG) neurons when nerve growth factor (NGF) is withheld [13]. In this model, a decrease in available NGF leads to local DLK activation, which in turn activates JNK, which then phosphorylates and thus stabilizes DLK,

allowing DLK accumulation and further activation of a stress response. DLK in lysates from degenerating retinas runs more slowly than that of DLK from injured RGCs, which could be because DLK is not being phosphorylated in degenerating retinas as happens in injured DRG neurons. This could mean that DLK is accumulating by a different as of yet unidentified mechanism.

The promising results in the Rho S334ter rats coupled with the elevated levels of DLK in degenerating retinas warranted further testing of sunitinib. It was tested using several different techniques in mouse models of retinal degeneration. From Zhiyong Yang's unpublished work with sunitinib, it was known that systemically delivered sunitinib was protective for RGCs in an adult mouse model of optic nerve injury; therefore, our first experiment testing sunitinib in models of retinal degeneration utilized daily systemic delivery in mouse pups at a number of different doses beginning at p6, an age before any morphological evidence of degeneration is recognizable. One of the models tested was the mouse equivalent of the Rho S334ter rat (Rho Q344ter) at multiple doses and the other was the *rd1* mouse strain. The initially tested higher doses (30 and 50 mg/kg daily), which are doses that have been active in other models, resulted in toxicity and the pups died after 2-4 days of treatment. The second experiment in which no significant toxicity was noted, failed to demonstrate neuroprotection in that the retinas of the treated animals had the same ONL thickness ratio as the vehicle treated animal (Figure 4). Because the delivery of sunitinib to the retina was never confirmed, it was possible that drug delivery was the problem and therefore intravitreal injection was attempted next.

Using a range of doses of intravitreal sunitinib in two different experiments in the Rho Q344ter mouse strain, we did not observe any evidence of neuroprotection in the sunitinib injected animals. The first experiment (Figure 5) resulted in a number of toxic effects and/or injection artifacts (data not shown). The second experiment (Figure 6), had none of these negative effects, but still failed to show evidence of neuroprotective effects, even though the same dose was tested that Dr. LaVail used that showed neuroprotection in the rat model. The reason for this difference remains unclear, but could reflect differences in pharmacokinetics between rat and mouse eyes.

In a pilot study, a slow release formulation of sunitinib was tested in a minipig model of autosomal dominant retinal degeneration (Figure 7). No attempt was made to confirm sunitinib delivery to the photoreceptor layer of the retina. The behavior of the microspheres was unknown in an eye as large as a pig eye, though they had shown efficacy in a rat model of glaucoma (Zhiyong Yang, unpublished data). The lack of dispersal of the microspheres at the highest doses was an unexpected result. It is possible that a significant amount of the sunitinib was sequestered in these accumulations and was unable to diffuse properly to the photoreceptor layer. In the 11 transgenic minipigs that received sunitinib in three different doses, none of them showed consistent neuroprotection regardless of whether they received one or two injections, although some local and not statistically significant areas of increased ONL thickness were observed. It is possible that drug delivery to the pig retina was a problem despite receiving an intravitreal injection.

We also tested a new DLK inhibitor. It was tested intravitreally in both rats (UCSF) and mice (JHU). This new compound demonstrated neuroprotection in the Rho

S334ter rat model (Table 2 and Figure 8). It also showed mild neuroprotection in two *rd1* mice but not in any of the Rho Q344ter mice tested (Figure 9). These results provided additional support that DLK inhibition may be beneficial in photoreceptor degeneration.

There are no published reports of DLK being involved in modulating photoreceptor survival, though it is known to be involved in not only RGC death, but also dorsal root ganglion neurons [1, 15]. DLK is upstream of the JNK pathway that leads to apoptosis in neuronal cells. Of the myriad studies characterizing photoreceptor cell death in retinal degeneration, a few have implicated JNK activation as contributing to photoreceptor death [7, 8]. If there is a similar connection between DLK and JNK activation in degenerating photoreceptors as there is in RGCs and cortical neurons, it is possible that DLK inhibition could potentially lessen photoreceptor death in degeneration. The studies described here involving the Rho S334ter rat model of retinal degeneration showed positive effects when sunitinib or the potent novel DLK inhibitor were administered; however, this was not recapitulated in a number of different mouse models of retinal degeneration. It is possible, but probably unlikely, that the photoreceptor cell death mechanism in the Rho S334ter rat differs greatly from that of the Rho Q344ter mouse, which might help to explain the difference in response to sunitinib and DLK inhibitor administration. It seems more likely that issues of drug delivery and metabolism may account for the observed differences.

If it turns out that DLK is not involved in photoreceptor degeneration, this would suggest that sunitinib's ability to promote photoreceptor cell survival is due to inhibition of one or more other kinases. If that other kinase(s) can be determined, such identification

could provide a novel target(s) for the development of drugs that prevent or slow down the course of retinal degeneration.

References

1. Welsbie, D.S., et al., *Functional genomic screening identifies dual leucine zipper kinase as a key mediator of retinal ganglion cell death.* Proc Natl Acad Sci U S A, 2013. **110**(10): p. 4045-50.
2. Bessero, A.C., et al., *Role of the c-Jun N-terminal kinase pathway in retinal excitotoxicity, and neuroprotection by its inhibition.* J Neurochem, 2010. **113**(5): p. 1307-18.
3. Fernandes, K.A., et al., *JNK2 and JNK3 are major regulators of axonal injury-induced retinal ganglion cell death.* Neurobiol Dis, 2012. **46**(2): p. 393-401.
4. Ribas, V.T., et al., *Early c-Jun N-terminal kinase-dependent phosphorylation of activating transcription factor-2 is associated with degeneration of retinal ganglion cells.* Neuroscience, 2011. **180**: p. 64-74.
5. Sun, H., et al., *Protective effect of a JNK inhibitor against retinal ganglion cell loss induced by acute moderate ocular hypertension.* Mol Vis, 2011. **17**: p. 864-75.
6. Watkins, T.A., et al., *DLK initiates a transcriptional program that couples apoptotic and regenerative responses to axonal injury.* Proc Natl Acad Sci U S A, 2013. **110**(10): p. 4039-44.
7. Donovan, M., F. Doonan, and T.G. Cotter, *Differential roles of ERK1/2 and JNK in retinal development and degeneration.* J Neurochem, 2011. **116**(1): p. 33-42.
8. Shinde, V.M., et al., *ER stress in retinal degeneration in S334ter Rho rats.* PLoS One, 2012. **7**(3): p. e33266.
9. Karaman, M.W., et al., *A quantitative analysis of kinase inhibitor selectivity.* Nat Biotechnol, 2008. **26**(1): p. 127-32.

10. Sung, C.H., et al., *A rhodopsin gene mutation responsible for autosomal dominant retinitis pigmentosa results in a protein that is defective in localization to the photoreceptor outer segment.* J Neurosci, 1994. **14**(10): p. 5818-33.

11. Ross, J.W., et al., *Generation of an inbred miniature pig model of retinitis pigmentosa.* Invest Ophthalmol Vis Sci, 2012. **53**(1): p. 501-7.

12. Green, E.S., et al., *Characterization of rhodopsin mis-sorting and constitutive activation in a transgenic rat model of retinitis pigmentosa.* Invest Ophthalmol Vis Sci, 2000. **41**(6): p. 1546-53.

13. Huntwork-Rodriguez, S., et al., *JNK-mediated phosphorylation of DLK suppresses its ubiquitination to promote neuronal apoptosis.* J Cell Biol, 2013. **202**(5): p. 747-63.

14. Pozniak, C.D., et al., *Dual leucine zipper kinase is required for excitotoxicity-induced neuronal degeneration.* J Exp Med, 2013. **210**(12): p. 2553-2567.

15. Ghosh, A.S., et al., *DLK induces developmental neuronal degeneration via selective regulation of proapoptotic JNK activity.* J Cell Biol, 2011. **194**(5): p. 751-64.

	Injected eyes ONL thickness (μm) Mean +/- St dev	DMSO injected eyes ONL thickness (μm) Mean +/- St dev	Paired t-test results
Sunitinib single injection (N = 5)	18.0 +/- 7.0	8.6 +/- 0.5	0.038
Sunitinib two injections (N = 6)	13.7 +/- 3.3	8.5 +/- 1.2	0.0069

Table 1. Retinal thickness measurements in Rho S334ter mutant rats treated with intravitreal sunitinib. The photoreceptor degeneration of Rho S334ter rat retinas injected with 2 μL of 20 mg/mL sunitinib either once or twice was slower than uninjected control eyes. Six animals received a single injection at p9 and five animals received two injections (at p9 and p12). All animals were sacrificed at p19. Eyes that received either one or two injections of sunitinib had a statistically significantly slower degeneration compared to DMSO injected eyes.

	Injected eyes Rows of nuclei in the ONL Mean +/- St dev	Uninjected eyes Rows of nuclei in the ONL Mean +/- St dev	Paired t-test results
Novel DLK inhibitor (N = 4)	2.8 +/- 0.79	1.5 +/- 0.26	0.0460

Table 2. Rows of photoreceptor nuclei in Rho S334ter mutant rats injected with a novel DLK inhibitor. The photoreceptor degeneration of Rho S334ter rat retinas injected with 2 μL of 2 mM of a novel DLK inhibitor was slowed. Four animals received the DLK inhibitor at p8 and then all were sacrificed at p19. Eyes that received the novel DLK inhibitor had a statistically significantly slower degeneration compared to uninjected eyes.

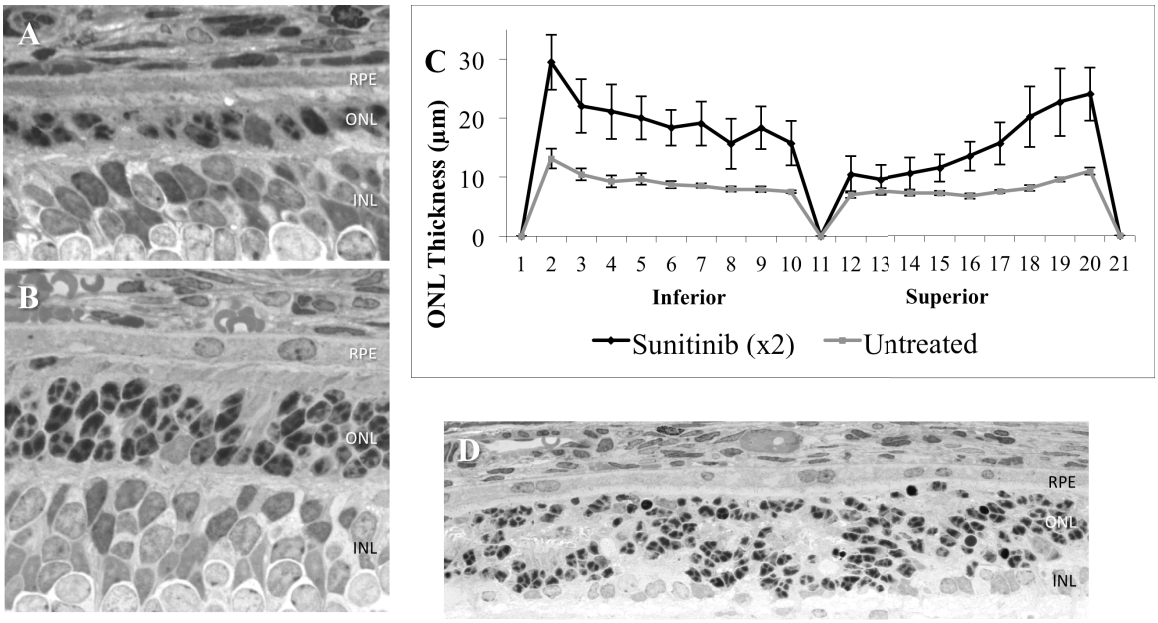

Figure 1. Representative retinal sections from Rho S334ter rats treated with sunitinib and ONL thickness measurements. A. Retinal section from a DMSO treated retina from a Rho S334ter rat sacrificed at p19. **B.** Representative retinal section from a Rho S334ter rat that received 2 µL of 20 mg/mL intravitreal sunitinib at p9 and p12 and then sacrificed at p19. Note that there are more photoreceptors remaining in the sunitinib treated eye than in the untreated retina. Plastic embedded, toluidine blue stained sections. **C.** Spider plot showing measurements of ONL thickness in a representative rat treated with 20 mg/mL of sunitinib at p9 and p12 and sacrificed at p19. The treated eye has a thicker ONL at all points measured compared to the untreated eye. Error bars represent the standard errors of the mean. **D.** Rosettes developed within the ONL in some eyes that received sunitinib. Similar rosettes developed in some eyes that received vehicle (DMSO) only as well as some eyes that received sunitinib. RPE = retinal pigmented epithelium, ONL = outer nuclear layer, INL = inner nuclear layer.

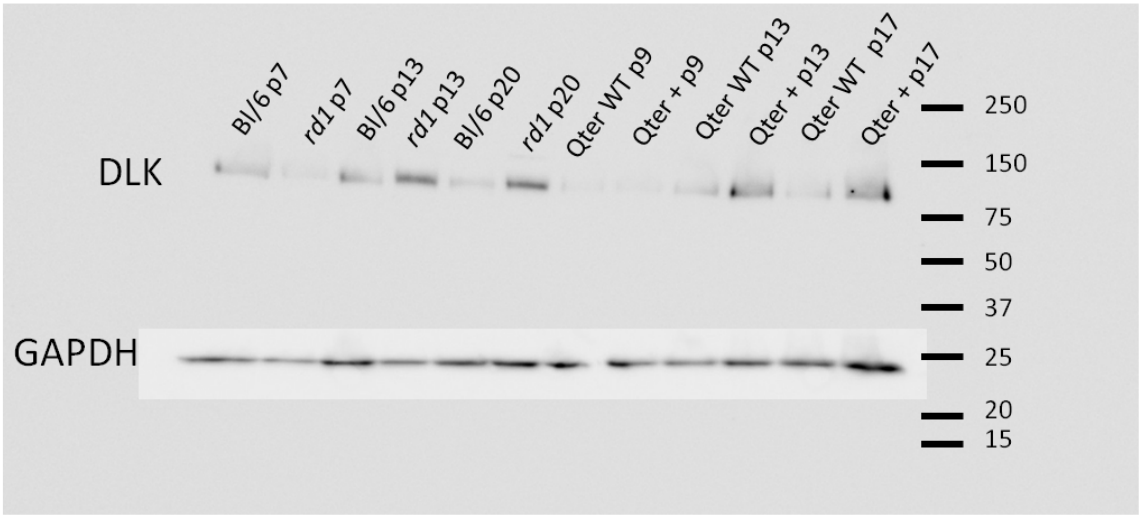

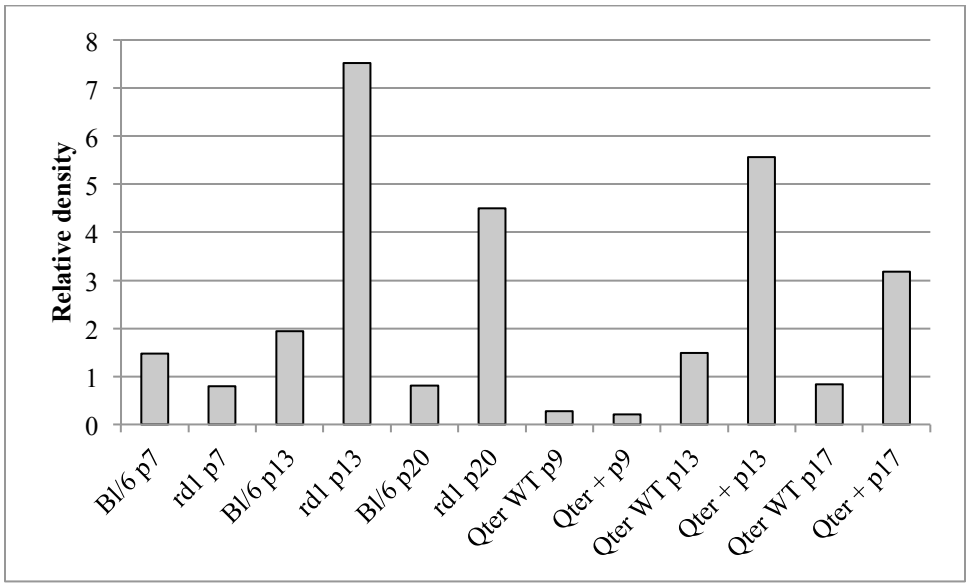

Figure 2. Western blot of DLK protein in degenerating mouse retinas. Blot demonstrates DLK protein levels in degenerating and age matched wild type whole retinal lysates from homozygous *rd1* and hemizygous Rho Q344ter mice. Top panel shows the blot for DLK with GAPDH as a loading control. Bottom panel shows the density of the DLK bands from the above blot normalized to the GAPDH bands as measured with Image J. Note that at the older ages for both strains, there is an increase in DLK protein compared to the age matched wild type controls. At p20 in *rd1* mice, there

are very few rods remaining, however, there is still an elevated amount of DLK protein present indicating the DLK protein is likely coming from cells other than photoreceptors. Qter p17 retinas have 4-6 rows of nuclei remaining in the ONL compared to 16-20 in the wild type, and therefore the DLK present in hemizygous Qter retinas at p17 could be from photoreceptors in addition to other retinal cells. Each lane represents retinal lysates from a single retina from a single animal. Bl/6 = C57BL/6, Qter = Rho Q344ter.

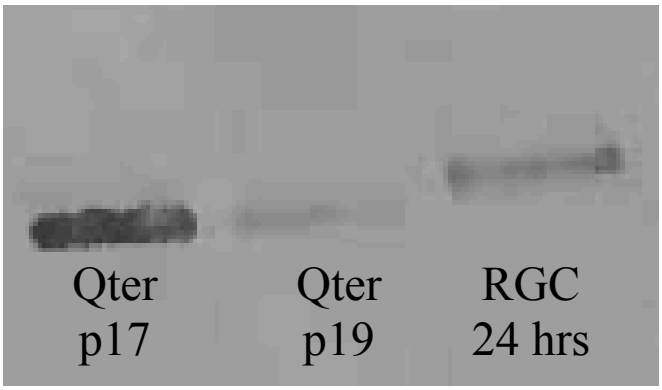

Figure 3. Western blot of DLK protein in Rho Q344ter mouse retinas and wild type mouse neurotrophin-starved RGCs. Qter whole retinal lysates are from 17 and 19 day old mouse pups and RGC lysate is from cells in culture for 24 hours without pharmacological or neurotrophic support. The DLK band in retinal lysates travels faster than that in RGC lysates. Qter = Rho Q344ter.

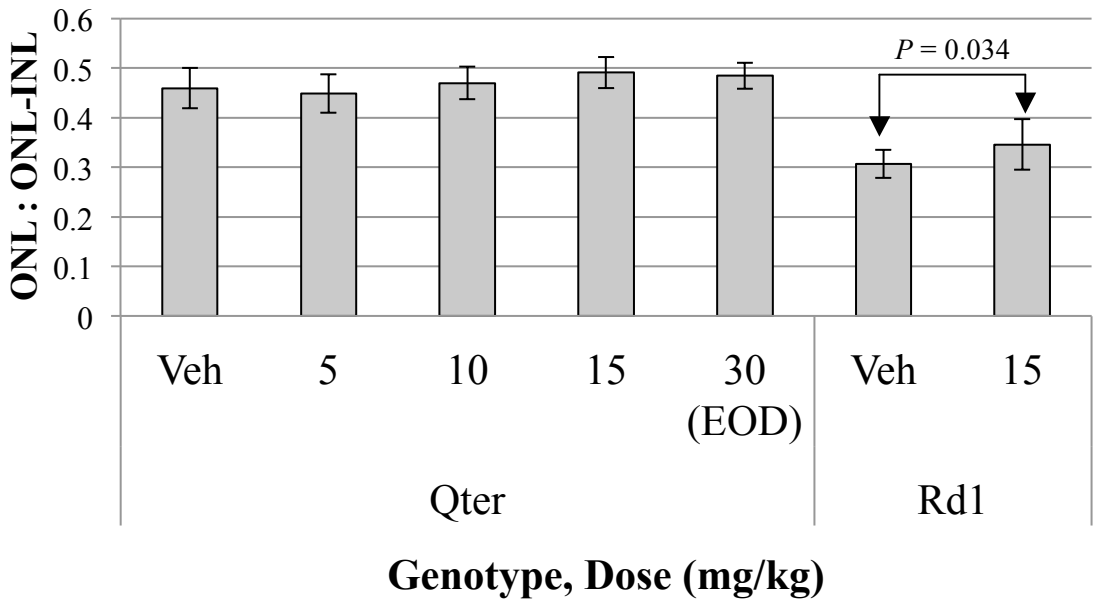

Figure 4. ONL : ONL-INL ratio after daily systemic delivery of sunitinib to hemizygous Rho Q344ter (Qter) mice and homozygous *rd1*. Pups were injected daily with sunitinib from p6 to p14 and then sacrificed on p15. Layer thicknesses were measured in paraffin embedded, hematoxylin and eosin-stained sections (one section from one eye from each mouse) at three points on both sides of the optic nerve head (six points total) and averaged for the whole eye. Error bars represent the standard deviations. There was no significant difference in any of the treatment groups compared to the vehicle injected eyes ($P > 0.05$). Veh = vehicle injected, EOD = every other day.

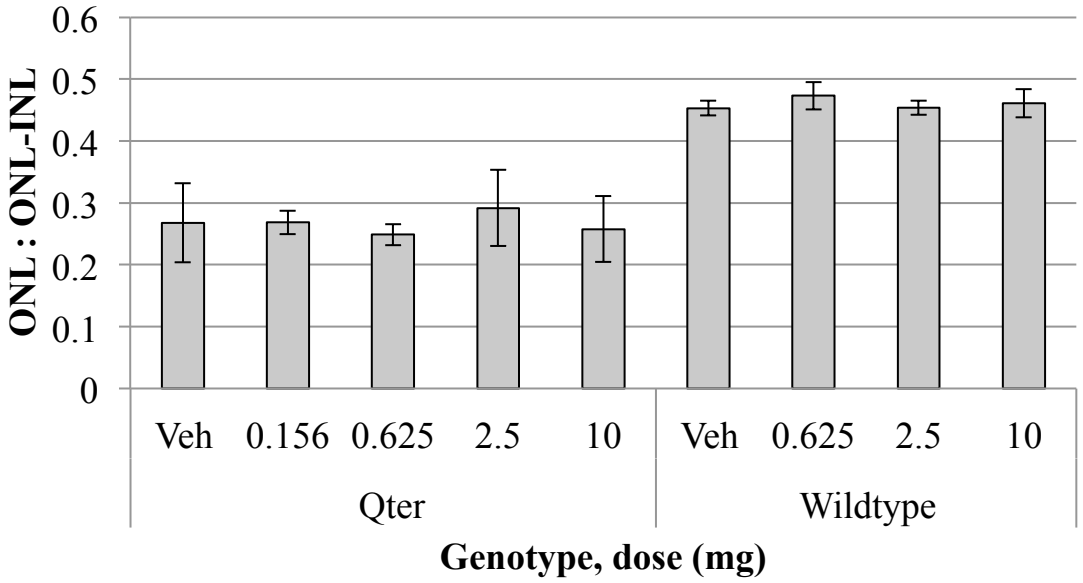

Figure 5. ONL : ONL-INL ratio after intravitreal injection of sunitinib in hemizygous Rho Q344ter (Qter) or wildtype mice. A single injection of sunitinib or vehicle was given to p11 pups, which were then sacrificed at p18 and retinas measured in paraffin embedded, hematoxylin and eosin stained sections. Each bar represents the average of two (0.156 mg dose) or three (Vehicle, 0.625, 2.5, 10 mg dose) eyes with the standard deviation. There was no significant difference in any of the treatment groups compared to the vehicle injected eyes ($P > 0.05$). Veh = vehicle.

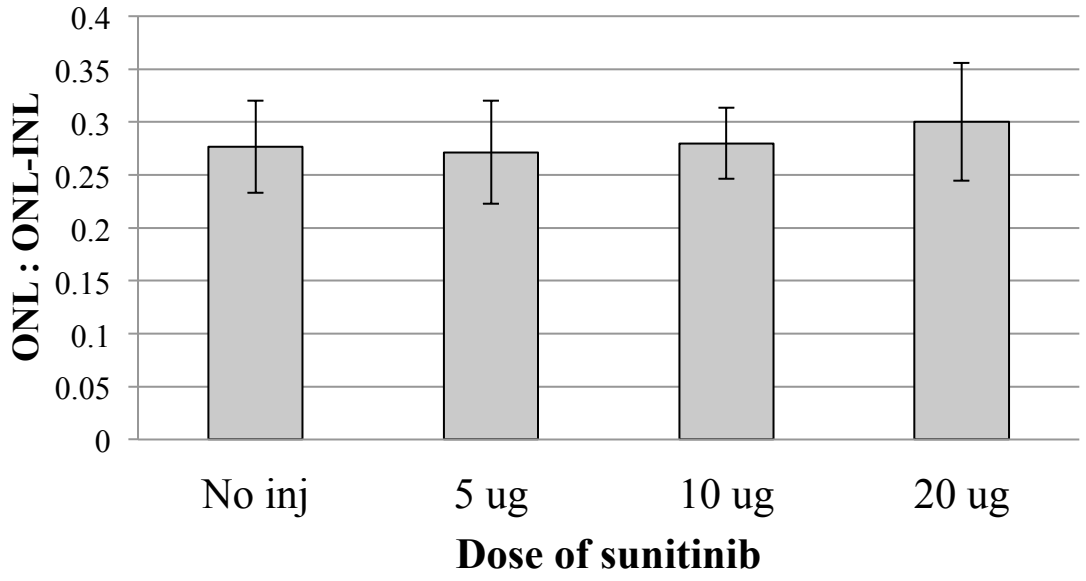

Figure 6. ONL : ONL-INL ratios from hemizygous Rho Q344ter mice treated with intravitreal sunitinib. The left eye of each pup was injected with sunitinib and the right eye was uninjected and served as a negative control. Pups were injected intravitreally at p11 and then sacrificed at p17. Layer thicknesses were measured in paraffin-embedded, hematoxylin and eosin stained sections. Each bar represents the average of measurements of all eyes in the treatment group with the standard deviation. There was no significant difference in any of the treatment groups compared to the uninjected eye ($P > 0.05$). No inj = uninjected.

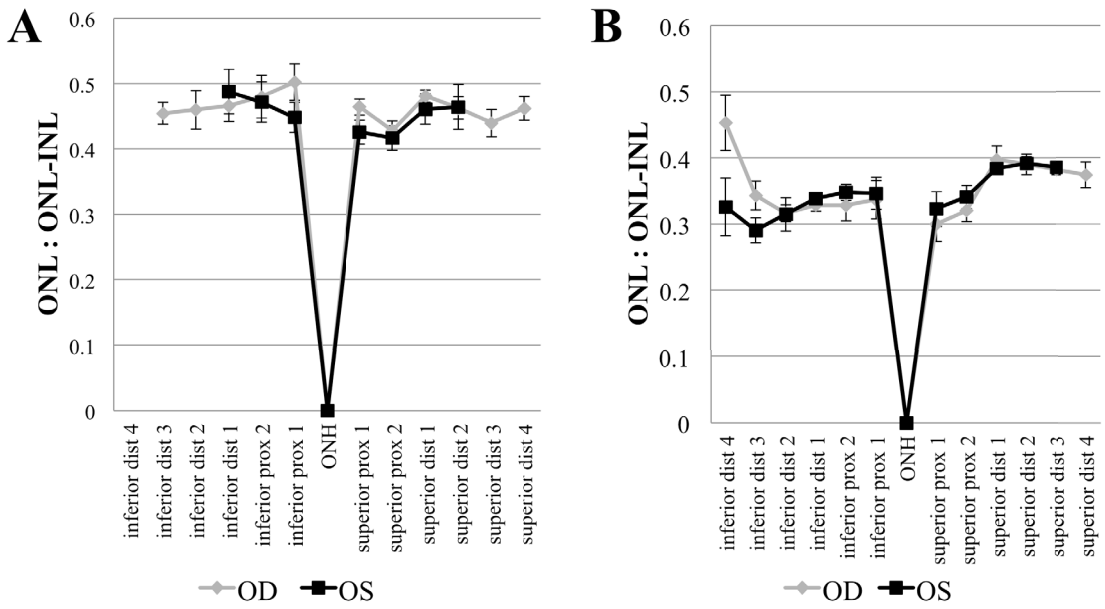

Figure 7. ONL : ONL-INL ratio in a wild-type and a hemizygous Rho P23H minipig treated with intravitreal slow release sunitinib. Piglets were injected intravitreally at p3 and p17 and then sacrificed at p30. Left eyes (OS) received sunitinib containing microspheres and right eyes (OD) received blank microspheres. **A.** Measurements from a wild-type piglet. **B.** Measurements from a transgenic Rho P23H piglet. Note that there were no apparent toxic effects in the wild-type pig, but there was also no protective effect in the transgenic piglet.

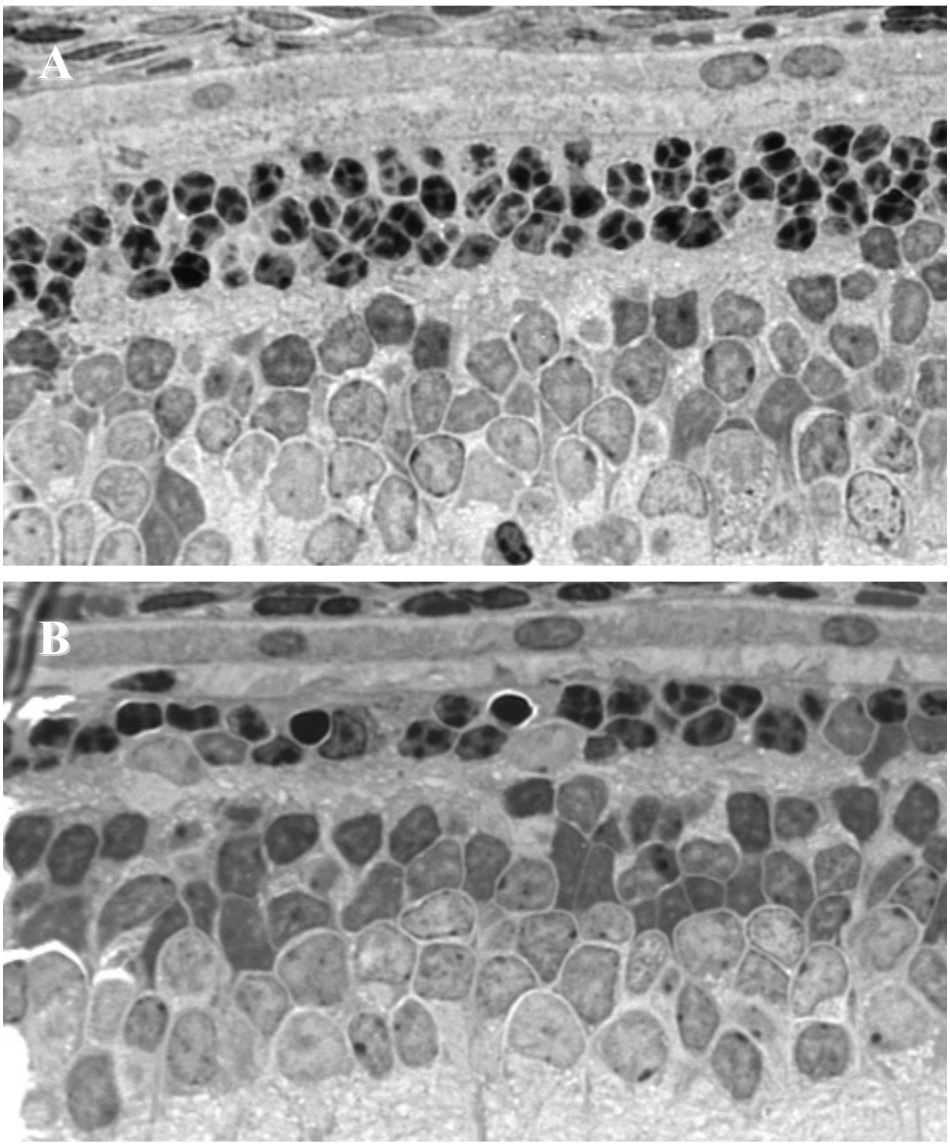

Figure 8. Representative retinal sections from Rho S334ter rats treated with a novel DLK inhibitor. Images represent retinas from a Rho S334ter rat eye that received the new small molecule (A) and an uninjected control retina (B). Pups were injected intravitreally at p8 with 2 μL of a 2 mM solution and then sacrificed at p19. The retina that received the DLK inhibitor (A) had three to four rows of nuclei in the outer nuclear layer (ONL) compared to the uninjected retina (B), which had only one to two rows of nuclei remaining in the ONL.

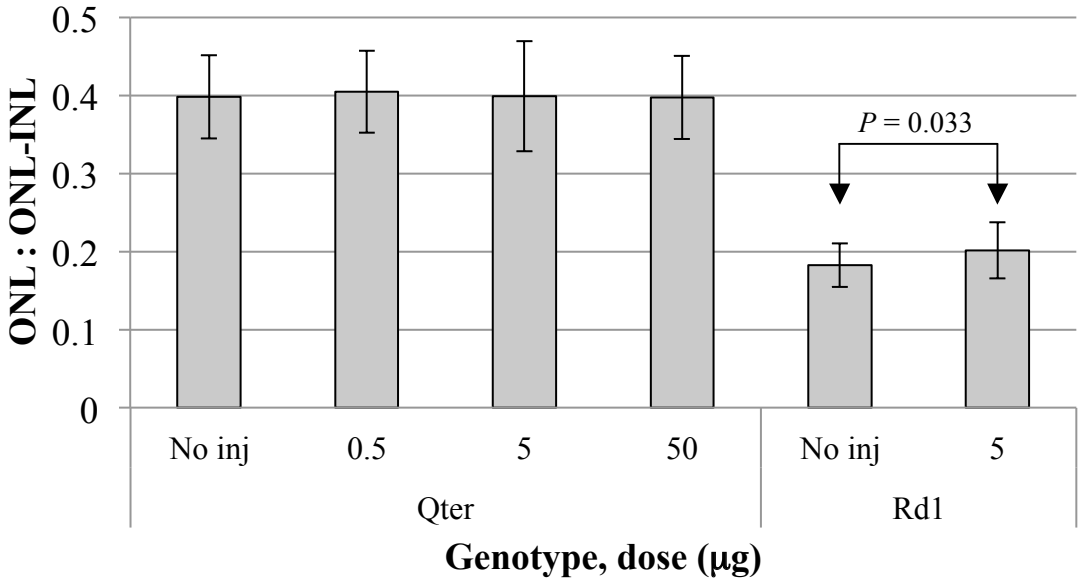

Figure 9. Results of the intravitreal injection of DLK inhibitor in hemizygous Rho Q344ter (Qter) and homozygous *rd1* mouse pups. The left eye of each pup was injected with the DLK inhibitor and the right eye was uninjected and served as a negative control. Pups were injected intravitreally at p11 and then sacrificed at p17. Layer thicknesses were measured in paraffin-embedded, hematoxylin and eosin stained sections Each bar represents the average of measurements of all eyes in the treatment group with the standard deviation. Single factor ANOVA reported no significant difference in the means of the Qter animals ($P > 0.05$). However, the *rd1* animals that received 5 μg of the DLK inhibitor did have significantly larger ONL : ONL-INL ratio ($P = 0.033$).

Chapter 2: Exploration of whether *Parp1* knockout promotes photoreceptor survival in murine models of retinal degeneration

Introduction

Poly (ADP-ribose) polymerase 1 (PARP1) is an enzyme that is involved in many different cellular processes, but is especially well known for its role in sensing DNA damage and initiating DNA repair. Interest in PARP1's role in neuronal cell death has increased in the past several years since its excess activation was recognized as playing a role in neuronal cell death in a process termed "parthanatos" (reviewed by Andrabi [1] and Fatokun [2]). DNA damage activates PARP1, which transfers ADP-ribose from nicotinamide adenine dinucleotide (NAD+) to other proteins as well as itself [3, 4]. Excess poly-ADP-ribose (PAR) accumulation in the cytoplasm leads to translocation of apoptosis-inducing factor (AIF) from the mitochondria to the nucleus, initiating DNA cleavage. Additionally, PARP1 activation can lead to a depletion of NAD+, which further contributes to cell death.

The role of PARP1 activation in retinal degeneration has been investigated by several groups. Photoreceptor cell death induced by N-methyl-N-nitrosurea (MNU), a DNA alkylating agent known to induce apoptosis in photoreceptors [5], can be prevented by both pharmacological PARP inhibition and supplementation with nicotinamide [6, 7]. An increase in PARP activity and PAR formation was found in *Pde6b* mutant mice (*rd1*) in the later stages of retinal degeneration, which correlated with oxidatively-damaged DNA and nuclear translocation of AIF [8]. Additionally, treatment with a PARP-specific inhibitor (PJ34) decreased cell death and resulted in more surviving photoreceptors in an

rd1 retinal explant culture system [8]. The detrimental effects of zaprinast, a PDE inhibitor that mimics photoreceptor cell death induced by *Pde6b* mutation, were decreased in a *Parp1* KO retinal explant system [9].

Because of the implication of PARP1 activity in photoreceptor degenerations, further investigations utilizing *Parp1* knockout (KO) mice were performed. *Parp1* KO mice were found to be resistant to MNU-induced photoreceptor degeneration up to 72 hours post-injection as evaluated by electroretinography (ERG) and spectral-domain optical coherence tomography (SD-OCT) (Xinrong Zhou, unpublished data, not shown). The effect of *Parp1* KO was evaluated after sodium iodate ($NaIO_3$) administration and also in the face of *Pde6b*-mutation induced retinal degeneration (*rd1*), with the hypothesis that *Parp1* KO would be protective in these two different retinal degeneration models.

Materials & Methods

All animals used in this research were treated in accordance with the ARVO statement for the use of animals in vision research and all protocols were approved by Johns Hopkins' institutional animal care and use committee. The *Parp1* KO mice were a gift from Valina Dawson.

Sodium iodate ($NaIO_3$) injections

Adult *Parp1* KO and *Parp1* wild type (WT) mice were injected intravenously via the tail vein with vehicle only (PBS), 20 or 40 mg/kg of $NaIO_3$ and euthanized with an isoflurane overdose followed by cervical dislocation at 36 days post-injection (dpi).

Parp1 KO / rd1 cross

Parp1 KO mice were bred to *rd1* mice and then F1 offspring were bred to obtain various genotype combinations. Offspring of these F2 crosses were evaluated at 14, 15, 16 and 17 days of age via retinal morphology. Pups were euthanized with an isoflurane overdose followed by cervical dislocation.

Tissue processing and image analysis

Following euthanasia, globes were collected, fixed in 4% paraformaldehyde overnight at 4 ^{o}C, routinely processed for paraffin embedding, sectioned at 5 μm and stained with hematoxylin and eosin. Slides were imaged at 100x with a Zeiss Axioplan 2 imaging system (Carl Zeiss Microscopy LLC, Thornwood, NY) and measurements taken using Image J [10]. Because of the undulating contour of the retinal layers after sodium iodate injection, simply measuring the layer thicknesses was insufficient. Instead, the area of the ONL was divided by the length of the measured retina. To evaluate the retinas of the genetic crosses of the *Parp1* KO and *rd1* mice, three points between the optic nerve head (ONH) and the limbus were measured and averaged on both sides of the ONH for a total of six measurements per eye. For each point, the thickness of the outer nuclear layer (ONL) and the thickness of the outer border of the ONL from the inner border of the inner nuclear layer (INL) were measured. To avoid artifacts of a distorted retinal section, the ratio of the ONL to the ONL-INL measurement was reported.

Statistical tests

Retinal thickness measurements of the *Parp1*/*rd1* animals were analyzed by a multilevel linear mixed effects model with a random intercept for the animal to account for the correlations among the repeated measures from the same animal.

Results

Sodium iodate damages RPE cells and causes a secondary photoreceptor degeneration [11]. Though the *Parp1* KO mice were shown to be resistant to MNU-induced photoreceptor damage in the short term, it was unknown whether photoreceptors from *Parp1* KO mice would be resistant to later degeneration. At 36 days post-injection we did not see evidence of increased photoreceptor survival in the *Parp1* KO mice. In fact, although not statistically significant, the *Parp1* KO mice showed more severe retinal degeneration in response to sodium iodate than the WT mice (Figure 1). However, there were likely technical issues with the experiment, as sodium iodate injection did not consistently induce ONL depletion in the WT mice.

The retinal thicknesses of a total of 30 animals of varying *Parp1* KO / *rd1* genotypes were evaluated. All of the *rd1* heterozygous animals' ONL:ONL-INL ratios were over 0.5 (data not shown), whereas those of *rd1* homozygous animals were all under 0.4 (Figure 2). Figure 2 shows all of the *rd1* homozygous animals analyzed and their Parp1 status. The animals in three of the five litters showed a significant difference between *Parp1* -/+ (het) and *Parp1* -/- (KO) in the face of *rd1* induced retinal degeneration at the time points analyzed.

Discussion

There has been increasing interest in PARP's role in retinal degeneration in the past several years, and these experiments were meant to further investigate the effect of *Parp1* KO on retinal degeneration.

The results of the sodium iodate injections were interesting in that not only did *Parp1* KO not protect against retinal degeneration, but seemed to result in greater degeneration (more severe ONL depletion) compared to wild type animals. Though *Parp1* KO was protective against MNU in a short term study (72 hrs), it was not evaluated at later time points following MNU injection. The sodium iodate experiment was carried out to 36 days post-injection without earlier evaluation. It is possible that the different time points of evaluation of the MNU and sodium iodate experiments can account for the differences seen (lack of protection from sodium iodate at 36 days post-injection). It is possible that *Parp1* KO retinas may eventually succumb to MNU-induced photoreceptor degeneration at later time points. It is also possible that the *Parp1* KO retinas may be resistant to initial damage caused by sodium iodate. Additional MNU and sodium iodate administration experiments should be repeated with similar evaluation time points to address this in the future.

The variation in photoreceptor degeneration of the *Parp1* WT animals that received sodium iodate suggests that technical issues with the drug administration may have played a role. Additionally, mice of a range of ages (4 to 20 weeks) were included in the study, which may have contributed to the observed experimental variability.

Animals in three of five evaluated litters of *Parp1* / *rd1* crosses showed a significant difference between *Parp1* -/- / *rd1* homozygous and *Parp1* +/- / *rd1*

homozygous. This result was with a relatively small number of animals; however, it does suggest that *Parp1* KO can be mildly protective against photoreceptor loss in the *rd1* model. Why some liters showed evidence of protection and others didn't is unclear. It doesn't appear that the age of the animals explains the difference since there were two 14 day-old litters, with one showing a statistically significant increase in survival and one not showing a significant difference. The finding of protection in some of the animals is consistent with the published findings that *Parp* inhibition in *rd1* explants increased the number of surviving photoreceptors [8]. These findings are also consistent with the report that photoreceptors from *Parp1* KO mice were partially resistant to treatment with zaprinast, which is a PDE6B inhibitor that mimics the *rd1* mutation [9]. These results, taken together with the published literature, suggest that *Parp1* KO is protective against retinal degeneration induced by *Pde6b* mutation; however, additional studies are warranted.

References

1. Andrabi, S.A., T.M. Dawson, and V.L. Dawson, *Mitochondrial and nuclear cross talk in cell death: parthanatos.* Ann N Y Acad Sci, 2008. **1147**: p. 233-41.
2. Fatokun, A.A., V.L. Dawson, and T.M. Dawson, *Parthanatos: mitochondrial-linked mechanisms and therapeutic opportunities.* Br J Pharmacol, 2014. **171**(8): p. 2000-16.
3. David, K.K., et al., *Parthanatos, a messenger of death.* Front Biosci (Landmark Ed), 2009. **14**: p. 1116-28.
4. Wang, Y., V.L. Dawson, and T.M. Dawson, *Poly(ADP-ribose) signals to mitochondrial AIF: a key event in parthanatos.* Exp Neurol, 2009. **218**(2): p. 193-202.
5. Tsubura, A., et al., *Animal models for retinitis pigmentosa induced by MNU; disease progression, mechanisms and therapeutic trials.* Histol Histopathol, 2010. **25**(7): p. 933-44.
6. Uehara, N., et al., *Nicotinamide blocks N-methyl-N-nitrosourea-induced photoreceptor cell apoptosis in rats through poly (ADP-ribose) polymerase activity and Jun N-terminal kinase/activator protein-1 pathway inhibition.* Exp Eye Res, 2006. **82**(3): p. 488-95.
7. Miki, K., et al., *Poly (ADP-ribose) polymerase inhibitor 3-aminobenzamide rescues N-methyl-N-nitrosourea-induced photoreceptor cell apoptosis in Sprague-Dawley rats through preservation of nuclear factor-kappaB activity.* Exp Eye Res, 2007. **84**(2): p. 285-92.

8. Paquet-Durand, F., et al., *Excessive activation of poly(ADP-ribose) polymerase contributes to inherited photoreceptor degeneration in the retinal degeneration 1 mouse.* J Neurosci, 2007. **27**(38): p. 10311-9.

9. Sahaboglu, A., et al., *PARP1 gene knock-out increases resistance to retinal degeneration without affecting retinal function.* PLoS One, 2010. **5**(11): p. e15495.

10. Abramoff, M.D., Magalhaes, Paulo J., Ram, Sunanda J, *Image Processing with ImageJ.* Biophotonics International, 2004. **11**(7): p. 36-42.

11. Kiuchi, K., et al., *Morphologic characteristics of retinal degeneration induced by sodium iodate in mice.* Curr Eye Res, 2002. **25**(6): p. 373-9.

Figures

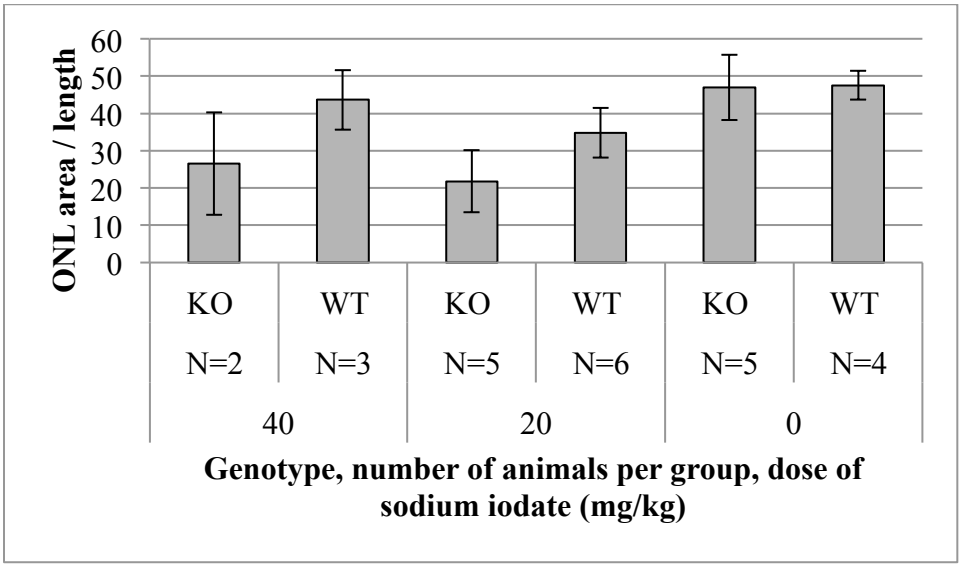

Figure 1. Morphological measurements of *Parp1* KO and WT retinas after sodium iodate injection. *Parp1* KO was not observed to be protective against systemic sodium iodate at 36 days post-injection. However, the sodium iodate injection did not consistently induce ONL depletion in WT mice, indicating possible variation in drug administration, or perhaps another experimental variable that was not determined. The animals varied in age from 4 to 20 weeks with approximately equal distribution across the groups.

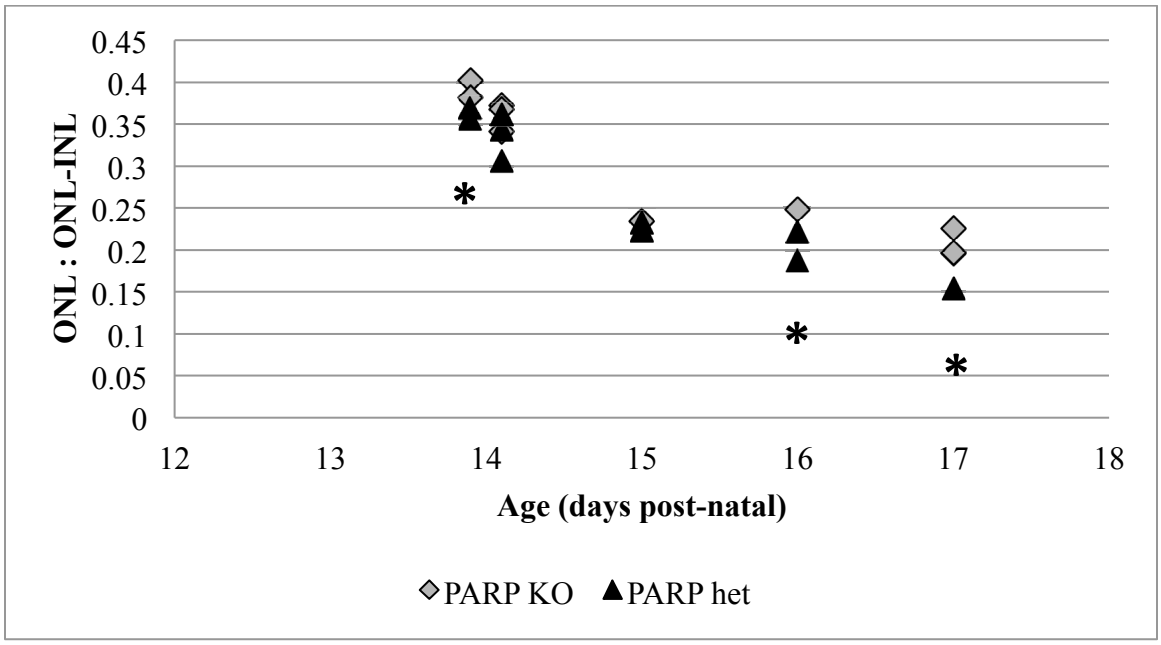

Figure 2: Morphological measurements of *Parp1*/*rd1* mutant animals. Animals heterozygous and homozygous for the *Parp* mutation in the face of homozygous *Pde6b* mutation (*rd1*) suggests *Parp1* KO may be protective. Each individual marker represents measurements from a single eye of an individual animal. Each grouping of ages represents animals from a single litter. There were two litters collected at 14 days of age – one showed significant protection, and one did not. * = significant difference between *Parp1* KO and *Parp1* heterozygous animals with $P < 0.05$.

Gillian Curtis Shaw
302 Norris Ct, Apt 5, Madison, WI 53703

Cell phone: (330) 608-6117 Email: gilliancshaw@gmail.com

EDUCATION

- Comparative Ocular Pathology Laboratory of Wisconsin, University of Wisconsin, School of Veterinary Medicine, Madison, WI
    - July 2014 to present
    - *Pathology Fellow:* I am a trainee in the lab of a very busy mail-in biopsy service that receives ocular pathological specimens from veterinary ophthalmologists and veterinarians from all over the world. Duties include grossing specimens as they arrive, histological evaluation and report writing.

- Cellular and Molecular Medicine Graduate Program, Johns Hopkins University, School of Medicine, Baltimore, MD
    - August 2008 to present
    - *PhD Candidate in Donald Zack's laboratory*: I am analyzing important promoter elements for retinal ganglion cell and photoreceptor enriched genes.

- Molecular and Comparative Pathobiology, JHU, SOM, Baltimore, MD
    - July 2007 to June 2014
    - *Postdoctoral Veterinary Pathology Trainee*: Duties included gross and histopathological examination of animals and biopsies from JHU, National Aquarium in Baltimore, Maryland Zoo in Baltimore and outside veterinary clinics and participating in relevant veterinary pathology training including a weekly slide conference

- Michigan State University College of Veterinary Medicine, East Lansing, MI
    - Degree awarded: DVM, May 2007
    - Cumulative GPA 3.68 / 4.0

- Michigan State University Comparative Medicine and Integrative Biology Graduate Program, East Lansing, MI
    - Degree awarded: MS, August 2007
    - Thesis: Further characterization of the retinopathy, globe-enlarged chicken
    - Cumulative GPA 3.92 / 4.0

- Kalamazoo College, Kalamazoo, MI
    - Degree awarded: BA Biology, June 2001
    - Cumulative GPA of 3.65 / 4.0

RESEARCH EXPERIENCE

- Comparative Ophthalmology Laboratory, MSU CVM, East Lansing, MI
    - May 2004 to August 2007
    - *Master's student*: My project encompassed the further characterization of the retinopathy, globe-enlarged (*rge*) chicken and includes immunohistochemistry, gene hunting, electron microscopic analysis and electroretinography. Duties also include supervising the maintenance of the *rge* chicken flock at MSU.
    - Research funded by NIH T-32 Student Research Training Grant

- USDA Avian Disease and Oncology Laboratory, East Lansing, MI
    - May 2003 to August 2003
    - *Research Assistant*: Aided in furthering the diagnosis of Marek's Disease in chickens using immunohistochemistry and real time PCR
    - Experience funded by an NIH T-35 Summer Research Grant

- Veterinary Parasitology Laboratory, Ohio State College of Veterinary Medicine, Columbus, OH
    - June through July 2000
    - *Research Assistant:* Tested fenbendazole and its efficacy against the common gastrointestinal parasites of llamas and alpacas.
    - Duties included restraining the animals and collecting, setting up and analyzing fecal samples. Results were submitted to fulfill Kalamazoo College's required Senior Individualized Project.

- Barking Dogs in Kennel Settings Research Project, Perth, Western Australia
    - August to November 1999
    - *Research Assistant:* Project determined that barking dogs in kennel settings in veterinary clinics and animal shelters is hazardous to human hearing.
    - Duties included taking measurements of dogs barking using a decibel meter, determining whether they were hazardous to human hearing and then writing up the results.

PUBLICATIONS

- Tuxbury KA, **Shaw GC**, Montali RJ, Clayton LA, Kwiatkowski NP, Dykstra MJ, Mankowski JL. Fusarium solani species complex associated with carapace lesions and branchitis in captive American horseshoe crabs Limulus polyphemus. Dis Aquat Organ. 2014 Jul 3;109(3):223-30.

- Fuller JA, **Shaw GC**, Bonnet-Wersinger D, Hansen BS, Berlinicke CA, Inglese J, Zack DJ. A high content screening approach to identify molecules neuroprotective for photoreceptor cells. Adv Exp Med Biol. 2014;801:773-81.

- **Shaw GC**, Berlinicke C, Zack DJ. Synaptotagmin 11: A Model for the Study of Retinal Ganglion Cell (RGC) Transcriptional Regulation ARVO Meeting Abstracts March 26, 2012 53:1533

- Baxter VK, **Shaw GC**, Sotuyo NP, Carlson CS, Olson EJ, Zink MC, Mankowski JL, Adams RJ, Hutchinson EK, Metcalf Pate KA. Serum albumin and body weight as biomarkers for the antemortem identification of bone and gastrointestinal disease in the common marmoset. PLoS One. 2013 Dec 6;8(12):e82747.

- **GC Shaw**, DS Welsbie, Z Yang, CA Berlinicke, DJ Zack. Regulation of retinal ganglion cell gene expression: development of an electroporation-based method for the study of *cis*-acting regulatory elements. Abstract in: *Vet Pathol* November 2010 47: 1S-2S.

- Miki A, Miki K, Ueno S, Wersinger DM, Berlinicke C, **Shaw GC**, Usui S, Wang Y, Zack DJ, Campochiaro PA. Prolonged blockade of VEGF receptors does not damage retinal photoreceptors or ganglion cells. *J Cell Physiol*. 2010 Jul;224(1):262-72.

- **GC Shaw**, KK Brennan, TL Southard, MC Zink. Metabolic bone disease in a colony of common marmosets (*Callithrix jacchus*). Abstract in: *Vet Pathol,* September 2009; vol. 46, 5: pp. 1020-1083.

- **G. Shaw**, K. Brennan, T. Southard, S. Trembley, D. Huso, C. Morrell, K. Tuxbury, R. Montali, N. Kwiatkowski, W. Merz, J. Mankowski. Chitinolytic Shell Disease and Branchitis in Captive American Horseshoe Crabs (*Limulus polyphemus*). Abstract in: *Vet Pathol,* September 2008; vol. 45, 5: pp. 730-791.

- Montiani-Ferreira F, **Shaw G**, Mattos BC, Russ HH, Vilani RG. Reference values for selected ophthalmic diagnostic tests of the capuchin monkey (Cebus apella). *Vet Ophthalmol*. 2008 May-Jun;11(3):197-201.

- Montiani-Ferreira F, **Shaw GC**, Geller AM, Petersen-Jones SM. Electroretinographic features of the retinopathy, globe enlarged (rge) chick phenotype. *Mol Vis.* 2007 Apr 4;13:553-65.

- Montiani-Ferreira F, Fischer A, Cernuda-Cernuda R, Kiupel M, DeGrip WJ, Sherry D, Cho SS, **Shaw GC**, Evans MG, Hocking PM, Petersen-Jones SM. Detailed histopathologic characterization of the retinopathy, globe enlarged (rge) chick phenotype. *Mol Vis*. 2005 Jan 13;11:11-27.

- **Shaw G**, Montiani-Ferreira F, & Petersen-Jones SM. Pharmacological dissection of the electroretinogram of the retinopathy, globe enlarged (rge) chicken. *ARVO Meeting Abstracts,* May 1, 2005 46:5260.

POSTER / ORAL PRESENTATIONS

- Association for Research in Vision & Ophthalmology, May 2013
  - Poster Presentation: Transcriptional regulation of synaptotagmin 11 in retinal ganglion cells

- Association for Research in Vision & Ophthalmology, May 2012 and 23RD Annual Wilmer Research Meeting, April 2012
  - Poster Presentation: Synaptotagmin 11: A Model for the Study of Retinal Ganglion Cell (RGC) Transcriptional Regulation

- 62nd annual meeting of the American College of Veterinary Pathology, December 2011
  - Case presentation at the Ocular Pathology Mystery Slide Conference: Corneal stromal defect and ectasia (staphyloma), with iris prolapse, broad anterior synechia and Descemet's membrane rupture in a Chihuahua

- 17th Annual CL Davis Zoo & Wildlife Pathology Workshop at the 43rd Annual meeting of the American Association of Zoo Veterinarians, October 2011
  - Oral presentation: Metabolic Bone Disease in a Common Marmoset

- 61st annual meeting of the American College of Veterinary Pathology, October and November 2010 & 22nd Annual Wilmer Research Meeting April 2011
  - Poster: Regulation of retinal ganglion cell gene expression: development of an electroporation-based method for the study of *cis*-acting regulatory elements

- 60th annual meeting of the American College of Veterinary Pathology, December 2009
  - Poster: Metabolic bone disease in a colony of common marmosets (*Callithrix jacchus*)

- 59th annual meeting of the American College of Veterinary Pathology, November 2008
  - Poster: Chitinolytic Shell Disease and Branchitis in Captive American Horseshoe Crabs (Limulus polyphemus)

- 15TH annual CL Davis Zoo & Wildlife Pathology Workshop at the 40th Annual meeting of the American Association of Zoo Veterinarians, October 2008
  - Oral Presentation: Ocular Mycobacteriosis in a Madagascar Tomato Frog

- Phi Zeta Research Day (MSU CVM) 2005
  - Poster: The search for the gene and causative mutation responsible for the retinopathy, globe-enlarged (rge) chicken: a positional candidate gene approach

- ARVO (Association for Research in Vision and Ophthalmology) 2005, Phi Zeta Research Day (MSU CVM) and the Merck-Merial Student Research Symposium 2005
    - Poster: Pharmacological dissection of the electroretinogram of the Retinopathy, globe-enlarged (*rge*) chicken

- Phi Zeta Research Day (MSU CVM) 2003
    - Poster: New techniques for the diagnosis of Marek's disease in chickens

AWARDS

- NIH Loan Repayment Program, July 2012-June 2014
- K12 Award through Wilmer Eye Institute, October 2011 – June 2014
- Young Investigator Award, category of Natural Disease, Second place for poster entitled "Metabolic bone disease in a colony of common marmosets (*Callithrix jacchus*)", 60th Annual meeting of the American College of Veterinary Pathologists, December 2010
- Young Investigator Award, category of Diagnostic Pathology, Third place for poster entitled "Chitinolytic Shell Disease and Branchitis in Captive American Horseshoe Crabs (Limulus polyphemus)", 59th Annual meeting of the American College of Veterinary Pathologists, November 2008
- CVM General Scholarship, 2006
- Salsbury Scholarship, 2006
- Member of The Phi Zeta Honorary Society of Veterinary Medicine, 2006
- NIH T-32 Training Grant, 2005
- NIH T-35 Training Grant, 2003
- Merck/Tanaka Award for Veterinary Sciences, 2003
- Veterinary Camp Scholarship, 2002
- CVM General Scholarship, 2002

TEACHING EXPERIENCE

- <u>Ocular Pathology Lectures</u>
    - Pathology for Graduate Students: Basic Mechanisms (300.713), 2008, 2009, 2010, 2011, 2012, 2013
    - Comparative Pathobiology & Genetically Engineered Mice (680.701), Johns Hopkins School of Medicine, 2010, 2012
    - Ophthalmic Phenotyping of Mutant Mice for the JHU Mouse Pathobiology and Phenotyping Short Course, 2012, 2013

- <u>Mouse dissection lab</u>
    - 2010, 2011, 2012 Mouse Pathobiology and Phenotyping Course

- <u>Toxicological Pathology of the Eye Lecture</u>
    - Environmental Toxicological Pathology (187.620.01), Johns Hopkins School of Public Health 2010, 2011, 2012, 2013

- Mouse model of asthma lecture
    - Comparative Pathobiology & Genetically Engineered Mice, May 2008

- Veterinary Microbiology Tutor, MSU CVM, East Lansing
    - January to May 2004
    - *Tutor*: Individually tutored a student to help him understand the most important aspects of veterinary microbiology

- Veterinary Histology Teaching Assistant, MSU CVM, East Lansing
    - August to December 2003
    - *Teaching Assistant*: Helped first year vet students identify cells and tissues as they navigated the histology laboratory exercises

CLINICAL VETERINARY EXPERIENCE

- Maryland SPCA, Baltimore, MD
    - January 2008 to June 2014
    - *Veterinarian*: Spay, neuter & vaccinate feral cats

- Milwood Animal Clinic, Portage, MI
    - February 2001 to July 2002
    - *Small Animal Veterinary Technician:* Checked in animals for surgery, prepared pre-surgical meds, induced and monitored anesthesia, assisted in surgery, communicated with clients, phlebotomy, radiographed, stocked, tracked items to be ordered, weekend care of in-house patients and general restraint of small animals including exotics

- Emergency Pet Clinic, Inc., Bedford Hts, OH
    - June '98 to Aug. '98, Dec. '98, June '99, Aug. '00, Dec. '00
    - *Veterinary Technician:* Answered the phone, communicated with clients, restrained animals for examination, administered treatments, filled prescriptions, took radiographs, used automatic blood analyzing machines and took care of patients in the clinic.

- Western Australian Rural Sheep Farms, Western Australia
    - January 2000
    - *Veterinarian/Farm Consultant's Assistant:* Restrained and mustered sheep during shearing, collected blood samples for selenium trials, collected and analyzed fecal samples, and learned how to work with sheep dogs and about a sheep farmer's way of life.

WORK EXPERIENCE

- Mary Rheuben's Residence, Holt, MI
    - May 2003 to May 2006
    - *Manual Laborer*: Duties include cleaning horse stalls, managing manure, sheep work (vaccinating, deworming, feeding), mowing the lawn, planting and weeding both vegetable garden and flower beds and other tasks as needed.

- Nutrition Kitchen Care Taker, Veterinary Teaching Hospital, East Lansing, MI
    - November 2002 to March 2004
    - *Cleaner and Stocker*: Duties included keeping the nutrition kitchen clean, stocking canned and dry dog and cat food and managing the hospital's inventory of available pet foods.

- Center for International Programs, Kalamazoo College, Kalamazoo, MI
    - September 2000 to June 2001
    - *Peer Advisor*: Duties include helping students learn about and choose a study abroad program, advising them in the application process and preparing them for their experiences abroad.

- Residential Life, Kalamazoo College, Kalamazoo, MI
    - September 1998 to June 1999 and March 2000 to June 2000
    - *Residential Advisor*: Duties included being a resource person for the first year students, keeping order in the residence halls and programming activities for residents.

REFERENCES

Donald J. Zack, MD, PhD
Department of Ophthalmology, School of Medicine, Johns Hopkins University
Phone (410) 502-5230 Email dzack@jhmi.edu

Joseph Mankowski, PhD, DVM, DACVP
Department of Molecular and Comparative Pathobiology, School of Medicine, Johns Hopkins University
Phone (410) 955-9770 Email jmankows@jhmi.edu

M. Christine Zink, DVM, PhD, DACVP
Department of Molecular and Comparative Pathobiology, School of Medicine, Johns Hopkins University
Phone (410) 955-9770 Email mczink@jhmi.edu

Simon Petersen-Jones, DVet, PhD, DECVO
Small Animal Clinical Sciences, College of Veterinary Medicine, Michigan State University
Phone (517) 353-3278 Email peter315@cvm.msu.edu